



HAL
open science

Achieving High Affinity for a Bacterial Lectin with Reversible Covalent Ligands

Giulia Antonini, Anna Bernardi, Emilie Gillon, Alberto Dal Corso, Monica Civera, Laura Belvisi, Annabelle Varrot, Sarah Mazzotta

► **To cite this version:**

Giulia Antonini, Anna Bernardi, Emilie Gillon, Alberto Dal Corso, Monica Civera, et al.. Achieving High Affinity for a Bacterial Lectin with Reversible Covalent Ligands. *Journal of Medicinal Chemistry*, 2024, 67 (21), pp.19546-19560. 10.1021/acs.jmedchem.4c01876 . hal-04777715

HAL Id: hal-04777715

<https://hal.science/hal-04777715v1>

Submitted on 12 Nov 2024

HAL is a multi-disciplinary open access archive for the deposit and dissemination of scientific research documents, whether they are published or not. The documents may come from teaching and research institutions in France or abroad, or from public or private research centers.

L'archive ouverte pluridisciplinaire **HAL**, est destinée au dépôt et à la diffusion de documents scientifiques de niveau recherche, publiés ou non, émanant des établissements d'enseignement et de recherche français ou étrangers, des laboratoires publics ou privés.

ACHIEVING HIGH AFFINITY FOR A BACTERIAL LECTIN WITH REVERSIBLE COVALENT LIGANDS

Giulia Antonini,^a Anna Bernardi,^a Emilie Gillon,^b Alberto Dal Corso,^a Monica Civera,^a Laura Belvisi,^{a*} Annabelle Varrot,^{b*} Sarah Mazzotta^{a*}

a. Università degli Studi di Milano, Dipartimento di Chimica, 20133 Milano, Italy;

b. Univ. Grenoble Alpes, CNRS, CERMAV, 38000 Grenoble, France

KEYWORDS: *Glycomimetics, carbohydrates, covalent ligands, salicylaldehyde, lectins*

ABSTRACT:

High-affinity monovalent ligands for lectins are challenging to develop due to weak binding interactions. This study investigates the potential of rationally designed covalent ligands targeting the *N*-terminal domain of BC2L-C lectin from *Burkholderia cenocepacia*, a pathogen causing severe respiratory infections in immunocompromised patients. Anti-adhesion therapy is emerging as a complementary approach against such infections and bacterial lectins are suitable targets. The fucose-specific BC2L-C-*Nt* recognizes blood group oligosaccharides on host cells. Using a computational approach, we designed reversible covalent competitive ligands that include a fucoside anchor and a salicylaldehyde warhead targeting Lys108 near the fucose-binding site. Several candidates were synthesized and tested using competition experiments. The most effective ligand improved the IC₅₀ of methyl-fucoside by two orders of magnitude, matching the affinity of the native H-type 1 trisaccharide. Control experiments confirmed the importance of both fucose anchor and salicylaldehyde moiety in the ligand's affinity. Mass analysis confirmed covalent interaction with Lys108.

1. INTRODUCTION

The increase of antibacterial resistance has become an emergency for public health, compromising the efficacy of traditional antibiotics and leading to clinical implications.^{1,2} *Burkholderia cenocepacia* is one of closely related species of the *Burkholderia cepacia* complex that is widely distributed in the environment and in particular in soil. This Gram-negative bacterium presents intrinsic resistance to many antibiotics and has emerged as a highly harmful pathogen for immunocompromised individuals.³⁻⁵ It causes nosocomial pulmonary infections in cystic fibrosis and chronic granulomatous patients, increasing the mortality rate and the risk to develop the so-called “cepacia syndrome”.⁴⁻⁶

As for many other pathogens, infections by *B. cenocepacia* require an initial adhesion step to host cells, which is mediated by bacterial lectins. These proteins can specifically bind glycans expressed on the host cell surface, enabling the following infection process.⁷⁻¹⁰ Thus, complementary antimicrobial therapies (antiadhesion, antibiofilm), that are much needed in view of the current bacterial resistance emergency, can be developed by inhibiting bacterial lectins' binding to host tissue.¹¹ The lectin BC2L-C from *B. cenocepacia* is an intriguing target due to its dual carbohydrate specificity. Its hexamer features a C-terminal dimeric domain that binds to bacterial glycans with heptose/mannose specificity and an N-terminal trimeric domain that interacts with fucosylated glycans and in particular with histo-blood group oligosaccharides, including H-type 1 and H-type 3.^{8,9} Knockout studies suggest a role for this lectin in biofilm stabilization.¹² The N-terminal domain forms three identical binding sites at each protomer interface and shows millimolar affinity for α -methyl-L-fucoside and micromolar affinity for histo-blood group oligosaccharides,^{8,13} which suggests a possible role in host adhesion for this domain. We have recently reported the first synthetic glycomimetic ligands for BC2L-C-Nt, obtained by engaging simultaneously its fucose binding site and a secondary site that extends in the direction of the β -substituent on fucose anomeric carbon.¹⁴⁻¹⁷ This first series of molecules includes a β -fucosylamide hit, compound **1** (Figure 1A), that showed a 159 μ M Kd for the lectin and thus an order of magnitude gain over α -methyl fucoside, which presents a Kd of 2700 μ M.

Despite the interesting results obtained from this first generation of ligands, the affinity for the target lectin remains modest and further optimization is required to obtain suitable candidates for *in vitro* cellular tests. Nevertheless, the development of efficient inhibitors of lectins is exceedingly difficult to achieve, due to the unfavourable characteristics of lectins' binding sites, which entail weak interaction energies.^{18,19} The use of covalent ligands represents a powerful strategy to enhance both the ligand's affinity and selectivity towards a particular target. These ligands exhibit strong and prolonged interactions with the protein target by forming an intermolecular covalent bond.²⁰⁻²² The process involves an electrophilic unit in the ligand reacting with a nucleophilic functionality in an amino acid residue close to the binding site.

The past decade has witnessed a resurgence of interest in covalent inhibitors in medicinal chemistry, with several approved drugs, including anti-infective ones.²⁰ Indeed, covalent ligands are particularly well-suited for the inhibition of microbial targets, where complete functional impairment of the target protein is not a concern. To the best of our knowledge, there are still no approved covalent drugs targeting lectins and just a few examples of covalent compounds designed to target lectins have been reported in the literature.^{23,24} The first covalent ligand of a bacterial lectin was described in 2017 by A. Titz and co-workers. It contains a modified D-galactose anchor and an epoxide electrophile, which targets a cysteine residue in *Pseudomonas aeruginosa*'s lectin LecA.²³ More recently, L. Hartmann and colleagues have reported a group of D-mannose glycomacromolecules functionalized with a catechol moiety that can slowly oxidize and irreversibly engage nucleophilic residues in Concanavalin A.²⁴

Here, we describe the development of salicylaldehyde-based reversible covalent ligands of BC2L-C-*Nt*, designed to target a lysine residue in the vicinity of its fucose binding site. Reversible covalent inhibition mitigates some of the possible negative effects of covalent ligands. To date, this strategy has been used to target human enzymes (mainly kinases and proteases),^{25,26} but it is also valuable to target microbial proteins, because can prevent 'off-target' irreversible modifications that may lead to toxic effects for the host.²⁶ Out of the various warheads that have been developed to achieve reversible covalent inhibition,²⁶⁻²⁸ those used to engage Lys residues often entail the use of a boronic acid. This is not a viable option for carbohydrate ligands, that would effectively coordinate to the warhead. *Ortho*-hydroxy benzaldehydes (salicylaldehydes) have also been used as portable and mild electrophiles to engage with Lys ϵ -amino groups in aqueous media. They have a proven ability to react with a broad range of Lys residues in the proteome,²⁹⁻³¹ and reversibly form H-bond stabilized imine adducts, which can act synergistically with ligand/protein non-covalent forces, stabilizing the complex (Figure 1B).

To design reversible covalent ligands for BC2L-C-*Nt*, we started from the SAR previously obtained for glycomimetic inhibitors and developed a docking manifold which allowed to identify and prioritize a set of candidates. They were synthesized, evaluated through a set of biophysical techniques and characterized as covalent ligands by mass spectrometry (MS). Our results are reported below.

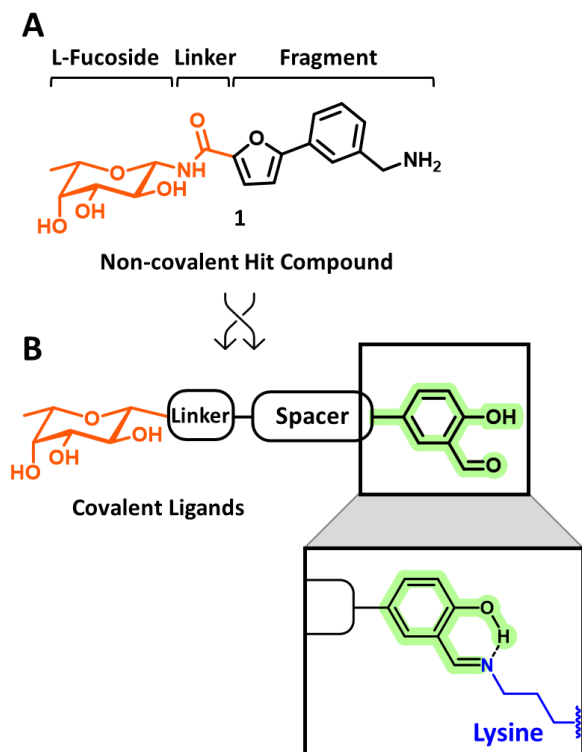


Figure 1. Towards reversible covalent ligands for BC2L-C-*Nt*. (A): structure of the non-covalent hit compound **1** obtained in previous work,¹⁴ (B): general structure of salicylaldehyde-bearing covalent ligands designed to target a Lys side chain near the fucose binding site, as highlighted in the box.

2. RESULTS AND DISCUSSION

2.1. Design

To design covalent ligands for BC2L-C-*Nt*, we focused on the identification of a suitable amino acid residue for covalent bond formation, as well as on the selection of an appropriate electrophilic warhead. Upon analysis of the available crystal structures of the protein in complex with various fucosylated ligands (PDB ID: 7BFY, 2WQ4, 7OLU, 7OLW, 8BRO, 6TIG and 6TID), the nucleophilic residue Lys108 emerged as a potential candidate, due to its proximity to the previously identified secondary site near the fucose binding region (Figure 2). Lysine residues typically show poor nucleophilicity at physiological pH as their ϵ -amino groups are mostly protonated. Thus, the reactivity of Lys108 was estimated through *in silico* calculations of local pK_a values with the Rosetta webtool³² considering different available crystal structures of BC2L-C-*Nt* in the *apo* form and in complex with synthetic ligands or natural oligosaccharides. Interestingly, the calculated average pK_a value (10.07 ± 0.25) was the lowest among the five Lys residues in the protein (Figure 2), suggesting that the amino group of Lys108 may be partially

neutral at physiological pH and may act as a nucleophile more effectively than the other four Lys residues in each protomer, that are more basic.

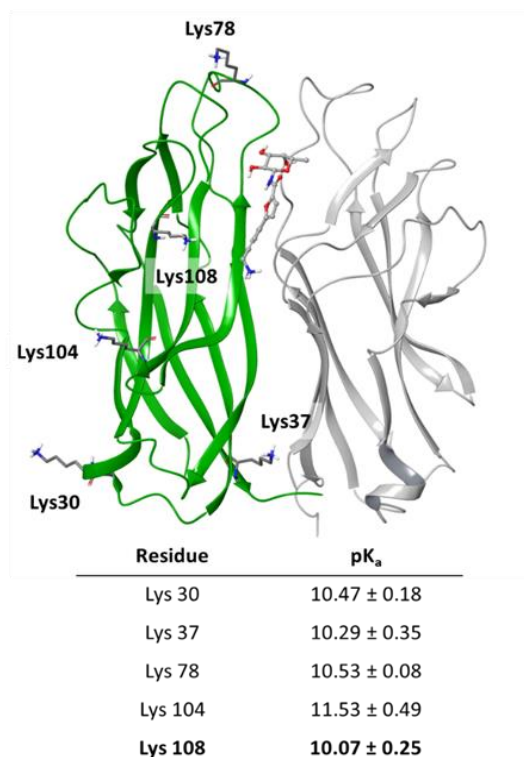


Figure 2. The *N*-terminal domain of BC2L-C. One of the three binding interfaces from the crystal structure of BC2L-C-*Nt* in complex with **1** (PDB ID: 8BRO) is shown. The lysine residues are highlighted in one of the protomers (chain C, green). The pK_a values of Lys(ε-NH₂) collected in the table are average values calculated using different available crystal structures of BC2L-C-*Nt* in the *apo* form and in complex with fucosylated ligands (PDB ID: 7BFY, 2WQ4, 7OLU, 7OLW, 8BRO, 6TIG and 6TID). The pK_a value of a typical lysine residue on the surface of a protein is around 10.4.^{33,34}

Our previous work on BC2L-C-*Nt* ligands¹⁴⁻¹⁷ showed that the crevice separating the fucose binding site from Lys108 can be engaged productively by extended aromatic fragments, such as the (aminomethyl-phenyl)-furan fragment in **1** (Figure 1A), installed at fucose anomeric carbon through an amide linker in the β-configuration. We initially examined the possibility of modifying the structure of **1** by adding a salicylaldehyde moiety directed towards the lysine side chain. Since some *in silico* experimentation failed to produce convincing candidates, we switched to a strategy that incorporates a salicylaldehyde warhead directly into the structure of new glycomimetic ligands (Figure 1B). To fit the active chemotype, the new blueprint includes a suitable aromatic spacer between the linker and the salicylaldehyde moiety, replacing the furan in **1** (Figure 1B). As a linker, we examined an alkyne, an amide or a 1,4-triazole, already used and validated in the first generation of non-covalent BC2L-C-*Nt* ligands.^{14,15} The spacer was chosen among aromatic and heteroaromatic fragments, based on the distance between the fucose anomeric carbon

and the Lys108 side chain. Most of the selected spacers consist of a functionalized benzene ring that can establish π - π stacking interactions with Tyr58 in the secondary site, a stabilizing interaction that was shown to enhance ligand affinity.¹⁶

A total of 56 compounds were designed and analysed *in silico* by means of docking protocols. Docking algorithms for covalent ligands are available and appropriate procedures have been reported.³⁵ However, a specific challenge is presented here by the characteristics of lectins' binding sites, which are shared by BC2L-C-Nt. The fucose site is shallow and solvent exposed (see Figure 3) and does not provide the strong physical constraint of ligands within a confined space, which is typical of enzymes. This means that the covalent bond with the target residue can be formed, but the sugar portion can still fluctuate in and out of its binding site, due to torsional strain in the bound linker. In other words, the bound pose of the putative ligand must be sufficiently pre-organized for covalent interaction with the target residue, in order to avoid straining the carbohydrate portion out of its binding pose. This can hardly be evaluated by "traditional" covalent docking protocols. Thus, we developed a docking workflow to address this issue. First, standard docking was performed exploiting a previously defined protocol (Figure 3A),¹⁵ based on the XP scoring function of Glide.³⁶ A maximum of 10 poses for each ligand were saved and a first filter was applied to remove those compounds that did not display a distance between the reactive electrophilic and nucleophilic groups lower than 10 Å in all poses (structures collected in Table SI-1). This left 36 compounds, and their top-ranked pose was selected as the starting structure to perform covalent docking using CovDock.³⁷ For each remaining candidate, 10 poses were saved, all having the imine bond well established between the ligand aldehyde group and the ϵ -amino group of Lys108 (Figure 3B). The poses obtained from covalent docking were evaluated based on their ability to maintain in all poses the interactions and the conformation of the L-fucose core observed in available X-ray structures of non-covalent ligands. In particular, the presence of the following H-bond interactions was monitored: Fuc-OH-2 with Arg111 side chain; Fuc-OH-3 with Thr74 side chain; and Fuc-OH-4 with Arg85 side chain (Figure 3). The three ligands which did not satisfy these criteria (shown in Table SI-2) were filtered away. As a result of this workflow, 33 compounds matching the chosen criteria were selected (collected in Table SI-3) and, in order to prioritize their synthesis, they were analyzed for their ability to form additional interactions within the binding site, fitting the established pharmacophore for β -fucosides in BC2L-C-Nt. In details, ligands establishing (T-shaped) π - π stacking interactions with the Tyr58 side chain (Figure 3B) were prioritized because our previous work¹⁴⁻¹⁶ had shown that this feature plays an important role in the ligand binding affinity. Additional stabilizing interactions between ligand and protein, including the formation of an intramolecular hydrogen bond between the imine nitrogen and the *ortho*-hydroxyl group of the aldehyde warhead, were flagged as selection criteria.

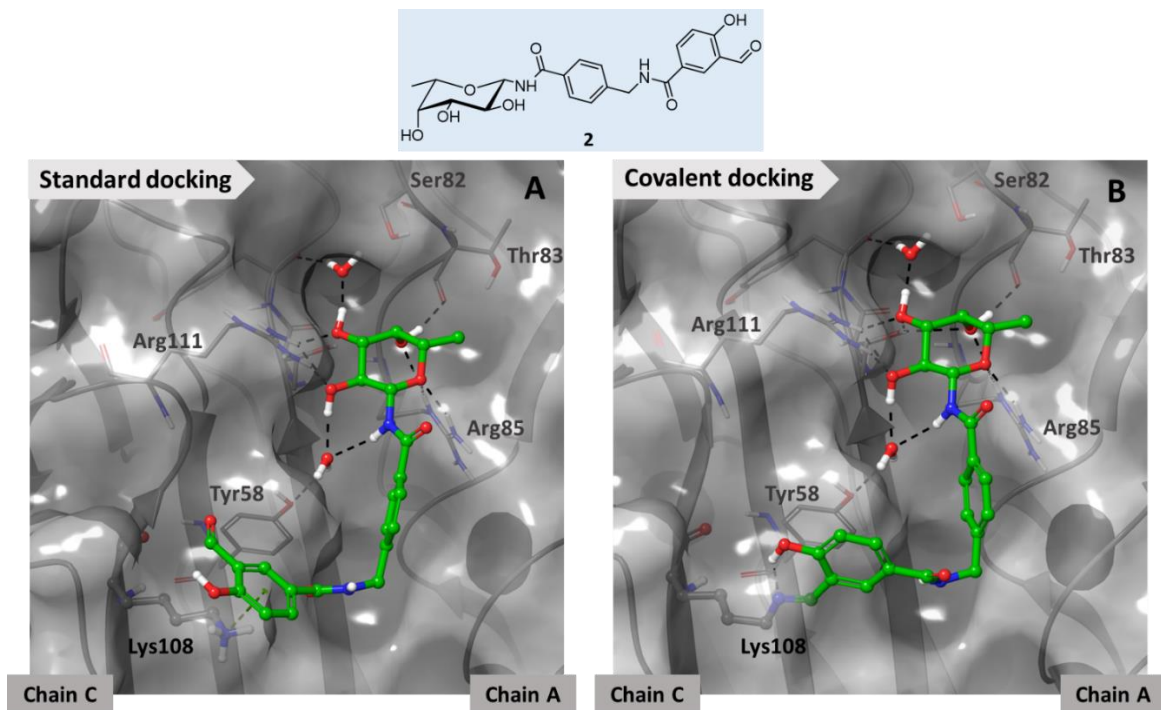


Figure 3. Docking pose of ligand **2** obtained from (A) standard docking and (B) covalent docking. PDB ID: 2WQ4 was used to prepare the docking model. Two highly conserved water molecules are retained in docking calculations; H-bond interactions are depicted as black dashed line. Selected poses obtained from standard and covalent docking for compounds **3-5** are reported in Supporting Information, Figure SI-1.

The structure of all the compounds screened, as well as a full description of the screening protocol and of the filters adopted to prioritize synthesis are reported as Supporting Information (Tables SI-1 to SI-3 and corresponding discussion). Figure 3 shows two typical poses for standard docking and covalent docking of one ligand (compound **2**) which passed both filters and satisfied the above criteria. The corresponding poses for a candidate (compound **A12**, Table SI-1) which did not satisfy the first filter is shown in Figure SI-2.

Finally, the 14 candidates from this group that include an amide linker were preferred over the alkyne- and triazole-containing ligands, based on synthetic feasibility and, as a first attempt to obtain a proof of concept, the synthesis of four of them was prioritized (compounds **2-5**, Figure 4).^{14,15} The selected glycomimetics depicted in Figure 4 differ in the spacer, which is either a *para*- (compounds **2** and **3**) or a *meta*-substituted (compounds **4** and **5**) benzoic acid, as well as in the length of the tether connecting the

spacer to the terminal salicylaldehyde moiety. Selected poses obtained from standard and covalent docking of **3-5** are reported in Supporting Information, Figure SI-1. They served as ideal examples for evaluating the impact of these structural differences that are common to the remaining 10 amide candidates (see Table SI-3) on the interaction with the target lectin domain.

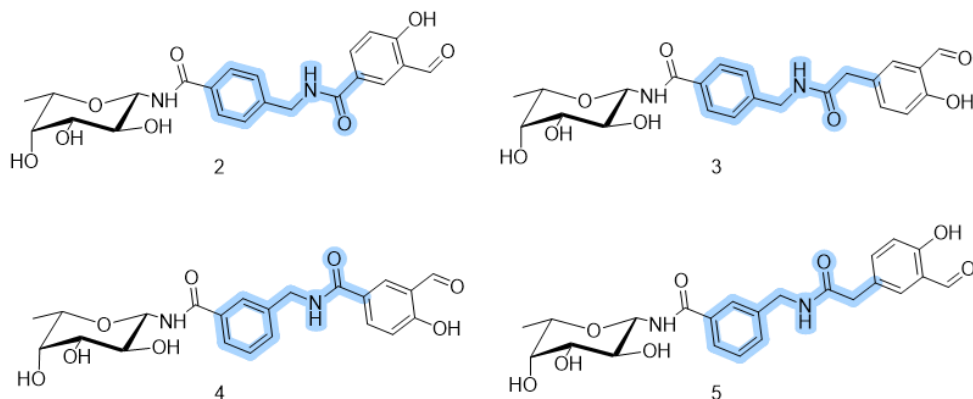
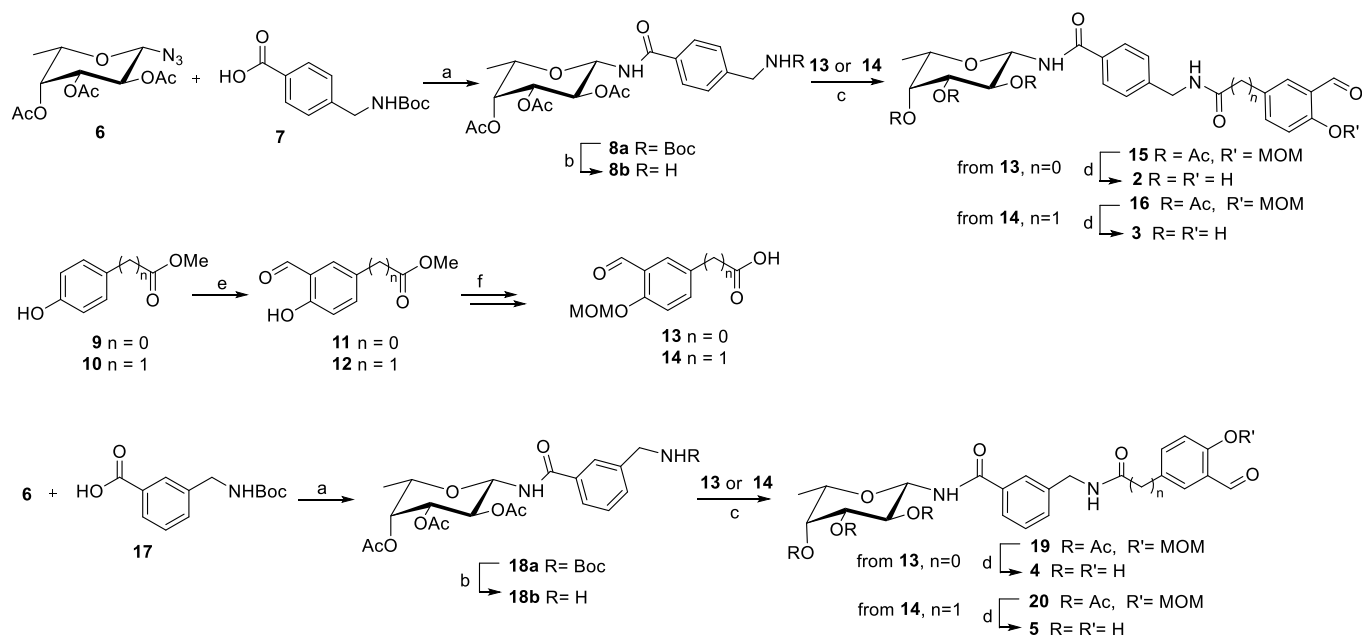


Figure 4. Covalent glycomimetic ligands prioritized for the synthesis. The variable part of the compounds is highlighted in blue. Compounds **2** and **3** present a *para*-substituted benzene spacer, while **4** and **5** have a *meta*-substituted spacer. They differ also for the length of the chain that connects the spacer to the terminal salicylaldehyde moiety.

2.2. Synthesis

Ligands **2-5** (Figure 4) were synthesized by condensation of a β-fucosylamide scaffold with the salicylaldehyde moiety, as summarized in Scheme 1. The fucoside intermediates **8b** and **18b** were synthesized by Staudinger ligation of the β-fucosylazide **6**^{14,15} with acid **7** or **17**, respectively (PMe₃, 1-ethyl-3-(3-dimethylaminopropyl)carbodiimide EDC, hydroxybenzotriazole HOBt, *N,N*-diisopropylethylamine DIPEA 79%), followed by Boc removal. The electrophilic warheads containing the salicylaldehyde moiety (**13** and **14**, Scheme 1) were obtained from commercially available *para*-hydroxy esters **9** and **10**, which differ for the chain length. An *ortho*-formylation reaction under Skattebøl condition (MgCl₂, paraformaldehyde, Et₃N)^{38,39} afforded the salicylaldehyde intermediates **11** and **12** (51% and 77%, respectively). They were protected on the phenolic hydroxyl group as MOM ethers before ester hydrolysis in basic conditions to obtain acids **13** and **14** that were coupled to **8b** and **18b** (*N*-Hydroxysuccinimide NHS, EDC). Ligands **2-5** were finally obtained upon full deprotection in acidic conditions (Scheme 1).



Scheme 1. Synthesis of **2-5**. Reagent and conditions: a) PMe_3 , EDC, HOBT, DIPEA, CH_2Cl_2 , 79%; b) TFA/ CH_2Cl_2 97%; c) NHS, EDC, DIPEA, CH_2Cl_2 , 52 – 57%; d) HCl conc., EtOH/ CHCl_3 , 43 – 57%; e) MgCl_2 , paraformaldehyde, Et_3N , MeCN, 51% (**11**) 77% (**12**); f) MOMCl, DIPEA, CH_2Cl_2 ; LiOH· H_2O , THF/ H_2O , 81% (**13**) 93% (**14**), over two steps.

As negative controls, the L-fucosylamide **21** and the D-glucosylamide **22** (Figure 5) were also synthesized through a similar synthetic strategy (see Supporting Information). The fucose derivative **21** features the same core structure of **3** but lacks the aldehyde function in the distal aromatic ring. The glucosylamide **22** shares with **3** the aglycone portion, including the electrophilic warhead, but contains a different monosaccharide, which is known not to bind to BC2L-C-*Nt* carbohydrate recognition domain.⁹ Analysis of the interaction of these controls with the lectin was employed to dissect the relative role of the sugar moiety and of the electrophilic warhead in determining the affinity of **2-5**.

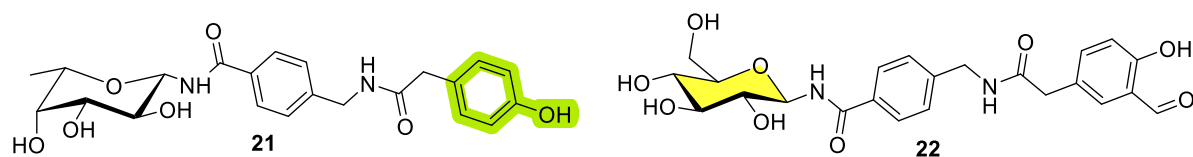


Figure 5. Negative controls **21** and **22**. Structural differences relative to ligand **3** are highlighted: in green the distal aromatic ring in **21**, lacking the aldehyde group; in yellow the glucose ring that replaces the fucose core in **22**.

2.3. Biophysical evaluation

A preliminary evaluation of ligands **3** and **5** using a thermal shift assay showed a positive shift of about 2°C (see blue curves in Figure SI-3, with $T_m \sim 75^\circ\text{C}$), suggesting a strong and stabilizing interaction provided by ligand binding. This shift was not observed with ligands devoid of electrophilic units (e.g. **1**, see the green curve in Figure SI-3), indicating that the additional interaction formed by **3** and **5** could be due to a covalent bond.

Motivated by these results, the full set of compounds was further investigated, mainly through Surface Plasmon Resonance (SPR) and mass spectrometry.

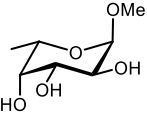
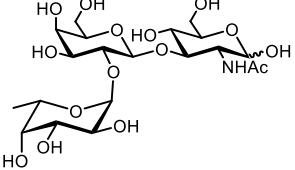
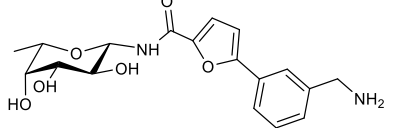
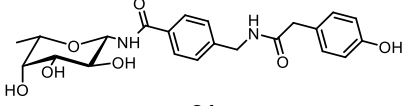
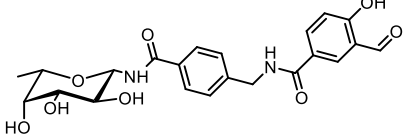
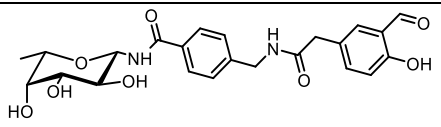
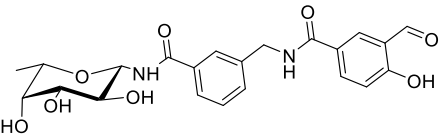
2.3.1. SPR competition assays

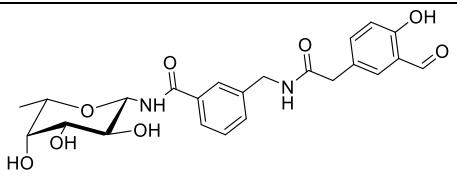
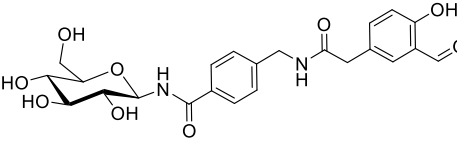
A competition assay was set up using SPR to investigate the interaction of **2-5** with BC2L-C-Nt. The competition experiments were carried out using a fucosylated chip generated in house (see experimental section) and injecting solutions of the lectin domain mixed with ligands at decreasing concentrations. IC_{50} were obtained from the resulting inhibition curves (see Supporting Information Figure SI-6). The fucosylamide **21**, which lacks the aldehyde functionality but is otherwise identical to **3**, and the glucosylamide **22**, which contains the same spacer-aldehyde system as **3**, but replaces the fucose moiety with a sugar which is not recognized by BC2L-C-Nt,⁹ were included as negative controls. Our hit ligand **1** and the native ligand H type-1 trisaccharide **23** were added as positive, non-covalent controls and as a calibration for the assay relative to the known Isothermal Titration Calorimetry (ITC) data (Table SI-4). The results obtained are collected in Table 1.

The competition experiments performed on the H type-1 trisaccharide **23** and on ligand **1** (Table 1, entries 2 and 3) resulted in IC_{50} values that were consistent with the known K_d for these compounds, thus validating the SPR experiment. For the negative control **21** (entry 4), saturation could not be achieved and an IC_{50} value higher than 2 mM was estimated. Comparison with the $K_d 2.7 \pm 0.7$ mM reported for α -methyl-L-fucoside **24** (entry 1) and the $IC_{50} 103 \pm 5$ μM obtained for the β - fucosylamide **1** in the same experiment (entry 3) suggests that the aglycon portion of **21** is not contributing significantly to the interaction. However, when the same aglycone bears the aldehyde warhead, as in **3** (entry 6), the competition experiment yields an IC_{50} value of 34.9 ± 4.7 μM . This is the same affinity range as the H type-1 trisaccharide **23**, while gaining almost 2 orders of magnitude over **21**. Thus, the salicylaldehyde moiety clearly has a key role in enhancing the interaction between the protein and the ligand. Ligands **2**, **4** and **5** (entries 5, 7 and 8, respectively) showed IC_{50} values in the same range of activity as **3**, with minor variations depending on the length of the chain (**3** vs **2**, **5** vs **4**) and the substitution pattern of the first aromatic ring (**2** vs **4** and **3** vs **5**). The best result ($IC_{50} 27.7 \pm 1.6$ μM) was obtained with **2**, featuring the

para-substituted spacer and the shorter chain. Collectively, these results show a strong correlation between the presence of the salicylaldehyde moiety and the strength of the interaction, suggesting that the significant difference in the IC₅₀ value of **21** and those of aldehyde-containing compounds **2-5** may depend on the formation of a covalent bond. Additionally, the low activity of the glucoside **22** (entry 9) strongly suggests that the sugar drives the interaction, and the aldehyde stabilizes it by specifically ligating a nearby lysine.

Table 1. SPR competition assays^a

Entry	Ligand	IC ₅₀ (μM) SPR
1	 24	2700 ± 700 ^b
2	 23	19.9 ± 0.31
3	 1	103 ± 5
4	 21	> 2000
5	 2	27.7 ± 1.6
6	 3	34.9 ± 4.7
7	 4	74.3 ± 3.6

8		50.5 ± 9.5
5		
9		> 2000
22		

^a IC₅₀ values obtained from SPR competition assays by inhibiting binding of BC2L-C-*Nt* to fucosylated chip; ^b K_d, as measured by ITC from ref 13.

2.3.2. MS analysis

MS is usually employed to identify the presence of a covalent binding mode, which can be detected as a mass peak corresponding to the covalently linked adduct.⁴⁰

We investigated the formation of a covalent adduct between BC2L-C-*Nt* and ligands **2-5** by MALDI-TOF analysis, comparing the MS spectra of the free protein with those of protein/ligand mixtures at various stoichiometric ratios. Figure 6 shows the spectrum of a 1:200 mixture of protein and ligand **3** incubated for 24 h at room temperature in pH 8.0 buffer. Comparison with the protein spectrum shown on the upper trace shows a mass shift of 440 Da (ligand – H₂O) which corresponds to the formation of a condensation product and agrees with the presence of an imine adduct. Similar results were obtained also with **2**, **4** and **5** (see Supporting Information Figures SI-7 to SI-9), suggesting the ability of all these ligands to covalently engage one amino group of the protein.

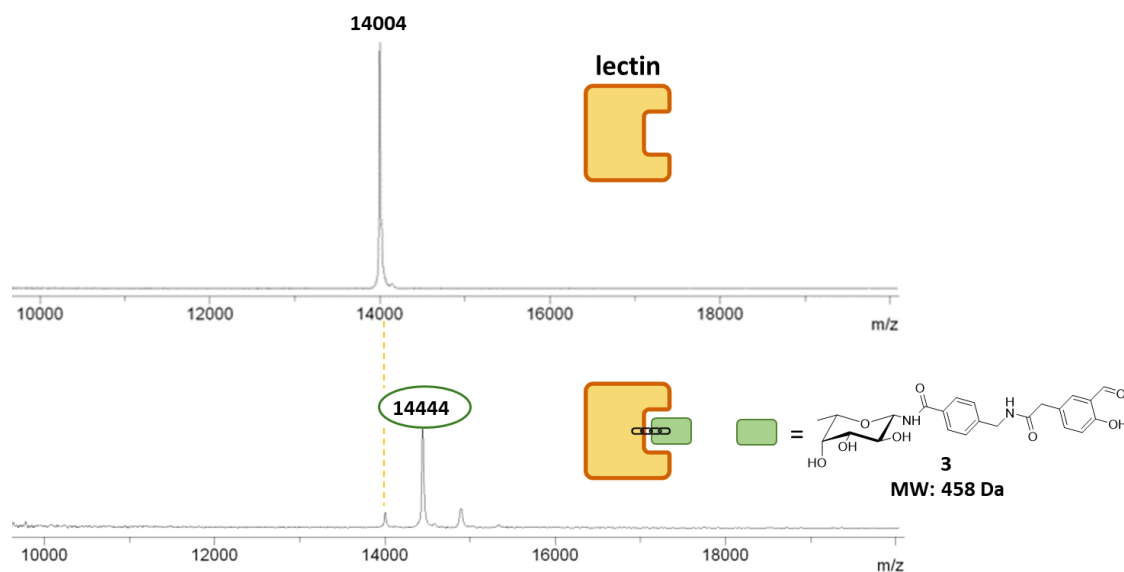


Figure 6. MALDI MS experiments (2,3-Dihydroxybenzoic acid DHB matrix). upper trace: BC2L-C-*Nt*; bottom trace: 1:200 mixture of protein and ligand **3** incubated for 24 h at room temperature in pH 8.0 buffer. The protein mass shift corresponds to the condensation adduct.

Control experiments were performed at 1:10 protein:ligand ratio using **3** (24 h and 2 h incubation, Figures 7 and SI-10, respectively) and negative controls **21** and **22** (Figure 7). The shift of the protein peak (440 Da) was observed only upon addition of **3** (Figure 7, bottom trace), while no shifted peak was detected with either negative controls (upper and middle traces), suggesting that no covalent adduct is formed with either **21** or **22**. As an additional control, the spectrum was obtained also at 1:200 protein:**22** ratio, confirming the result (Figure SI-11). For compound **21**, this observation is consistent with the absence of the electrophilic warhead, responsible for the covalent bond formation. The result for the glucose-analogue **22** indicates that the fucoside moiety also plays a key role: by non-covalently anchoring the ligand within the binding site it forces the warhead in proximity of Lys108 side chain and promotes covalent bond formation. The interplay between both binding units enables effective inhibition.

It is worth mentioning at this point, that compound **A12** (Table SI-1), one of the ligands filtered out by the docking workflow, was also tested in MALDI-MS experiments as an additional validation of the computational protocol, showing no formation of covalent adducts (see Figure SI-12).

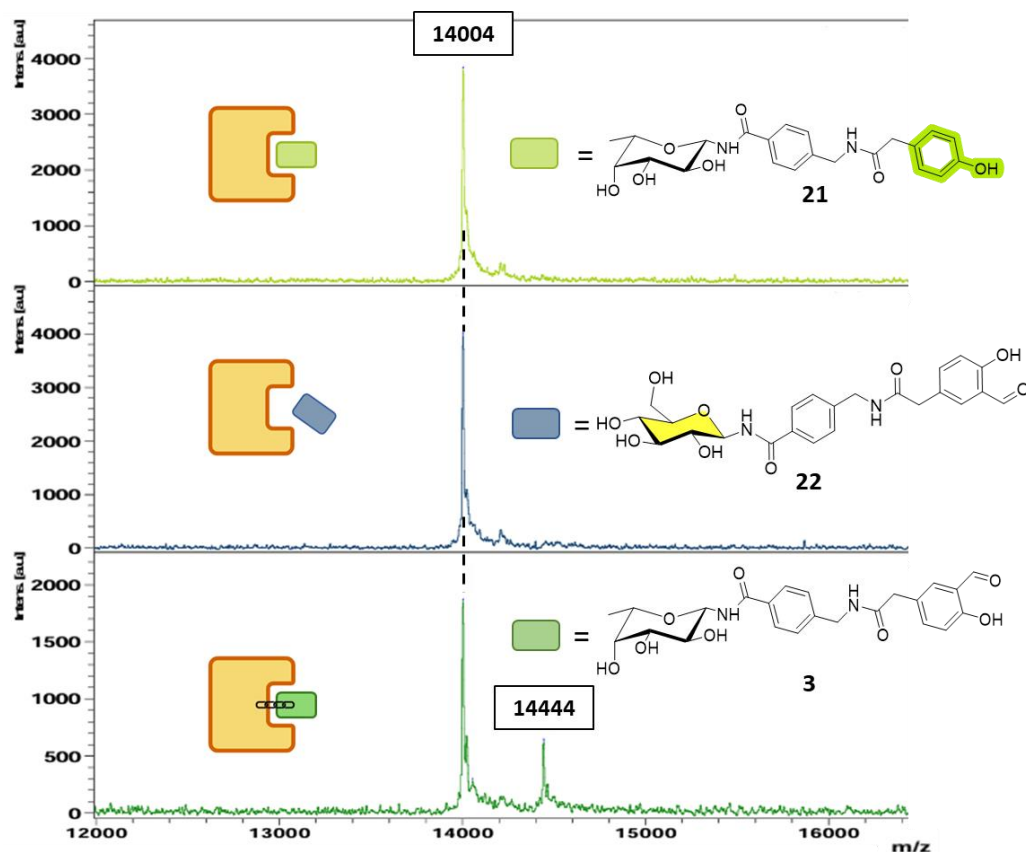


Figure 7: MALDI MS of 1:10 BC2L-C-*Nt*:ligand mixtures, incubated for 24 h at pH 8 (sinapinic acid matrix). Upper trace: protein + **21**; middle trace: protein + **22**; bottom trace: protein + **3**.

The results reported above clearly support that the aldehyde functionality in ligands **2-5** reacts with a nucleophilic nitrogen residue in BC2L-C-*Nt* pocket, producing a strong stabilizing interaction of the protein/ligand complex. The ligands successfully compete against immobilized fucose, as shown by the SPR experiments, suggesting that both the fucose binding site and a nucleophilic amino group are involved in complex formation.

Conceivably, imine formation occurs at Lys108, which, among the five Lys residues in the monomer, is the closest to the fucose binding site. Unfortunately, co-crystallization or soaking trials of BC2L-C-*Nt* with ligands **2-5** were unsuccessful and only led to the *apo* structure, which has prevented further structural analysis by X-ray crystallography up to now. Crystals could be obtained in a variety of space group (H32, P6₃, C2 and P2₁2₁2₁), but, in all these forms Lys108 is close to symmetry axes or neighbouring protomers. This suggests that, upon imine formation the aglycone rings may clash with symmetric protomers and disrupt crystal contacts due to lack of space. Although disappointing, this result is in line with the observation of crystal cracking induced by salicylaldehyde derivatives, recently reported by Tzalis and Ottmann during the development of aldehyde binders for the adapter protein 14-3-3 σ .⁴¹ We

also observed this phenomenon while soaking some crystals for an extended time, which led to their disappearance after a few hours.

Thus, in an effort to pinpoint which of the lysine residues is covalently linked to the ligand, we turned our attention to LC-MS/MS analysis of the peptides obtained by trypsin digestion of a protein:ligand complex. Ligand **2** was selected for this experiment, because it displayed the best affinity for BC2L-C-*Nt*. Before digestion, the ligand:protein mixture was treated with NaBH₄ to reduce the intermolecular imine bond and to allow detection of the covalent adduct (see Supporting Information for LC-MS spectra and analysis, Figure SI-13 and SI-14). A modified 105-111 heptapeptide GQWKSVR was found in the LC-MS trace of the digested complex, and a fragment corresponding to the hexapeptide QWKSVR modified by condensation and reduction ($z=3$) (405.21829) was observed in its MS/MS spectrum (Figure 8). No other Lys residues were found to be modified.

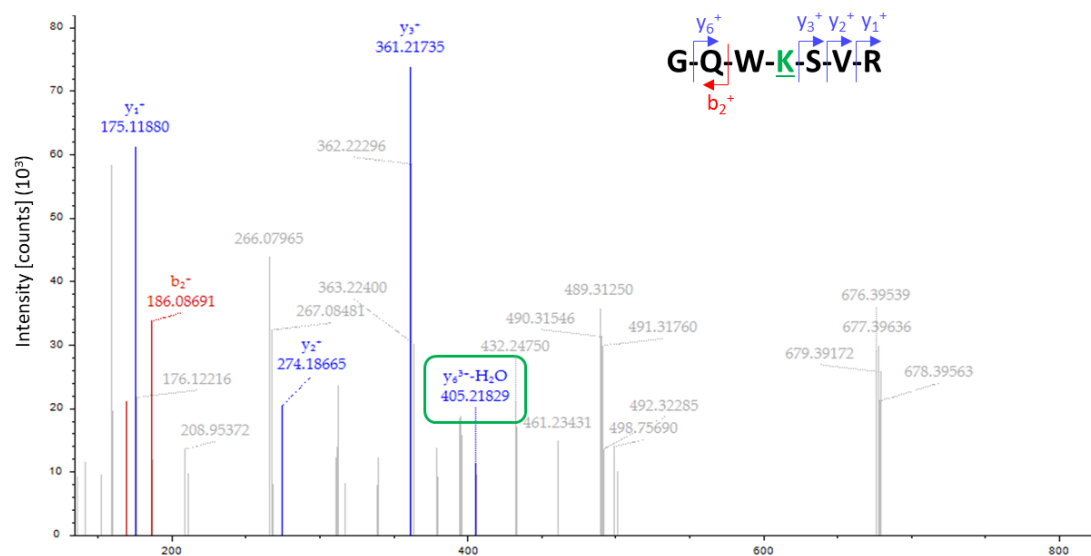


Figure 8. MS/MS spectrum of the lysine modified peptide GQWKSVR ($MH^+ = 1288.63108$ Da; $m/z = 430.21521$, $z=3$) after incubation with **2** and reduction. The fragment in the green box corresponds to the hexapeptide QWKSVR modified by condensation and reduction after water loss ($z=3$) (405.21829).

3. CONCLUSIONS

We described here the development of a set of covalent glycomimetic ligands targeting a lysine residue of the bacterial lectin BC2L-C-*Nt* from *B. cenocepacia* opportunistic pathogen. More than 50 fucosides bearing a salicylaldehyde electrophilic warhead were designed and evaluated *in silico* following a docking workflow specifically devised for lectins, which allowed the identification of most promising candidates. Candidate ligands containing a β -amide linker were prioritized for synthesis considering feasibility.

A synthetic pathway was developed and 4 candidates were prepared, compounds **2-5**, which consist of the combination of sugar scaffold and electrophilic tag. Appropriate negative controls were also synthesized, lacking either the aldehyde warhead (compound **21**) or the fucose anchor (**22**).

All the compounds were evaluated for their affinity with the target using competition SPR experiments, based on their ability to inhibit BC2L-C-*Nt* binding to a fucosylated chip. The resulting IC₅₀ values (comprised between 27.7 μ M and 74.3 μ M) represent an improvement of two orders of magnitude over the simple parent monosaccharide. In particular, the best ligand **2** had the same inhibitory potency of the BC2L-C-*Nt* native ligand H-type 1 trisaccharide **23**. For the first time, a synthetic monovalent glycomimetic ligand of this lectin reaches the same affinity of a natural oligosaccharide.

To confirm the covalent interaction with the lectin, MALDI-MS experiments were performed, observing a shift in the protein peak that corresponds to a condensation protein:ligand adduct. Experiments in the same conditions were carried out on negative controls **21** and **22**, lacking the aldehyde group or the fucose core, neither of which showed shifted peaks in the MS spectra. These results suggests that the aldehyde moiety is responsible for the covalent adduct formation and for the affinity improvement, while the fucose core is required to initiate the interaction and allow proximity to Lys108. Covalent bond formation between the ligands and Lys108 was confirmed by LC-MS/MS analysis of the peptides resulting from enzymatic digestion of the complex formed by **2** and BC2L-C-*Nt*, after stabilization by NaBH₄ reduction. To dissect the atomic details of the binding of the covalent linkage and confirm the pose obtained by docking, new crystallographic studies are required to uncover new crystal forms, whereby the Lys108 residue is not close to symmetry axes.

Covalent stabilization of lectin-sugar complexes has rarely been attempted.^{23,24} Its rational design is particularly challenging, because, unlike enzymes, lectins have large and permissive binding sites, and very low affinity for their native ligands. The characteristic binding mode of carbohydrates in lectins' sites is highly dynamic and entails rapid off-rates. This implies that, if a carbohydrate-based ligand is not sufficiently pre-organized to comfortably adopt a covalently bound pose, formation of the covalent bond

can easily pull the carbohydrate portion out of its binding site. In turn, this means that covalent ligands do not necessarily succeed in blocking competitive binding to the sugar-recognition site. With this in mind, we have elaborated and described here a docking workflow based on a combined analysis of poses generated by standard docking and covalent docking that allowed to prioritize for synthesis a very small number of candidates that were successfully tested in competitive binding assays. Thus, with this work, we have validated a viable computational protocol to design covalent lectin ligands, that we expect to be generally applicable. We also have produced a synthetically accessible monovalent fucoside which binds to BC2L-C-*Nt* as strongly as one of its minimal native oligosaccharide ligands, the H-type 1 trisaccharide **23**.

4. EXPERIMENTAL SECTION

4.1. Computational studies

All the calculations were performed using the Schrödinger Suite through Maestro graphical interface (Schrödinger Release 2018–1). The new glycomimetics were prepared for docking calculations using the LigPrep⁴² tool to create energy 3D minimized structures, generating the protonation states at physiological conditions (pH 7 ± 2).

Atomic coordinates from the crystal structure of BC2L-C-*Nt* in complex with MeSe- α -L-Fuc (PDB 2WQ4) were taken from the Protein Data Bank. The asymmetric unit involves three peptide chains with three identical carbohydrate ligands (MeSe- α -L-Fuc) displaying identical binding pose, thus only one binding site (located between chains A and C) was used for docking calculations. In addition, two highly conserved water molecules, HOH2195 (w1) and HOH2194 (w2), that mediate interactions of ligands with the protein, were retained in the binding site. The system was prepared using the Protein Preparation Wizard of the Maestro graphical user interface. The hydrogen atoms were added and pKa was calculated for protein residues using the PROPKA method at pH 7.4. Then, the protein-ligand complex was subjected to restrained minimization with convergence of heavy atoms to an RMSD of 0.3 Å using the OPLS3 force field. In accordance with our previous docking calculations,^{14,15} the third chain of the trimeric protein which is not involved in the considered binding site (that is chain B) was removed, simplifying the protein model. The final dimeric structure was used to generate the grid for docking calculations as already described.¹⁵

Docking calculations were performed using Glide (Grid-based Ligand Docking with Energetics) version 7.8, applying the flexible docking approach, and employing the extra precision (XP) scoring function with the OPLS3 force field.⁴³ The poses were analysed verifying the protein-ligand interactions. The distance between the oxygen atom of the aldehyde group of ligands and the nitrogen atom of Lys108(ϵ -NH₂) group was monitored, selecting compounds with distance values lower than 10 Å in all poses. For the selected compounds, the top-scored pose was chosen as starting structure to perform the subsequent covalent docking.

The covalent docking protocol CovDock available in the Schrödinger Suite Release 2018–1 (version 1.3)³⁷ was employed to generate binding poses of ligands while forcing the covalent bond between the aldehyde and the ϵ -NH₂ group of Lys108. Starting from conventional non-covalent poses, the docked ligand was confined to a grid box with center in the ligand centroid and automatic box size. A custom imine condensation reaction type was defined to select only aldehyde moieties as reactive group of ligands. Additional setups include docking mode in pose prediction, affinity score calculation using Glide, and 10 output poses per ligand.

The poses obtained were examined in detail, verifying mainly the position of the sugar moiety, its conformation as well as its interactions with the protein. To confirm that the fucose binding mode is consistent with available crystal structures, the presence of the following hydrogen bond interactions was monitored: Fuc-OH-2 with Arg111 side chain; Fuc-OH-3 with Thr74 side chain; and Fuc-OH-4 with Arg85 side chain. We applied the following geometric criteria for protein-ligand hydrogen bonds: the distance between the donor hydrogen atom and acceptor atoms should be ≤ 2.5 Å (D—H \cdots A); the donor angle between the donor-hydrogen-acceptor atoms should be $\geq 120^\circ$ (D—H \cdots A); and the acceptor angle between the hydrogen-acceptor-bonded atom atoms should be $\geq 90^\circ$ (H \cdots A—X). In addition, the formation of other non-covalent interactions was monitored, such as the presence of an intramolecular hydrogen bond involving the nitrogen atom of formed imine and the *ortho*-hydroxyl group of the salicylaldehyde moiety.

4.2. Prediction of lysine pKa values

The pKa values of the Lys(ϵ -NH₂) groups in BC2L-C-*Nt* shown in Figure 2 were predicted with the Rosetta pKa protocol³² available on the Rosetta Online Server That Includes Everyone (ROSIE),⁴⁴ giving flexibility to the side chain of all residues within 5 Å from the target residue and considering different crystal structures of BC2L-C-*Nt* in complex with synthetic ligands, oligosaccharides and in the *apo* form (PDB ID: 7BFY, 2WQ4, 7OLU, 7OLW, 8BRO, 6TIG and 6TID).

4.3. General procedures for synthesis

All reagents and anhydrous solvents were purchased from Merck, aber or Carbosynth. THF was dried over sodium/benzophenone and freshly distilled, while Et₃N was dried over calcium hydride. MgCl₂ and paraformaldehyde were dried over P₂O₅ prior to use. Et₃N and CH₃CN were freshly distilled. Reactions were monitored by analytical TLC performed on Silica Gel 60 F254 plates (Merck) and TLC Silica gel 60 RP-18 F254s (Merck) and were analysed with UV detection (254 and 365nm) and/or staining with ammonium molybdate acid solution, potassium permanganate alkaline solution, and ninhydrin stain. Purification by flash column chromatography was performed using silica gel 60 (40–63 μm, Merck), and automated flash chromatography was performed with a Biotage Isolera Prime system, and SNAP ULTRA cartridges were employed. HPLC purifications were performed with a Dionex Ultimate 3000 equipped with Dionex RS Variable Wavelength Detector (column: Atlantis Prep T3 OBDTM 5μm 19 x 100mm, flow 15 mL min⁻¹ unless stated otherwise), and was used at a flow rate of 10.0 mL/min. NMR experiments were conducted on a Bruker AVANCE 400 MHz instrument at 298 K. The ¹³C-NMR spectra are Attached Proton Test J-modulated spin-echo (APT). MS spectra were recorded on a Thermo Fischer LCQ apparatus (ESI ionization); high resolution mass spectra (HRMS) were acquired on Synapt G2-Si QToF mass spectrometer (Waters)—Zspray ESI-probe (Waters) for electrospray ionization. All compounds were purified by RP-HPLC. The H-type 1 trisaccharide **23** was purchased from Elicityl S.A.. 4-(*t*-butyloxycarbonylaminoethyl)benzoic acid **7** was purchased from aber; 3-cyanobenzoic acid **25**, *p*-hydroxybenzoic acid methyl ester **9**, methyl 4-hydroxyphenylacetate **10** were purchased from Merck. 2,3,4,6-Tetra-*O*-acetyl-β-D-glucosyl azide **34** was prepared as described in literature.⁴⁵ The synthesis of intermediates azide **6**, acid **17**, negative controls **21**, **22** and **A12** (Table SI-1) are described in Supporting Information. The purity of all the final compounds was confirmed to be ≥ 95% by HPLC (H₂O + 0.1% TFA/CH₃CN + 0.1% TFA: 0-26 min, 0-100%; 26-36 min, 100%). HPLC traces for ligands **2-5**, **21** and **22** are reported in Supporting Information (Section 9).

4.4. General procedures for the synthesis of **13** and **14**

Skattebøl formylation³⁸: To a suspension of paraformaldehyde (6.8 mol equiv) and anhydrous MgCl₂ (3 mol equiv) in dry CH₃CN under N₂ atmosphere, the phenol **9** or **10** was added as a solution in dry CH₃CN (final conc. = 0.2 or 0.3 M). The mixture was stirred 10 min. and then dry Et₃N (3.5 or 4 mol equiv) was added. The reaction mixture was stirred at reflux until the phenol was converted completely (4.5 h). The mixture was cooled to room temperature and quenched with 1 N HCl (until pH=2) and extracted with Et₂O (x4). The combined organic layers were washed with brine (x2), dried over anhydrous Na₂SO₄ and

concentrated under vacuum. The crude product was purified by flash chromatography using *n*-Hex/AcOEt as eluents.

The resulting phenol **11** or **12** (1 mol equiv) was dissolved in anhydrous CH₂Cl₂ (0.5 M) under nitrogen, and *i*Pr₂EtN (1.5 mol equiv) was added. The mixture was stirred for 5 min. at room temperature and then cooled to 0°C. Methoxymethyl chloride (MOMCl, 1.5 mol equiv) was added dropwise, and the reaction mixture was stirred 10 min. at 0°C and then 4 h at room temperature. The mixture was diluted with CH₂Cl₂ and washed with a NaHCO₃ sat. solution (x1) and H₂O (x2). The organic phase was dried (Na₂SO₄) and concentrated under reduced pressure, and the crude product was purified by flash chromatography on silica gel.

The resulting methyl ester (1 mol equiv) was dissolved in a 3:1 mixture of THF/H₂O (conc. = 0.25 M), lithium hydroxide monohydrate (LiOH·H₂O, 3 mol equiv) was added and the mixture was stirred at room temperature until complete deprotection (3h). 1 N HCl was added (until pH=2) and the solution was extracted with AcOEt (x3). The combined organic layers were dried over Na₂SO₄ and concentrated under reduced pressure affording the acid product, used in subsequent steps without further purification.

Methyl-3-formyl-4-hydroxybenzoate (11) - The product was obtained from methyl 4-hydroxybenzoate **9** (Et₃N 4.5 mol equiv, final (conc. = 0.3 M) using 4 mol equiv eq of Et₃N and the general procedure for Skattebøl formylation (reaction time: 16h). It was purified by flash chromatography on silica gel (*n*-Hex/AcOEt 9:1 to 8:2) affording the pure product as a yellow solid. Y = 51%. R_f (*n*-Hex/AcOEt 2:1) = 0.67. MS (ESI) calcd for C₉H₈O₄ [M - H]⁻ *m/z*: 179.16; found: 179.19. Characterization data in accordance with the literature.⁴⁶ ¹H NMR (400 MHz, CDCl₃) δ 11.39 (s, 1H, Ph-OH), 9.95 (s, 1H, COH), 8.32 (d, *J* = 2.2 Hz, 1H, Ph-H-2), 8.19 (dd, *J* = 8.8 Hz, *J* = 2.1 Hz, 1H, Ph-H-6), 7.04 (d, *J* = 8.8 Hz, 1H, Ph-H-5), 3.93 (s, 3H, OCH₃).

Formyl-4-(methoxymethoxy)benzoic acid (13) - The MOM-protection of compound **11** (0.70 mmol) was performed using the general procedure and afforded the intermediate *methyl 3-formyl-4-(methoxymethoxy)benzoate*, which was purified by flash chromatography on silica gel (*n*-Hex/AcOEt 8:2) obtaining the pure product as a yellow oil. Y = 95%. R_f (*n*-Hex/AcOEt 4:1) = 0.32. MS (ESI) calcd for C₁₁H₁₂O₅ [M + Na]⁺ *m/z*: 247.05; found: 247.26. Characterization data in accordance with the literature.⁴⁷ ¹H NMR (400 MHz, CDCl₃) δ 10.49 (s, 1H, COH), 8.51 (d, *J* = 2.1 Hz, 1H, Ph-H-2), 8.21 (dd, *J* = 8.8 Hz, *J* = 2.2 Hz, 1H, Ph-H-6), 7.28 (d, *J* = 8.9 Hz, 1H, Ph-H-5), 5.37 (s, 2H, OCH₂ MOM), 3.91 (s, 3H, OCH₃), 3.54 (s, 3H, OCH₃).

The intermediate *methyl 3-formyl-4-(methoxymethoxy)benzoate* was deprotected using the general procedure for methyl ester hydrolysis (156 mg, 0.57 mmol, 1 mol equiv), affording compound **13** as a

pale yellow foam. Y = 98%. Rf (*n*-Hex/AcOEt 1:1 + 0.1 % FA) = 0.20. MS (ESI) calcd for C₁₀H₁₀O₅ [M + Na]⁺ *m/z*: 233.05; found: 233.28. ¹H NMR (400 MHz, CDCl₃) δ 10.50 (s, 1H, COH), 8.60 (d, *J* = 2.3 Hz, 1H, Ph-H-2), 8.27 (dd, *J* = 8.8 Hz, *J* = 2.3 Hz, 1H, Ph-H-6), 7.32 (d, *J* = 8.8 Hz, 1H, Ph-H-5), 5.39 (s, 2H, OCH₂ MOM), 3.55 (s, 3H, OCH₃ MOM).

Methyl 2-(3-formyl-4-hydroxyphenyl)acetate (12) - The product was obtained from methyl 4-hydroxyphenylacetate **10** (conc. = 0.2 M) using 3.5 eq of Et₃N and the general procedure for Skattebøl formylation (reaction time: 4.5h). It was purified by flash chromatography on silica gel (*n*-Hex/AcOEt 7:3 to 6:4) affording the pure product as a yellowish oil. Y = 77%. Rf (*n*-Hex/AcOEt 3:1) = 0.26. MS (ESI) calcd for C₁₀H₁₀O₄ [M - H]⁻ *m/z*: 193.05; found: 193.31. Characterization data in accordance with the literature.⁴⁸ ¹H NMR (400 MHz, CDCl₃) δ 10.95 (s, 1H, Ph-OH), 9.88 (s, 1H, COH), 7.47 (d, *J* = 2.3 Hz, 1H, Ph-H-2), 7.44 (dd, *J* = 8.5 Hz, *J* = 2.3 Hz, 1H, Ph-H-6), 6.96 (d, *J* = 8.5 Hz, 1H, Ph-H-5), 3.71 (s, 3H, OCH₃), 3.62 (s, 2H, Ph-CH₂).

2-(3-formyl-4-(methoxymethoxy)phenyl)acetic acid (14) - The MOM-protection of compound **12** (0.94 mmol) was performed using the general procedure and afforded the intermediate *methyl 2-(3-formyl-4-(methoxymethoxy)phenyl)acetate*, which was purified by flash chromatography on silica gel (*n*-Hex/AcOEt 6:4) obtaining the pure product as a colourless oil. Y = 88%. Rf (*n*-Hex/AcOEt 6:4) = 0.51. ¹H NMR (400 MHz, CDCl₃) δ 10.48 (s, 1H, COH), 7.72 (d, *J* = 2.3 Hz, 1H, Ph-H-2), 7.46 (dd, *J* = 8.6 Hz, *J* = 2.4 Hz, 1H, Ph-H-6), 7.20 (d, *J* = 8.6 Hz, 1H, Ph-H-5), 5.29 (s, 2H, OCH₂ MOM), 3.69 (s, 3H, OCH₃), 3.60 (s, 2H, Ph-CH₂), 3.52 (s, 2H, OCH₃ MOM). The intermediate *2-(3-formyl-4-(methoxymethoxy)phenyl)acetate* (0.82 mmol) was deprotected using the general procedure for methyl ester hydrolysis, affording compound **14** as a yellowish foam. Y = 90%. Rf (CH₂Cl₂/MeOH 95:5) = 0.41. MS (ESI) calcd for C₁₁H₁₂O₅ [M + Na]⁺ *m/z*: 247.06 ; found: 247.33. ¹H NMR (400 MHz, CDCl₃) δ 10.48 (s, 1H, COH), 7.74 (d, *J* = 2.3 Hz, 1H, Ph-H-2), 7.46 (dd, *J* = 8.6 Hz, *J* = 2.4 Hz, 1H, Ph-H-6), 7.21 (d, *J* = 8.6 Hz, 1H, Ph-H-5), 5.30 (s, 2H, OCH₂ MOM), 3.64 (s, 2H, Ph-CH₂), 3.52 (s, 2H, OCH₃ MOM). ¹³C chemical shifts extrapolated from HSQC exp.: 136.8 (Ph-C-6), 129.1 (Ph-C-2), 115.4 (Ph-C-5), 94.6 (OCH₂ MOM), 56.4 (OCH₃ MOM), 39.4 (Ph-CH₂).

4.5. Synthesis of (4-(aminomethyl)benzamido)-2,3,4-tri-*O*-acetyl-β-*L*-fucopyranose (**8b**) -

Acid **7** (commercially available, 121 mg, 0.48 mmol, 1 eq) was suspended in anhydrous CH₂Cl₂ (4.8 mL) and EDC·HCl (101 mg, 0.53 mmol, 1.1 eq) was added, together with HOBt (72 mg, 0.53 mmol, 1.1 eq) and iPr₂EtN (185 μL, 1.06 mmol, 2.2 eq). The resulting solution was stirred at room temperature for 1 h under N₂ atmosphere. Meanwhile, in another reaction flask, the azide **6** (151 mg, 0.48 mmol, 1 eq) was dissolved in anhydrous CH₂Cl₂ (3 mL) and cooled to 0°C under N₂ atmosphere. A 1M solution of PMe₃

in toluene (0.72 mL, 1.5 eq) was slowly added, and the reaction mixture was stirred at room temperature for 30 min., verifying the reduction of the azide by TLC (*n*-Hex/AcOEt/1:1). Then, the activated acid solution was added to the iminophosphorane intermediate, and the final solution was stirred overnight at room temperature. After 18h, the mixture was diluted with CH₂Cl₂ and washed with a sat. solution of NH₄Cl (x2), a sat. aqueous solution of NaHCO₃ (x2) and brine. The organic layer was dried over anhydrous Na₂SO₄, filtered and concentrated to dryness. The product was purified by automatic flash chromatography (SFAR 10 g, *n*-Hex/AcOEt 7:3 to 5:5) to give the amide **8a** as a white foam. Y = 79%. R_f (*n*-Hex/AcOEt 1:1) = 0.34. MS (ESI) calcd for C₂₅H₃₄N₂O₁₀ [M + Na]⁺ *m/z*: 545.21; found: 545.83. ¹H NMR (400 MHz, CDCl₃) δ 7.71 (d, *J* = 8.2 Hz, 2H, Ph-H-2 + Ph-H-6), 7.33 (d, *J* = 8.1 Hz, 2H, Ph-H-3 + Ph-H-5), 7.05 (d, *J* = 8.7 Hz, 1H, NHCO), 5.39–5.28 (m, 2H, H-1 + H-4), 5.24–5.17 (m, 2H, H-2 + H-3), 4.94 (bs, 1H, NHBoc), 4.34 (s, 2H, Ph-CH₂), 3.99 (q, *J* = 6.3 Hz, 1H, H-5), 2.17 (s, 3H, OAc), 2.02 (s, 3H, OAc), 2.00 (s, 3H, OAc), 1.45 (s, 9H, Boc), 1.20 (d, *J* = 6.4 Hz, 3H, H-6). ¹³C chemical shifts extrapolated from HSQC exp.: 127.5 (Ph-C-2, Ph-C-6), 127.4 (Ph-C-3, Ph-C-5), 79.0 (C-1), 71.1 (C-3), 70.8 (C-5), 70.4 (C-4), 68.6 (C-2), 44.1 (Ph-C), 28.3 (Boc), 20.6–20.5 (OAc), 16.1 (C-6).

8a was dissolved in CH₂Cl₂ (conc. = 0.01 M), and TFA was added (CH₂Cl₂ /TFA 9:1). The mixture was stirred at room temperature until complete removal of the Boc group was observed by TLC (9:1 CH₂Cl₂/MeOH 9:1). The reaction mixture was concentrated under reduced pressure and TFA was removed by co-evaporation with MeOH. The residue was dissolved in CH₂Cl₂ and washed with a NaHCO₃ sat. solution. The aqueous solution was extracted with CH₂Cl₂ (x3), and the combined organic layers were dried over anhydrous Na₂SO₄ and concentrated under vacuum to afford **8b** as a white foam. Y = 97%. R_f (CH₂Cl₂/MeOH 95:5) = 0.30. MS (ESI) calcd for C₂₀H₂₆N₂O₈ [M + H]⁺ *m/z*: 423.18; found: 423.26. ¹H NMR (400 MHz, CDCl₃) δ 7.74 (d, *J* = 8.2 Hz, 2H, Ph-H-2 + Ph-H-6), 7.39 (d, *J* = 8.2 Hz, 2H, Ph-H-3 + Ph-H-5), 7.06 (d, *J* = 8.9 Hz, 1H, NHCO), 5.40–5.32 (m, 2H, H-1 + H-4), 5.25–5.18 (m, 2H, H-2 + H-3), 4.02 (q, *J* = 6.4 Hz, 1H, H-5), 3.93 (s, 2H, Ph-CH₂), 2.18 (s, 3H, OAc), 2.03 (s, 3H, OAc), 2.02 (s, 3H, OAc), 1.22 (d, *J* = 6.4 Hz, 3H, H-6). ¹³C chemical shifts extrapolated from HSQC exp.: 127.5 (Ph-C-2, Ph-C-6), 127.3 (Ph-C-3, Ph-C-5), 79.1 (C-1), 71.2 (C-3), 70.9 (C-5), 70.5 (C-4), 68.7 (C-2), 46.0 (Ph-CH₂), 20.8–20.6 (OAc), 16.1 (C-6).

4.6. Synthesis of (3-(aminomethyl)benzamido)-2,3,4-tri-*O*-acetyl-β-*L*-fucopyranose (**18b**) –

Acid **17** (100 mg, 0.4 mmol, 1 eq.) was suspended in anhydrous CH₂Cl₂ (4 mL) and EDC·HCl (85 mg, 0.44 mmol, 1.1 eq) was added, together with HOBt (59 mg, 0.44 mmol, 1.1 eq) and *i*Pr₂EtN (154 μL, 0.88 mmol, 2.2 eq). The resulting solution was stirred at room temperature for 1 h under N₂ atmosphere. Meanwhile, in another reaction flask, the azide **6** (126 mg, 0.4 mmol, 1 eq) was dissolved in anhydrous CH₂Cl₂ (2.5 mL) and cooled to 0°C under N₂ atmosphere. A 1M solution of PMe₃ in toluene (0.6 mL, 1.5

eq) was slowly added, and the reaction mixture was stirred at room temperature for 30 min., verifying the reduction of the azide by TLC (AcOEt/Hex 1:1). Then, the activated acid solution was added to the iminophosphorane intermediate, and the final solution was stirred overnight at room temperature. After 18h, the mixture was diluted with CH₂Cl₂ and washed with a sat. solution of NH₄Cl (x2), a sat. aqueous solution of NaHCO₃ (x2) and brine. The organic layer was dried over anhydrous Na₂SO₄, filtered and concentrated to dryness. The product was purified by flash chromatography on silica gel (n-Hex/AcOEt 6:4 to 4:6) to give the product **18a** as a white foam. Y = 79%. Rf (n-Hex/AcOEt 1:1) = 0.24. MS (ESI) calcd for C₂₅H₃₄N₂O₁₀ [M - H]⁻ m/z: 521.21; found: 521.85. ¹H NMR (400 MHz, CDCl₃) δ 7.73 (s, 2H, Ph-H-2), 7.60 (d, *J* = 7.6 Hz, 1H, Ph-H-6), 7.47 (d, *J* = 7.5 Hz, 1H, Ph-H-4), 7.41 (t, *J* = 7.5 Hz, 1H, Ph-H-5), 7.03 (d, *J* = 8.6 Hz, 1H, NHCO), 5.40-5.36 (m, 2H, H-1 + H-4), 5.25-5.18 (m, 2H, H-2 + H-3), 4.90 (bs, 1H, NHBoc), 4.37 (d, *J* = 5.9 Hz, 2H, Ph-CH₂), 4.01 (q, *J* = 6.3 Hz, 1H, H-5), 2.19 (s, 3H, OAc), 2.04 (s, 3H, OAc), 2.02 (s, 3H, OAc), 1.47 (s, 9H, Boc), 1.22 (d, *J* = 6.4 Hz, 3H, H-6). ¹³C chemical shifts extrapolated from HSQC exp.: 131.25 (Ph-C-4), 128.9 (Ph-C-5), 126.4 (Ph-C-2), 125.7 (Ph-C-6), 78.9 (C-1), 71.2 (C-3), 70.9 (C-5), 70.4 (C-4), 68.6 (C-2), 44.2 (Ph-C), 28.6 (Boc), 20.6-20.5 (OAc), 16.0 (C-6).

18a was dissolved in CH₂Cl₂ (conc. = 0.01 M), and TFA was added (CH₂Cl₂ /TFA 9:1). The mixture was stirred at room temperature until complete removal of the Boc group observed in TLC (9:1 CH₂Cl₂/MeOH). The reaction mixture was concentrated under reduced pressure and the excess of TFA was removed by co-evaporation with MeOH. The residue was dissolved in CH₂Cl₂ and washed with a NaHCO₃ sat. solution. The aqueous solution was extracted with CH₂Cl₂ (x3), and the combined organic layers were dried over anhydrous Na₂SO₄ and concentrated in vacuo to afford **18b** as a white foam. Y = 95%. Rf (CH₂Cl₂/MeOH 95:5) = 0.24. MS (ESI) calcd for C₂₀H₂₆N₂O₈ [M + H]⁺ m/z: 423.18; found: 423.37. ¹H NMR (400 MHz, CDCl₃) δ 7.77 (s, 2H, Ph-H-2), 7.61 (d, *J* = 7.7 Hz, 1H, Ph-H-6), 7.49 (d, *J* = 7.7 Hz, 1H, Ph-H-4), 7.41 (t, *J* = 7.6 Hz, 1H, Ph-H-5), 7.05 (d, *J* = 8.9 Hz, 1H, NHCO), 5.42-5.33 (m, 2H, H-1 + H-4), 5.26-5.18 (m, 2H, H-2 + H-3), 4.02 (q, *J* = 6.2 Hz, 1H, H-5), 3.93 (s, 2H, Ph-CH₂), 2.19 (s, 3H, OAc), 2.04 (s, 3H, OAc), 2.02 (s, 3H, OAc), 1.22 (d, *J* = 6.4 Hz, 3H, H-6). ¹³C chemical shifts extrapolated from HSQC exp.: 131.2 (Ph-C-4), 129.0 (Ph-C-5), 126.2 (Ph-C-2), 125.5 (Ph-C-5), 79.1 (C-1), 71.3 (C-3), 71.0 (C-5), 70.6 (C-4), 68.8 (C-2), 46.2 (Ph-CH₂), 21.0-20.8 (OAc), 16.3 (C-6).

4.7. General procedures for the synthesis of ligands 2-5

General procedure for coupling: The carboxylic acid (**13** or **14** 1 eq) was dissolved in anhydrous CH₂Cl₂ (conc. = 0.5 M), and then NHS (1.1 eq) and EDC·HCl (1.1 eq) were added. The mixture was stirred at room temperature for 8 h. In another reaction flask, to a solution of the amine (**8b** or **18b**, 1 eq) in

anhydrous CH₂Cl₂ (1 M), iPr₂EtN (3 eq) was added, and the mixture was combined with the solution of the activated acid. The resulting reaction mixture was stirred at room temperature overnight. After 20 h, the mixture was diluted with CH₂Cl₂ and washed with sat. solution of NH₄Cl (x2), sat. aqueous solution of NaHCO₃ (x2) and brine. The organic phase was dried over anhydrous Na₂SO₄, concentrated under reduced pressure, and the crude product was purified by column chromatography using *n*-Hex/Acetone as eluents.

General procedure for protecting groups removal⁴⁹: The acetylated, MOM-protected coupling product (1 eq) was dissolved in a mixture of 96%-ethanol and CHCl₃, and conc. HCl (10 eq) was added (EtOH/CHCl₃/HCl 4:1:1). The reaction mixture was stirred at 40°C until complete deprotection, as verified by TLC (CH₂Cl₂/MeOH 95:5). The solvents were removed under reduced pressure, and the residue was subjected to flash column chromatography.

(4-((3-formyl-4-hydroxybenzamido)methyl)benzamido)- β -L-fucopyranose (**2**) - Coupling of **8b** (236 mg, 0.56 mmol, 1 eq) and acid **13** (117 mg, 0.56 mmol, 1 eq) using the general procedure for coupling afforded the protected intermediate (4-((3-formyl-4-(methoxymethoxy)benzamido)methyl)benzamido)-2,3,4-tri-*O*-acetyl- β -L-fucopyranose **15**, which was purified by flash chromatography on silica gel (*n*-Hex/Acetone 2:1 to 1.5:1) to a white foam. Y = 57%. R_f (*n*-Hex/Acetone 1:1) = 0.40. MS (ESI) calcd for C₃₀H₃₄N₂O₁₂ [M - H]⁻ m/z: 613.20; found: 613.18. ¹H NMR (400 MHz, CDCl₃) δ 10.37 (s, 1H, COH), 8.17 (d, *J* = 2.3 Hz, 1H, Ph(SA)-H-2), 8.10 (dd, *J* = 9.0 Hz, *J* = 2.4 Hz, 1H, Ph(SA)-H-6), 7.62 (d, *J* = 8.2 Hz, 2H, Ph-H-2 + Ph-H-6), 7.29 (d, *J* = 8.0 Hz, 2H, Ph-H-3 + Ph-H-5), 7.22 (d, *J* = 8.3 Hz, 1H, Ph(SA)-H-5), 7.15 – 7.03 (m, 2H, NHCO + Fuc-NHCO), 5.38 – 5.20 (m, 4H, H-1 + H-4 + OCH₂ MOM), 5.19 – 5.08 (m, 2H, H-2 + H-3), 4.67 – 4.52 (m, 2H, Ph-CH₂), 3.94 (q, *J* = 6.3 Hz, 1H, H-5), 3.43 (s, 3H, OCH₃ MOM), 2.10 (s, 3H, OAc), 1.94 (s, 6H, OAc), 1.13 (d, *J* = 6.4 Hz, 3H, H-6). ¹³C chemical shifts extrapolated from HSQC exp.: 136.3 (Ph(SA)-C-6), 127.9 (Ph-C-2, Ph-C-6), 127.8 (Ph-C-3, Ph-C-5), 126.6 (Ph(SA)-C-2), 115.3 (Ph(SA)-C-5), 95.4 (OCH₂ MOM), 79.0 (C-1), 71.6 (C-3), 70.8 (C-5), 70.7 (C-4), 68.8 (C-2), 56.8 (OCH₃ MOM), 44.0 (Ph-CH₂), 20.7 (OAc), 16.1 (C-6).

Deprotection of **15** according to the general procedure for protecting group removal (80 mg, 0.13 mmol, 1 eq) resulted in **2**, which was purified by flash chromatography on silica gel (CH₃Cl/MeOH 85:15), affording the pure product as a white foam. Y = 57%. R_f (CH₃Cl/MeOH 8:2) = 0.38. Samples for interaction studies were further purified by semi-preparative RP-HPLC (H₂O + 0.1% TFA/CH₃CN) with gradient: 0-1 min, 10%; 1-10 min, 10-45%; 10-13 min, 45-100%. t_r = 6.22 min. HRMS (ESI) calcd for C₂₂H₂₃N₂O₈ [M+H]⁺ m/z: 443.1454; found 443.1454. ¹H NMR (400 MHz, DMSO d₆) δ 11.25 (s, 1H, Ph(SA)-OH), 10.32 (s, 1H, COH), 9.11 (t, *J* = 5.9 Hz, 1H, NHCO), 8.75 (d, *J* = 8.8 Hz, 1H, Fuc-NHCO), 8.27 (d, *J* = 2.3 Hz, 1H, Ph(SA)-H-2), 8.06 (dd, *J* = 8.7 Hz, *J* = 2.4 Hz, 1H, Ph(SA)-H-6), 7.89 (d, *J* = 8.3

Hz, 2H, Ph-H-2 + Ph-H-6), 7.38 (d, $J = 8.3$ Hz, 2H, Ph-H-3 + Ph-H-5), 7.08 (d, $J = 8.7$ Hz, 1H, Ph(SA)-H-5), 4.90 (t, $J = 8.9$ Hz, 1H, H-1), 4.72 (m, 2H, OH), 4.52 (d, $J = 5.5$ Hz, 2H, Ph-CH₂), 4.46 (d, $J = 3.9$ Hz, 1H, OH), 3.65 – 3.57 (m, 2H, H-2 + H-5), 3.49 (t, $J = 3.3$ Hz, 1H, H-4), 3.45 – 3.35 (m, 1H, H-3), 1.12 (d, $J = 6.4$ Hz, 3H, H-6). ¹³C NMR (100 MHz, DMSO d₆) δ 191.1 (COH), 166.9 (NHCO), 165.6 (NHCO), 163.5 (Ar quat.), 143.6 (Ar quat.), 135.7 (Ph(SA)-C-6), 133.2 (Ar quat.), 128.6 (Ph(SA)-C-2), 128.2 (Ph-C-2 + Ph-C-6), 127.3 (Ph-C-3 + Ph-C-5), 125.9 (Ar quat.), 122.3 (Ar quat.), 117.7 (Ph(SA)-C-5), 81.1 (C-1), 74.8 (C-3), 72.1 (C-5), 71.7 (C-4), 69.5 (C-2), 42.8 (Ph-CH₂), 17.2 (C-6).

(4-((2-(3-formyl-4-hydroxyphenyl)acetamido)methyl)benzamido)- β -L-fucopyranose (3) - Coupling of **8b** (124 mg, 0.29 mmol, 1 eq) with acid **14** (65 mg, 0.29 mmol, 1 eq) according to the general procedure for coupling afforded the intermediate (4-((2-(3-formyl-4-(methoxymethoxy)phenyl)acetamido)methyl)benzamido)-2,3,4-tri-O-acetyl- β -L-fucopyranose **16**, which was purified by flash chromatography on silica gel (*n*-Hex/Acetone, 7:3 to 5:5) to a white foam. Y = 52%. R_f (*n*-Hex/Acetone 1:1) = 0.31. MS (ESI) calcd for C₃₁H₃₆N₂O₁₂ [M + Na]⁺ m/z : 651.22; found: 651.74. ¹H NMR (400 MHz, CDCl₃) δ 10.48 (s, 1H, COH), 7.73-7.69 (m, 3H, Ph(SA)-H-2 + Ph-H-2 + Ph-H-6), 7.50 (dd, $J = 8.6$ Hz, $J = 2.4$ Hz, 1H, Ph(SA)-H-6), 7.28-7.22 (m, 3H, Ph(SA)-H-5 + Ph-H-3 + Ph-H-5), 7.03 (d, $J = 8.8$ Hz, 1H, Fuc-NHCO), 5.80 (t, $J = 5.6$ Hz, 1H, NHCO), 5.39-5.35 (m, 2H, H-1 + H-4), 5.30 (s, 2H, OCH₂ MOM) 5.24-5.18 (m, 2H, H-2 + H-3), 4.46 (d, $J = 5.9$ Hz, 2H, Ph-CH₂), 4.01 (q, $J = 6.4$ Hz, 1H, H-5), 3.60 (s, 2H, Ph(SA)-CH₂), 3.53 (s, 3H, OCH₃ MOM), 2.19 (s, 3H, OAc), 2.03 (s, 3H, OAc), 2.02 (s, 3H, OAc), 1.21 (d, $J = 6.4$ Hz, 3H, H-6). ¹³C chemical shifts extrapolated from HSQC exp.: 136.8 (Ph(SA)-C-6), 128.8 (Ph(SA)-C-2), 127.7 (Ph-C-2, Ph-C-6), 127.6 (Ph-C-3, Ph-C-5), 115.9 (Ph(SA)-C-5), 94.8 (OCH₂ MOM), 75.5 (C-1), 71.1 (C-3), 70.9 (C-5), 70.5 (C-4), 68.7 (C-2), 56.6 (OCH₃ MOM), 43.3 (Ph-CH₂), 42.5 (Ph(SA)-CH₂), 20.8-20.6 (OAc), 16.1 (C-6).

Deprotection of **16** according to the general procedure for protecting group removal (89.6 mg, 0.14 mmol, 1 eq) resulted in **3**, which was purified by automatic inverse phase flash chromatography (SFAR C18 D, H₂O/CH₃CN 9:1 to 5:5) to give the product as a white solid. Y = 43%. R_f (H₂O/CH₃CN 7:3) = 0.5. Samples for interaction studies were further purified by semi-preparative RP-HPLC (H₂O + 0.1% TFA/CH₃CN) with gradient: 0-1 min, 10-20%; 1-10 min, 20-50%, 10-13 min, 50-100%. tr = 6.33 min. $[\alpha]_D^{18} = 5.5$ (c 1, MeOH). HRMS (ESI) calcd for C₂₃H₂₆N₂O₈ [M-H]⁻ m/z : 457.1611; found 457.1609. ¹H NMR (400 MHz, DMSO d₆) δ 10.60 (s, 1H, Ph(SA)-OH), 10.26 (s, 1H, COH), 8.76 (d, $J = 8.8$ Hz, 1H, Fuc-NHCO), 8.60 (t, $J = 5.9$ Hz, 1H, NHCO), 7.85 (d, $J = 8.3$ Hz, 2H, Ph-H-2 + Ph-H-6), 7.57 (d, $J = 2.3$ Hz, 1H, Ph(SA)-H-2), 7.43 (dd, $J = 8.5$ Hz, $J = 2.3$ Hz, 1H, Ph(SA)-H-6), 7.28 (d, $J = 8.3$ Hz, 2H, Ph-H-3 + Ph-H-5), 6.95 (d, $J = 8.4$ Hz, 1H, Ph(SA)-H-5), 4.89 (t, $J = 8.9$ Hz, 1H, H-1), 4.31 (d, $J = 5.9$ Hz, 2H, Ph-CH₂), 3.63-3.56 (m, 2H, H-2 + H-5), 3.48 (d, $J = 3.0$ Hz, 1H, H-4), 3.45 (s, 2H, Ph(SA)-CH₂), 3.38

(dd, $J = 9.3$ Hz, $J = 3.2$ Hz, 1H, H-3), 1.11 (d, $J = 6.4$ Hz, 3H, H-6). ^{13}C NMR (100 MHz, DMSO d_6) δ 191.8 (COH), 170.8 (NHCO), 166.8 (NHCO), 160.0 (Ar quat), 143.4 (Ar quat.), 137.6 (Ph(SA)-C-6), 133.2 (Ar quat.), 129.5 (Ph(SA)-C-2), 128.2 (Ph-C-2 + Ph-C-6), 127.8 (Ar quat.), 127.2 (Ph-C-3 + Ph-C-5), 122.5 (Ar quat.), 117.6 (Ph(SA)-C-5), 81.1 (C-1), 74.8 (C-3), 72.1 (C-5), 71.7 (C-4), 69.5 (C-2), 42.3 (Ph-CH₂), 41.5 Ph(SA)-CH₂), 17.3 (C-6).

(3-((3-formyl-4-hydroxybenzamido)methyl)benzamido)- β -L-fucopyranose (**4**) - Coupling of **18b** (125 mg, 0.29 mmol, 1 eq) and **13** (61 mg, 0.29 mmol, 1 eq) according to the general procedure for coupling afforded the intermediate product (3-((3-formyl-4-(methoxymethoxy)benzamido)methyl)benzamido)-2,3,4-tri-O-acetyl- β -L-fucopyranose **19**, which was purified by flash chromatography on silica gel (*n*-Hex/acetone 2:1 to 1.5:19 to a white foam. Y = 45%. Rf (*n*-Hex/Acetone 1:1) = 0.44. MS (ESI) calcd for C₃₀H₃₄N₂O₁₂ [M - H]⁻ m/z: 613.20; found: 613.26. ^1H NMR (400 MHz, CDCl₃) δ 10.36 (s, 1H, COH), 8.18 (d, $J = 2.5$ Hz, 1H, Ph(SA)-H-2), 8.09 (dd, $J = 8.8$ Hz, $J = 2.2$ Hz, 1H, Ph(SA)-H-6), 7.68 (s, 1H, Ph-H-2), 7.53 (d, $J = 7.7$ Hz, 1H, Ph-H-6), 7.44 (d, $J = 7.5$ Hz, 1H, Ph-H-4), 7.30 (t, $J = 7.9$ Hz, 1H, Ph-H-5), 7.26-7.14 (m, 3H, Ph(SA)-H-5 + Fuc-NHCO + NHCO), 5.38-5.20 (m, 4H, H-1 + H-4 + OCH₂ MOM), 5.20 – 5.04 (m, 2H, H-2 + H-3), 4.56 (m, 2H, Ph-CH₂), 3.97-3.89 (m, 1H, H-5), 3.45 (s, 3H, OCH₃ MOM), 2.10 (s, 3H, OAc), 1.93 (s, 6H, OAc), 1.12 (d, $J = 6.3$ Hz, 1H, H-6). ^{13}C chemical shifts extrapolated from HSQC exp.: 136.2 (Ph(SA)-C-6), 132.6 (Ph-C-4), 129.4 (Ph-C-5), 127.1 (Ph-C-2 + Ph(SA)-C-2), 126.9 (Ph-C-6), 115.6 (Ph(SA)-C-5), 95.0 (OCH₂ MOM), 79.6 (C-1), 71.7 (C-3), 71.3 (C-5), 70.4 (C-4), 68.7 (C-2), 56.9 (OCH₃ MOM), 43.9 (Ph-CH₂), 21.0 (OAc), 20.9 (OAc), 16.4 (C-6).

Deprotection of **19** according to the general procedure for protecting group removal (58 mg, 0.094 mmol, 1 eq) resulted in **4**, which was purified by flash chromatography on silica gel (CH₃Cl/MeOH 85:15), affording the pure product as a white foam. Y = 60%. Rf (CH₃Cl/MeOH 8:2) = 0.31. Samples for the interaction studies were further purified by semi-preparative RP-HPLC (H₂O + 0.1% TFA/CH₃CN) with gradient: 0-1 min, 10%; 1-10 min, 10-45%; 10-13 min, 45-100%. tr = 6.50 min. HRMS (ESI) calcd for C₂₂H₂₃N₂O₈ [M+H]⁺ m/z: 443.1454; found 443.1456. ^1H NMR (400 MHz, DMSO) δ 11.24 (s, 1H, Ph(SA)-OH), 10.32 (s, 1H, COH), 9.09 (t, $J = 5.7$ Hz, 1H, NHCO), 8.80 (d, $J = 8.8$ Hz, 1H, Fuc-NHCO), 8.27 (d, $J = 2.3$ Hz, 1H, Ph(SA)-H-2), 8.06 (dd, $J = 8.7$, 2.4 Hz, 1H, Ph(SA)-H-6), 7.87 (s, 1H, Ph-H-2), 7.81 (d, $J = 7.6$ Hz, 1H, Ph-H-6), 7.47 (d, $J = 7.8$ Hz, 1H, Ph-H-4), 7.41 (t, $J = 7.9$ Hz, 1H, Ph-H-4), 7.07 (d, $J = 8.7$ Hz, 1H, Ph(SA)-H-5), 4.90 (t, $J = 8.9$ Hz, 1H, H-1), 4.72 (m, 2H, OH), 4.50 (d, $J = 5.9$ Hz, 2H, Ph-CH₂), 4.45 (d, $J = 3.6$ Hz, 1H, OH), 3.66-3.56 (m, 2H, H-2 + H-5), 3.52-3.47 (m, 1H, H-4), 3.43 – 3.35 (m, 1H, H-3), 1.12 (d, $J = 6.4$ Hz, 3H, H-6). ^{13}C NMR (100 MHz, DMSO d_6) δ 191.1 (COH), 167.1 (NHCO), 165.5 (NHCO), 163.4 (Ar quat), 140.2 (Ar quat.), 135.7 (Ph(SA)-C-6), 134.7 (Ar quat.), 130.7 (Ph-C-4), 128.7 (Ph(SA)-C-2), 128.6 (Ph-C-5), 127.3 (Ph-C-2), 126.4 (Ph-C-6), 125.9 (Ar quat.), 122.3

(Ar quat.), 117.7 (Ph(SA)-C-5), 81.0 (C-1), 74.8 (C-3), 72.1 (C-5), 71.7 (C-4), 69.5 (C-2), 43.0 (Ph-CH₂), 17.2 (C-6).

(3-((2-(3-formyl-4-hydroxyphenyl)acetamido)methyl)benzamido)- β -L-fucopyranose (**5**) – Coupling of **18b** (120 mg, 0.28 mmol, 1 eq) with acid **14** (62.8 mg, 0.28 mmol, 1 eq) according to the general procedure for coupling afforded the intermediate product (3-((2-(3-formyl-4-(methoxymethoxy)phenyl)acetamido)methyl)benzamido)-2,3,4-tri-O-acetyl- β -L-fucopyranose **20**, which was purified by flash chromatography on silica gel (*n*-Hex/Acetate, 7:3 to 5:5) to a white solid. Y = 64%. Rf (*n*-Hex/Acetone 1:1) = 0.30. MS (ESI) calcd for C₃₁H₃₆N₂O₁₂ [M + Na]⁺ *m/z*: 651.22; found: 652.07. ¹H NMR (400 MHz, CDCl₃) δ 10.48 (s, 1H, COH), 7.73 (d, 1H, *J* = 2.4 Hz, Ph(SA)-H-2), 7.64-7.61 (m, 2H, Ph-H-2 + Ph-H-6), 7.51 (dd, *J* = 8.6 Hz, *J* = 2.4 Hz, 1H, Ph(SA)-H-6), 7.40-7.37 (m, 2H, Ph-H-4 + Ph-H-5), 7.23 (d, *J* = 8.6 Hz, 1H, Ph(SA)-H-5), 7.07 (d, *J* = 8.8 Hz, 1H, Fuc-NHCO), 5.79 (t, *J* = 5.7 Hz, 1H, NHCO), 5.39-5.32 (m, 2H, H-1 + H-4), 5.30 (s, 2H, OCH₂ MOM) 5.23-5.18 (m, 2H, H-2 + H-3), 4.46 (d, *J* = 5.9 Hz, 2H, Ph-CH₂), 4.01 (q, *J* = 6.4 Hz, 1H, H-5), 3.62 (s, 2H, Ph(SA)-CH₂), 3.52 (s, 3H, OCH₃ MOM), 2.19 (s, 3H, OAc), 2.05 (s, 3H, OAc), 2.02 (s, 3H, OAc), 1.21 (d, *J* = 6.4 Hz, 3H, H-6). ¹³C chemical shifts extrapolated from HSQC exp.: 136.9 (Ph(SA)-C-6), 131.5 (Ph-C-4), 129.2 (Ph-C-5), 128.9 (Ph(SA)-C-2), 126.4 (Ph-C-2), 126.1 (Ph-C-6), 115.8 (Ph(SA)-C-5), 94.7 (OCH₂ MOM), 79.1 (C-1), 71.2 (C-3), 70.9 (C-5), 70.4 (C-4), 68.7 (C-2), 56.6 (OCH₃ MOM), 43.3 (Ph-CH₂), 42.5 (Ph(SA)-CH₂), 20.9-20.6 (OAc), 16.1 (C-6).

Deprotection of **20** (74 mg, 0.12 mmol, 1 eq) according to the general procedure for protecting group removal resulted in **5**, which was purified by automatic inverse phase flash chromatography (SFAR C18 D, from 100% H₂O to H₂O/MeOH 1:1) to give the product as a white solid. Y = 46%. Rf (H₂O/MeOH 1:1) = 0.6. Samples for interaction studies were further purified by semi-preparative RP-HPLC (H₂O + 0.1% TFA/CH₃CN) with gradient: 0-1 min, 10-20%; 1-10 min, 20-50%, 10-13 min, 50-100%. *t*_r = 6.43 min. HRMS (ESI) calcd for C₂₃H₂₆N₂O₈ [M + Na]⁺ *m/z*: 481.1587; found 481.1587. ¹H NMR (400 MHz, DMSO *d*₆) δ 10.60 (s, 1H, Ph(SA)-OH), 10.24 (s, 1H, COH), 8.79 (d, *J* = 8.8 Hz, 1H, Fuc-NHCO), 8.57 (t, *J* = 5.8 Hz, 1H, NHCO), 7.81-7.78 (m, 2H, Ph-H-2 + Ph-H-6), 7.56 (d, *J* = 2.2 Hz, 1H, Ph(SA)-H-2), 7.42 (dd, *J* = 8.4 Hz, *J* = 2.3 Hz, 1H, Ph(SA)-H-6), 7.39-7.37 (m, 2H, Ph-H-4 + Ph-H-5), 6.94 (d, *J* = 8.5 Hz, 1H, Ph(SA)-H-5), 4.90 (t, *J* = 8.9 Hz, 1H, H-1), 4.30 (d, *J* = 5.6 Hz, 2H, Ph-CH₂), 3.64-3.57 (m, 2H, H-2 + H-5), 3.48 (d, *J* = 2.8 Hz, 1H, H-4), 3.44 (s, 2H, Ph(SA)-CH₂), 3.38 (H-3, under the H₂O peak, chemical shift was extrapolated from COSY and HSQC exp.), 1.11 (d, *J* = 6.4 Hz, 3H, H-6). ¹³C NMR (100 MHz, DMSO *d*₆) δ 191.9 (COH), 170.6 (NHCO), 167.1 (NHCO), 159.9 (Ar quat), 139.9 (Ar quat.), 137.7 (Ph(SA)-C-6), 134.8 (Ar quat.), 130.6 (Ph-C-4), 129.6 (Ph(SA)-C-2), 128.6 (Ph-C-5), 127.8 (Ar

quat.), 127.3 (Ph-C-2), 126.5 (Ph-C-6), 122.4 (Ar quat.), 117.6 (Ph(SA)-C-5), 81.1 (C-1), 74.8 (C-3), 72.1 (C-5), 71.7 (C-4), 69.4 (C-2), 42.6 (Ph-CH₂), 41.5 Ph(SA)-CH₂, 17.3 (C-6).

4.8. Protein Sources for the Biophysical Studies

BC2L-C-*Nt* protein was expressed and purified in recombinant form as described previously^{13,50} and used for SPR and MALDI-MS experiments. For the proteolysis and LC-MS experiments the commercially available protein (FUJIFILM Wako Pure Chemical Corporation) was used.

4.9. SPR competition assays

Experiments were performed on a BIACORE X100 instrument (GE Healthcare) at 25 °C in running buffer 25 mM Hepes pH 8.0, 150 mM NaCl, 0.05% Tween 20, and 5 or 6.5% DMSO. Competition experiments were conducted using a fucosylated chip prepared using commercially available biotinylated L-fucose (20% mol of fucose and 5% mol of biotin, GlycoNZ) immobilized over a streptavidin sensor chip (SA, Cytiva) according to manufacturer. To establish the appropriate protein concentration for competition experiments, the apparent K_d of BC2L-C_{*Nt*} for the chip was determined (Figure SI-4). Competition experiments were performed with decreasing concentrations of ligands from 2000 μM to 15.625 μM or 12.33 μM. The samples were prepared mixing the ligand and protein (40 μM) in the running buffer and were incubated at room temperature for 2 h before being injected over the fucosylated chip performing multi-cycle affinity studies. The flow rate was set at 20 μL/min, with an association and dissociation time set to 200 s and 100 s respectively. Surface regeneration was performed after each analyte association/dissociation for 100 s injecting 10 mM L-fucose solution in the running buffer with a flow rate of 20 μL/min. Duplicates were performed for all ligands. Correction of the signal due to DMSO was performed constructing a 4-point solvent correction curve, using four solutions of the running buffer with different percentages of DMSO (from 4 to 10%). The final sensorgrams were obtained subtracting the reference channel 1 (no immobilized fucose) and the blank injection (running buffer without ligand and protein) and are reported as Supporting Information. IC₅₀ values were estimated from the inhibition curves using the online tool: “Quest Graph™ IC₅₀ Calculator” (AAT Bioquest, Inc., <https://www.aatbio.com/tools/ic50-calculator>) and are in agreement with those obtained with GraphPad Prism. Sensorgrams and inhibition curves are reported in Supporting information (Figures SI-5 and SI-6, respectively).

4.10. MALDI-TOF Mass analysis

Preliminary mass experiments at high ligand:protein ratio were performed using a Bruker autoflex speed instrument, equipped with a matrix-assisted laser desorption/ionization (MALDI) ionization source and a

TOF detector. Samples containing the protein with the ligand (ligand:protein 200:1, Figure 6 and Figures SI-7 to SI-9, SI-11 and SI-12) in buffer (25 mM Hepes pH 8.0 + 150 mM NaCl) were incubated at room temperature for 24 h, and then diluted with MilliQ water until a final concentration of protein of 25 μ M before mass analysis. The DHB/TA30 matrix was used (50mg/ml solution of DHB in TA30, TA30 = H₂O/Acetonitrile/TFA 70:30:0.1%).

Additional mass experiments were performed at 10:1 ligand:protein ratio (Figure 7 and Figure SI-10), using a MALDI TOF-TOF AutoflexIII Mass Spectrometer (Bruker Daltonics), equipped with the flexControl V. 3.0 & flexAnalysis V.3.0 software. The spectrometer calibration was performed using the protein calibration standard I mix (Bruker Daltonics), and considering a range between 3000 and 25000 Da. The “dried droplet” sample preparation method was employed; 1 μ l of a mixture of sinapinic acid (saturated in CH₃CN /0.1 % TFA=1/2) and analyte solution (1:1) was deposited onto the target plate. The resulting droplets were dried at room temperature. The acquisition parameters were the following: linear detector mode; positive voltage polarity; laser repetition rate at 200 Hz; 5000 shots per sample. Samples were prepared as above.

4.11. LC-MS analysis of BC2L-C-Nt:2 complex after NaBH₄ reduction and Trypsin digestion

The protein BC2L-C-Nt used in these experiments was purchased from FUJIFILM Wako Pure Chemical Corporation. Its full sequence is reported below (Lys108 underlined):⁵¹

PLLSASIVSAPVVTSETYVDIPGLYLDVAKAGIRDGKLQVILNVPTPYATGNNFPGIYFAIATNQGVVADGCFTYSSKVPESTGRMPFTLVATIDVGSVTFVKGQWKSVRGSAMHIDSYASLSAIWGTAAPSSQGSGNQGAETGGTGAGNIGG

To samples containing the protein (1.7 mg/mL) alone or mixed with ligand **2** (protein:ligand = 1:30) in 0.1X PBS pH 7.4 buffer, a solution of NaBH₄ in 10 mM NaOH was added (final NaBH₄ concentration: 1 mM) (adapted protocol).⁵² All samples were treated as following: i) reduction: with 1,4-dithiothreitol DTT 100 mM, at 55°C for 30 min. under stirring; ii) alkylation: with iodoacetamide IAA 150 mM, for 20 min. with no light, at room temperature; iii) Digestion: with Trypsin (0.10 μ g/ μ L) in Ambic 50 mM, incubating at 37°C overnight. Then, 0.5 μ L di TFA 100% was added to stop the reaction.

All samples were analysed at UNITECH OMICs (University of Milano, Italy) using: Dionex Ultimate 3000 nano-LC system (Sunnyvale CA, USA) connected to Orbitrap Exploris™ 240™ Mass Spectrometer (Thermo Scientific, Bremen, Germany) equipped with nano electrospray ion source. Peptide mixtures were pre-concentrated onto a PepMap 100 – 0.3x5mm C18 (Thermo Scientific) and separated on EASY-Spray column ES902, 25 cm x 75 μ m ID packed with Thermo Scientific Acclaim PepMap RSLC C18, 3

μm , 100 Å using mobile phase A (0.1 % formic acid in water) and mobile phase B (0.1% formic acid in acetonitrile 20/80, v/v) at a flow rate of 0.300 $\mu\text{L}/\text{min}$. The temperature was set to 35°C and the sample were injected in triplicates. The sample injection volume is 4 μL .

One blank was run between samples to prevent sample carryover. MS spectra were collected over an m/z range of 200 – 1100 Da at 60,000 resolutions (m/z 200), operating in the data dependent mode, cycle time 3 sec between masters scans. Higher-energy collisional dissociation (HCD) was performed with collision energy set at 35 eV. Polarity: positive.

Supporting Information

The Supporting Information is available free of charge at <http://pubs.acs.org>.

SI includes computational studies: computational workflow (Table SI-1-3), standard and covalent docking poses for ligands **3-5** (Figure SI-1) and compound **A12** (Figure SI-2); synthetic procedures for intermediate **6** and **17**, and for the negative controls **21**, **22** and **A12**; Thermal Shift Assays (Figure SI-3); Validation of SPR competition assays (Table SI-4); SPR competition assays – sensorgrams and inhibition curves (Figure SI-4-6); Mass MALDI-TOF spectra (Figure SI-7-12); LC-MS analysis (Figure SI-13 and Figure SI-14); NMR spectra of all new compounds (Section 8), HPLC traces for ligands **2-5**, **21** and **22** (Section 9). Molecular Formula Strings (CSV).

Primary data can be found in supporting information or can be requested to the authors

Corresponding author information

* Sarah Mazzotta

Università degli Studi di Milano, Dipartimento di Chimica, 20133 Milano, Italy

[orcid.org/ 0000-0003-0029-7003](https://orcid.org/0000-0003-0029-7003)

Email: sarah.mazzotta@unimi.it

* Laura Belvisi

Università degli Studi di Milano, Dipartimento di Chimica, 20133 Milano, Italy

[orcid.org/ 0000-0002-3593-2970](https://orcid.org/0000-0002-3593-2970)

Email: laura.belvisi@unimi.it

* Annabelle Varrot

Univ. Grenoble Alpes, CNRS, CERMAV, 38000 Grenoble, France

orcid.org/0000-0001-6667-8162

Email: Annabelle.varrot@cermav.cnrs.fr

Acknowledgment

The authors would like to thank the COSPECT Unitech at the Università degli Studi di Milano and the OMICs Unitech, an advanced core facility at the Università degli Studi di Milano for mass spectrometry analyses. The authors would like to thank the synchrotron SOLEIL (Saint Aubin, France) for access to beamlines Proxima 1 and 2 (Proposal Numbers 20210859) and technical support for the macromolecular crystallography experiments. We acknowledge the support of ICMG UAR 2607 for access to the mass spectrometry platform for the initial MALDI measurements and the help of Méлина Bellon for the expression and purification of BC2L-C-*Nt* samples.

Funding Sources

This research was supported by NextGeneration EU-MUR PNRR Extended Partnership initiative on Emerging Infectious Diseases (Project no. PE00000007, INF-ACT) and by Università degli Studi di Milano (UNIMI GSA-IDEA project). The instrument used for mass spectrometry analyses at the OMICs Unitech was funded by Regione Lombardia, regional law n° 9/2020, resolution n° 3776/2020. This work has been partially supported by the National Centre for Scientific Research (CNRS) and the CDP Glyco@alps (ANR-15-IDEX-02).

Abbreviation used

DHB, 2,3-Dihydroxybenzoic acid; DTT, 1,4-dithiotreitolo; EDC, 1-ethyl-3-(3-dimethylaminopropyl)carbodiimide; HCD; higher-energy collisional dissociation; HOBt, hydroxybenzotriazole; HRMS, high resolution mass spectrometry; IAA, iodoacetamide; ITC, Isothermal Titration Calorimetry; MS, mass spectrometry; NHS, N-Hydroxysuccinimide; SPR, Surface Plasmon Resonance.

REFERENCES

- (1) Varela, M. F.; Stephen, J.; Lekshmi, M.; Ojha, M.; Wenzel, N.; Sanford, L. M.; Hernandez, A. J.; Parvathi, A.; Kumar, S. H. Bacterial Resistance to Antimicrobial Agents. *Antibiotics* **2021**, *10*, 593. <https://doi.org/10.3390/antibiotics10050593>.
- (2) Mancuso, G.; Midiri, A.; Gerace, E.; Biondo, C. Bacterial Antibiotic Resistance: The Most Critical Pathogens. *Pathogens* **2021**, *10*, 1310. <https://doi.org/10.3390/pathogens10101310>.
- (3) Chattoraj, S. S.; Murthy, R.; Ganesan, S.; Goldberg, J. B.; Zhao, Y.; Hershenson, M. B.; Sajjan, U. S. *Pseudomonas Aeruginosa* Alginate Promotes *Burkholderia Cenocepacia* Persistence in Cystic Fibrosis Transmembrane Conductance Regulator Knockout Mice. *Infect Immun* **2010**, *78* (3), 984–993. <https://doi.org/10.1128/IAI.01192-09>.
- (4) Somayaji, R.; Yau, Y. C. W.; Tullis, E.; LiPuma, J. J.; Ratjen, F.; Waters, V. Clinical Outcomes Associated with *Burkholderia Cepacia* Complex Infection in Patients with Cystic Fibrosis. *Ann. Am. Thorac. Soc.* **2020**, *17*, 1542–1548. <https://doi.org/10.1513/AnnalsATS.202003-204OC>.
- (5) Drevinek, P.; Mahenthiralingam, E. *Burkholderia Cenocepacia* in Cystic Fibrosis: Epidemiology and Molecular Mechanisms of Virulence. *Clin. Microbiol. Infect.* **2010**, *16*, 821–830. <https://doi.org/10.1111/j.1469-0691.2010.03237.x>.
- (6) O'Connor, A.; Jurado-Martín, I.; Mysior, M. M.; Manzira, A. L.; Drabinska, J.; Simpson, J. C.; Lucey, M.; Schaffer, K.; Berisio, R.; McClean, S. A Universal Stress Protein Upregulated by Hypoxia Has a Role in *Burkholderia Cenocepacia* Intramacrophage Survival: Implications for Chronic Infection in Cystic Fibrosis. *Microbiologyopen* **2023**, *12*, e1311. <https://doi.org/10.1002/mbo3.1311>.
- (7) Lameignere, E.; Malinovská, L.; Sláviková, M.; Duchaud, E.; Mitchell, E. P.; Varrot, A.; Šedo, O.; Imberty, A.; Wimmerová, M. Structural Basis for Mannose Recognition by a Lectin from Opportunistic Bacteria *Burkholderia Cenocepacia*. *Biochemical Journal* **2008**, *411*, 307–318. <https://doi.org/10.1042/BJ20071276>.
- (8) Šulák, O.; Cioci, G.; Delia, M.; Lahmann, M.; Varrot, A.; Imberty, A.; Wimmerová, M. A TNF-like Trimeric Lectin Domain from *Burkholderia Cenocepacia* with Specificity for Fucosylated Human Histo-Blood Group Antigens. *Structure* **2010**, *18*, 59–72. <https://doi.org/10.1016/j.str.2009.10.021>.
- (9) Šulák, O.; Cioci, G.; Lameignère, E.; Balloy, V.; Round, A.; Gutsche, I.; Malinovská, L.; Chignard, M.; Kosma, P.; Aubert, D. F.; Marolda, C. L.; Valvano, M. A.; Wimmerová, M.; Imberty, A. *Burkholderia Cenocepacia* BC2L-C Is a Super Lectin with Dual Specificity and Proinflammatory Activity. *PLoS Pathog* **2011**, *7*, e1002238. <https://doi.org/10.1371/JOURNAL.PPAT.1002238>.
- (10) Marchetti, R.; Malinovska, L.; Lameignère, E.; Adamova, L.; De Castro, C.; Cioci, G.; Stanetty, C.; Kosma, P.; Molinaro, A.; Wimmerova, M.; Imberty, A.; Silipo, A. *Burkholderia Cenocepacia* Lectin A Binding to Heptoses from the Bacterial Lipopolysaccharide. *Glycobiology* **2012**, *22*, 1387–1398. <https://doi.org/10.1093/glycob/cws105>.

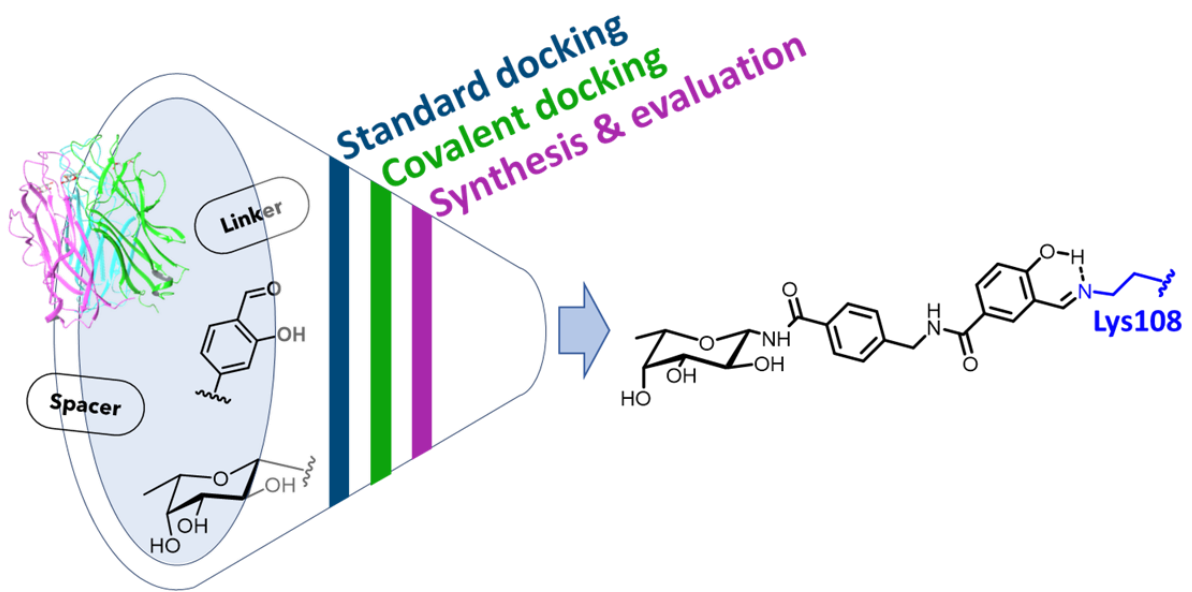
- (11) Asadi, A.; Razavi, S.; Talebi, M.; Gholami, M. A Review on Anti-Adhesion Therapies of Bacterial Diseases. *Infection* **2019**, *47*, 13–23. <https://doi.org/10.1007/s15010-018-1222-5>.
- (12) Inhülsen, S.; Aguilar, C.; Schmid, N.; Suppiger, A.; Riedel, K.; Eberl, L. Identification of Functions Linking Quorum Sensing with Biofilm Formation in *Burkholderia Cenocepacia* H111. *Microbiologyopen* **2012**, *1*, 225–242. <https://doi.org/10.1002/mbo3.24>.
- (13) Bermeo, R.; Bernardi, A.; Varrot, A. BC2L-C N-Terminal Lectin Domain Complexed with Histo Blood Group Oligosaccharides Provides New Structural Information. *Molecules* **2020**, *25*, 248. <https://doi.org/10.3390/MOLECULES25020248>.
- (14) Mazzotta, S.; Antonini, G.; Vasile, F.; Gillon, E.; Lundstrøm, J.; Varrot, A.; Belvisi, L.; Bernardi, A. Identification of New L-Fucosyl and L-Galactosyl Amides as Glycomimetic Ligands of TNF Lectin Domain of BC2L-C from *Burkholderia Cenocepacia*. *Molecules* **2023**, *28*, 1494. <https://doi.org/10.3390/MOLECULES28031494/S1>.
- (15) Bermeo, R.; Lal, K.; Ruggeri, D.; Lanaro, D.; Mazzotta, S.; Vasile, F.; Imberty, A.; Belvisi, L.; Varrot, A.; Bernardi, A. Targeting a Multidrug-Resistant Pathogen: First Generation Antagonists of *Burkholderia Cenocepacia*'s BC2L-C Lectin. *ACS Chem Biol* **2022**, *17*, 2899–2910. <https://doi.org/10.1021/acscchembio.2c00532>.
- (16) Antonini, G.; Civera, M.; Lal, K.; Mazzotta, S.; Varrot, A.; Bernardi, A.; Belvisi, L. Glycomimetic Antagonists of BC2L-C Lectin: Insights from Molecular Dynamics Simulations. *Front Mol Biosci* **2023**, *10*, 1201630. <https://doi.org/10.3389/fmolb.2023.1201630>.
- (17) Lal, K.; Bermeo, R.; Cramer, J.; Vasile, F.; Ernst, B.; Imberty, A.; Bernardi, A.; Varrot, A.; Belvisi, L. Prediction and Validation of a Druggable Site on Virulence Factor of Drug Resistant *Burkholderia Cenocepacia*. *Chemistry - A European Journal* **2021**, *27*, 10341–10348. <https://doi.org/10.1002/CHEM.202100252>.
- (18) Bernardi, A.; Sattin, S. Interfering with the Sugar Code: Ten Years Later. *Eur. J. Org. Chem.* **2020**, *2020*, 4652–4663. <https://doi.org/10.1002/ejoc.202000155>.
- (19) Weis, W. I.; Drickamer, K. Structural Basis of Lectin-Carbohydrate Recognition. *Annu. Rev. of Biochem.* **1996**, *65*, 441–473.
- (20) Boike, L.; Henning, N. J.; Nomura, D. K. Advances in Covalent Drug Discovery. *Nat. Rev. Drug Discov.* **2022**, *21*, 881–898. <https://doi.org/10.1038/s41573-022-00542-z>.
- (21) Lu, W.; Kostic, M.; Zhang, T.; Che, J.; Patricelli, M. P.; Jones, L. H.; Chouchani, E. T.; Gray, N. S. Fragment-Based Covalent Ligand Discovery. *RSC Chem. Biol.* **2021**, *2*, 354–367. <https://doi.org/10.1039/d0cb00222d>.
- (22) Keeley, A.; Petri, L.; Ábrányi-Balogh, P.; Keserű, G. M. Covalent Fragment Libraries in Drug Discovery. *Drug Discov. Today* **2020**, *25*, 983–996. <https://doi.org/10.1016/j.drudis.2020.03.016>.
- (23) Wagner, S.; Hauck, D.; Hoffmann, M.; Sommer, R.; Joachim, I.; Müller, R.; Imberty, A.; Varrot, A.; Titz, A. Covalent Lectin Inhibition and Application in Bacterial Biofilm Imaging. *Angew. Chem.* **2017**, *129*, 16786–16791. <https://doi.org/10.1002/ange.201709368>.

- (24) Fischer, L.; Steffens, R. C.; Paul, T. J.; Hartmann, L. Catechol-Functionalized Sequence-Defined Glycomacromolecules as Covalent Inhibitors of Bacterial Adhesion. *Polym. Chem.* **2020**, *11*, 6091–6096. <https://doi.org/10.1039/d0py00975j>.
- (25) Smith, S.; Keul, M.; Engel, J.; Basu, D.; Eppmann, S.; Rauh, D. Characterization of Covalent-Reversible EGFR Inhibitors. *ACS Omega* **2017**, *2*, 1563–1575. <https://doi.org/10.1021/acsomega.7b00157>.
- (26) Bandyopadhyay, A.; Gao, J. Targeting Biomolecules with Reversible Covalent Chemistry. *Curr. Opin. Chem. Biol.* **2016**, *34*, 110–116. <https://doi.org/10.1016/j.cbpa.2016.08.011>.
- (27) Zheng, M.; Chen, F. J.; Li, K.; Reja, R. M.; Haeffner, F.; Gao, J. Lysine-Targeted Reversible Covalent Ligand Discovery for Proteins via Phage Display. *J. Am. Chem. Soc.* **2022**, *144*, 15885–15893. <https://doi.org/10.1021/jacs.2c07375>.
- (28) Faridooon; Ng, R.; Zhang, G.; Li, J. J. An Update on the Discovery and Development of Reversible Covalent Inhibitors. *Med. Chem. Res.* **2023**, 1039–1062. <https://doi.org/10.1007/s00044-023-03065-3>.
- (29) Dal Corso, A.; Catalano, M.; Schmid, A.; Scheuermann, J.; Neri, D. Affinity Enhancement of Protein Ligands by Reversible Covalent Modification of Neighboring Lysine Residues. *Angew. Chem. Int. Ed.* **2018**, *57*, 17178–17182. <https://doi.org/10.1002/anie.201811650>.
- (30) Mason, M.; Belvisi, L.; Pignataro, L.; Dal Corso, A. A Tight Contact: The Expanding Application of Salicylaldehydes in Lysine-Targeting Covalent Drugs. *ChemBioChem* **2024**, *25*, e202300743. <https://doi.org/10.1002/cbic.202300743>.
- (31) Metcalf, B.; Chuang, C.; Dufu, K.; Patel, M. P.; Silva-Garcia, A.; Johnson, C.; Lu, Q.; Partridge, J. R.; Patskovska, L.; Patskovsky, Y.; Almo, S. C.; Jacobson, M. P.; Hua, L.; Xu, Q.; Gwaltney, S. L.; Yee, C.; Harris, J.; Morgan, B. P.; James, J.; Xu, D.; Hutchaleelaha, A.; Paulvannan, K.; Oksenberg, D.; Li, Z. Discovery of GBT440, an Orally Bioavailable R-State Stabilizer of Sick Cell Hemoglobin. *ACS Med. Chem. Lett.* **2017**, *8*, 321–326. <https://doi.org/10.1021/acsmchemlett.6b00491>.
- (32) Kilambi, K. P.; Gray, J. J. Rapid Calculation of Protein PKa Values Using Rosetta. *Biophys. J.* **2012**, *103*, 587–595. <https://doi.org/10.1016/j.bpj.2012.06.044>.
- (33) Platzer, G.; Okon, M.; McIntosh, L. P. PH-Dependent Random Coil ¹H, ¹³C, and ¹⁵N Chemical Shifts of the Ionizable Amino Acids: A Guide for Protein PK a Measurements. *J. Biomol. NMR* **2014**, *60*, 109–129. <https://doi.org/10.1007/s10858-014-9862-y>.
- (34) Pettinger, J.; Jones, K.; Cheeseman, M. D. Lysine-Targeting Covalent Inhibitors. *Angew. Chem. Int. Ed.* **2017**, *56*, 15200–15209. <https://doi.org/10.1002/anie.201707630>.
- (35) Scarpino, A.; Ferenczy, G. G.; Keserü, G. M. Comparative Evaluation of Covalent Docking Tools. *J Chem Inf Model* **2018**, *58*, 1441–1458. <https://doi.org/10.1021/acs.jcim.8b00228>.
- (36) Friesner, R. A.; Banks, J. L.; Murphy, R. B.; Halgren, T. A.; Klicic, J. J.; Mainz, D. T.; Repasky, M. P.; Knoll, E. H.; Shelley, M.; Perry, J. K.; Shaw, D. E.; Francis, P.; Shenkin, P. S. Glide: A New Approach for Rapid, Accurate Docking and Scoring. 1. Method and Assessment of Docking Accuracy. *J. Med. Chem.* **2004**, *47*, 1739–1749. <https://doi.org/10.1021/jm0306430>.

- (37) Zhu, K.; Borrelli, K. W.; Greenwood, J. R.; Day, T.; Abel, R.; Farid, R. S.; Harder, E. Docking Covalent Inhibitors: A Parameter Free Approach to Pose Prediction and Scoring. *J. Chem. Inf. Model.* **2014**, *54*, 1932–1940. <https://doi.org/10.1021/ci500118s>.
- (38) Hofsløkken, N. U.; Skattebol, L. Convenient Method for the Ortho-Formylation of Phenols. *Acta Chem. Scand.* **1999**, *53*, 258–262.
- (39) Sacco, G.; Stammwitz, S.; Belvisi, L.; Pignataro, L.; Dal Corso, A.; Gennari, C. Functionalized 2-Hydroxybenzaldehyde-PEG Modules as Portable Tags for the Engagement of Protein Lysine ϵ -Amino Groups. *Eur. J. Org. Chem.* **2021**, *11*, 1763–1767. <https://doi.org/10.1002/ejoc.202100160>.
- (40) Mons, E.; Kim, R. Q.; Mulder, M. P. C. Technologies for Direct Detection of Covalent Protein–Drug Adducts. *Pharmaceuticals* **2023**, *16*, 547. <https://doi.org/10.3390/ph16040547>.
- (41) Wolter, M.; Valenti, D.; Cossar, P. J.; Levy, L. M.; Hristeva, S.; Genski, T.; Hoffmann, T.; Brunsveld, L.; Tzalis, D.; Ottmann, C. Fragment-Based Stabilizers of Protein–Protein Interactions through Imine-Based Tethering. *Angew. Chem. Int. Ed.* **2020**, *59*, 21520–21524. <https://doi.org/10.1002/anie.202008585>.
- (42) Schrödinger Release 2018-1: LigPrep, Schrödinger, LLC, New York, NY, 2018.
- (43) Harder, E.; Damm, W.; Maple, J.; Wu, C.; Reboul, M.; Xiang, J. Y.; Wang, L.; Lupyán, D.; Dahlgren, M. K.; Knight, J. L.; Kaus, J. W.; Cerutti, D. S.; Krilov, G.; Jorgensen, W. L.; Abel, R.; Friesner, R. A. OPLS3: A Force Field Providing Broad Coverage of Drug-like Small Molecules and Proteins. *J. Chem. Theory Comput.* **2016**, *12*, 281–296. <https://doi.org/10.1021/acs.jctc.5b00864>.
- (44) Lyskov, S.; Chou, F. C.; Conchúir, S. Ó.; Der, B. S.; Drew, K.; Kuroda, D.; Xu, J.; Weitzner, B. D.; Renfrew, P. D.; Sripakdeevong, P.; Borgo, B.; Havranek, J. J.; Kuhlman, B.; Kortemme, T.; Bonneau, R.; Gray, J. J.; Das, R. Serverification of Molecular Modeling Applications: The Rosetta Online Server That Includes Everyone (ROSIE). *PLoS One* **2013**, *8*, e63906. <https://doi.org/10.1371/journal.pone.0063906>.
- (45) Bianchi, A.; Bernardi, A. Traceless Staudinger Ligation of Glycosyl Azides with Triaryl Phosphines: Stereoselective Synthesis of Glycosyl Amides. *J. Org. Chem.* **2006**, *71*, 4565–4577. <https://doi.org/10.1021/jo060409s>.
- (46) Qiu, Y.; Chan, S. T.; Lin, L.; Shek, T. L.; Tsang, T. F.; Barua, N.; Zhang, Y.; Ip, M.; Chan, P. K. sheung; Blanchard, N.; Hanquet, G.; Zuo, Z.; Yang, X.; Ma, C. Design, Synthesis and Biological Evaluation of Antimicrobial Diarylimine and –Amine Compounds Targeting the Interaction between the Bacterial NusB and NusE Proteins. *Eur. J. Med. Chem.* **2019**, *178*, 214–231. <https://doi.org/10.1016/j.ejmech.2019.05.090>.
- (47) Kumar, V.; Gandeepan, P. Green Synthesis of 3,4-Unsubstituted Isoquinolones through Rhodium(III)-Catalyzed C–H Activation and Annulation in Ethanol. *Eur. J. Org. Chem.* **2023**, *26*, e202300914. <https://doi.org/10.1002/ejoc.202300914>.
- (48) Wagener, T.; Pierau, M.; Heusler, A.; Glorius, F. Synthesis of Saturated N-Heterocycles via a Catalytic Hydrogenation Cascade. *Adv. Synth. Catal.* **2022**, *364*, 3366–3371. <https://doi.org/10.1002/adsc.202200601>.

- (49) Stepanova, E. V.; Belyanin, M. L.; Filimonov, V. D. Synthesis of Acyl Derivatives of Salicin, Salirepin, and Arbutin. *Carbohydr. Res.* **2014**, *388*, 105–111. <https://doi.org/10.1016/j.carres.2014.02.014>.
- (50) Bermeo Malo, R. Design, Synthesis and Evaluation of Antagonists towards BC2L-C, Université Grenoble Alpes/ Università degli Studi di Milano, 2021. <https://air.unimi.it/handle/2434/850474>.
- (51) Hoya, M.; Matsunaga, R.; Nagatoishi, S.; Ide, T.; Kuroda, D.; Tsumoto, K. Impact of Single-Residue Mutations on Protein Thermal Stability: The Case of Threonine 83 of BC2L-CN Lectin. *Int. J. Biol. Macromol.* **2024**, *272*, 132682. <https://doi.org/10.1016/j.ijbiomac.2024.132682>.
- (52) Diphosphopyridoxal, U.; Tagaya, M.; Nakano, K.; Fukui, T. A New Affinity Labeling Reagent for the Active Site of Glycogen Synthase. *J. Biol. Chem.* **1985**, *260*, 6670–6676.

Table of Contents



Supporting Information

Achieving High Affinity for a Bacterial Lectin with Reversible Covalent Ligands

Giulia Antonini,^a Anna Bernardi,^a Emilie Gillon,^b Alberto Dal Corso,^a Monica Civera,^a Laura Belvisi,^{a*} Annabelle Varrot,^{b*} Sarah Mazzotta^{a*}

a. Università degli Studi di Milano, Dipartimento di Chimica, 20133 Milano, Italy

b. Univ. Grenoble Alpes, CNRS, CERMAV, 38000 Grenoble, France

*Correspondence: sarah.mazzotta@unimi.it; laura.belvisi@unimi.it; annabelle.varrot@cermav.cnrs.fr

Table of contents

1. Computational studies	3
1.1 Computational workflow.....	3
Table SI-1. Compounds A1-A20 - did not pass Filter 1.....	5
Table SI-2. Compounds B1-B3 - passed Filter 1, but not Filter 2.....	6
Table SI-3. Compounds C1-C33 - passed both Filter 1 and Filter 2.	6
Figure SI-1. Standard and Covalent Docking poses of compounds 3-5.....	9
Figure SI-2. Standard and Covalent Docking poses of compound A12 from Table SI-1	11
2. Synthesis	12
2.1 Synthesis of (1,2,3,4-tri-O-acetyl β -L-fucopyranosyl) azide 6	12
2.2 Synthesis of acid 17	13
2.3 Synthesis of negative control 21	14
2.4 Synthesis of glucose negative control 22	17
2.5 Synthesis of compound A12 (Table SI-1)	19
3. Thermal Shift Assays	20
Figure SI-3. First derivatives of fluorescence curves obtained from TSA experiments.....	20
4. Validation of SPR competition assays: comparison with ITC experiments	21
Table SI-4. K_D values from ITC experiments for compounds 1 , 23 and 24	21
5. SPR competition assays – sensorgrams and inhibition curves	21
Figure SI-4. BC2L-C-Nt titration over the fucosylated surface.....	21
Figure SI-5. SPR sensorgrams.....	22
Figure SI-6. Inhibition curves.....	23
6. Mass MALDI-TOF analysis – additional spectra	24
Figure SI-7. MALDI-TOF spectra of a 1:10 mixture of protein and ligand 2	24

<i>Figure SI-8. MALDI-TOF spectra of a 1:4 mixture of protein and ligand 4</i>	25
<i>Figure SI-9. MALDI-TOF spectra of a 1:200 mixture of protein and ligand 5</i>	25
<i>Figure SI-10. MALDI-TOF spectra of a 1:10 mixture of protein and ligand 3 after 2 h incubation</i>	26
<i>Figure SI-11. MALDI-TOF spectra of a 1:200 mixture of protein and negative control 22</i>	26
<i>Figure SI-12. MALDI-TOF spectra of a 1:200 mixture of protein and A12 (Table SI-1)</i>	27
7. LC-MS analysis of BC2L-C-Nt:2 complex after NaBH₄ reduction and Trypsin digestion	27
7.1 <i>Figure SI-13. LC-MS analysis of the protein</i>	28
7.2 <i>Figure SI-14. LC-MS analysis of protein:2 mixture</i>	29
8. NMR spectra	30
9. HPLC traces for ligands 2-5, 21 and 22	51
10. References	53

1. Computational studies

1.1 Computational workflow

In this work we developed a docking workflow which allowed to prioritize a set of putative covalent ligands. With the aim of developing a robust protocol, that did not suffer from the known limitations of docking scores as reliable predictors of binding affinity, particularly in the study of lectin/glycomimetic interactions,^{1,2} standard and covalent docking approaches were applied in a combined manner exploiting the following filters as selection criteria.

Filter 1: All saved poses from standard docking of each of the 56 compounds designed must display a distance between the aldehyde carbonyl and Lys108 amino group ≤ 10 Å. This filter should allow to consider in some way the ligand pre-organization also for covalent binding, by checking the proximity of the ligand electrophilic warhead to the nucleophilic residue in the noncovalent complex. The ligands that did not pass this filter are listed in **Table SI-1** (20 compounds, A1 to A20). They were not further screened with the covalent docking protocol (except for compound **A12**, used as negative control for additional validation, see **Figure SI-2**).

Filter 2: The fucose moiety must form all the canonical interactions usually observed for the sugar within BC2L-C-Nt binding site in at least 8 of the 10 poses saved for each ligand by CovDock calculations. To confirm that the fucose binding mode is consistent with available crystal structures, the presence of the following H-bond interactions was monitored: Fuc-OH-2 with Arg111 side chain; Fuc-OH-3 with Thr74 side chain; and Fuc-OH-4 with Arg85 side chain. The ligands of the starting pool that passed *Filter 1*, but did not pass *Filter 2* were only 3 (B1 to B3) and are listed in **Table SI-2**. These compounds, likely because their spacer is too short, were unable to maintain the sugar core in the correct position within the binding site in almost all the saved poses from CovDock.

The ligands that passed both *Filter 1 and 2* are collected in **Table SI-3** (33 compounds, C1 to C33). In order to prioritize their synthesis, these ligands were then analyzed for their ability to form additional interactions within the binding site and their synthetic feasibility. Specifically, the poses obtained from covalent docking were examined to verify the presence of additional non-covalent interactions that could further stabilize the ligand within the binding site, thereby improving affinity. Our previous work³⁻⁵ had shown that (T-shaped) π stacking interactions with the Tyr58 side chain play an important role in the ligand binding affinity. Thus, all compounds with a functionalized benzene ring as a spacer (C1-C11 and C20-C33) were prioritized over those containing a triazole (C12-C18) or a PEG (C19) linker. As for synthetic feasibility, we prioritized compounds C20-C33,

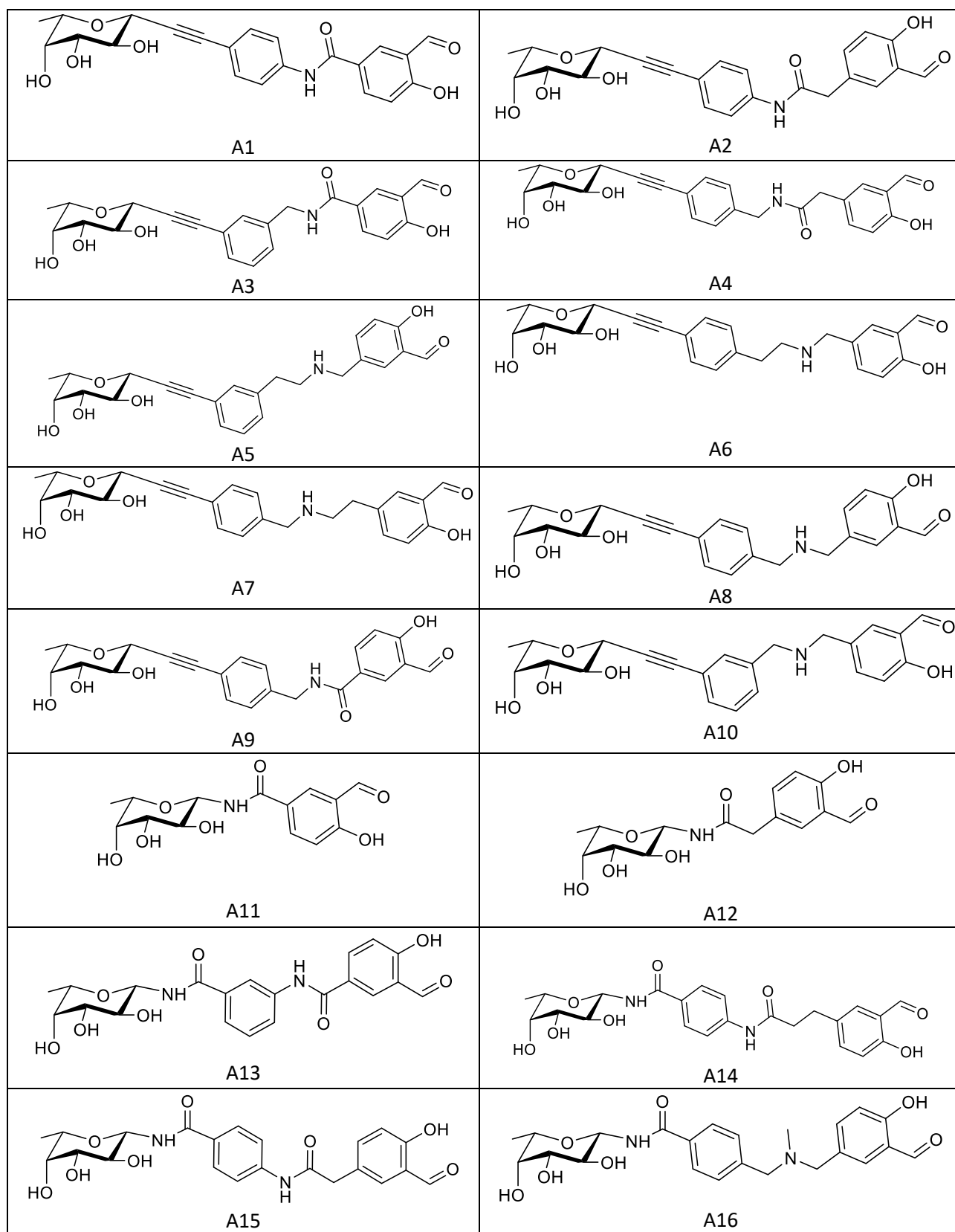
which contain a β -fucosylamide linker, over C1-C11, which feature an alkyne at the β -anomeric position, that requires several synthetic steps to be introduced.³

At the end of this analysis, 14 amide-containing compounds (C20-C33) remained. All featured the same benzene spacer, functionalized in the *meta* or *para* position with a salicylaldehyde warhead. They differed in the length of the chain connecting the spacer to the terminal electrophilic group, which contained either an amine or an amide group. As a first attempt to obtain covalent ligands targeting BC2LC-*Nt* lectin, only a few were synthesized as a proof of concept and the final four (C30-C33, compounds **2-5** in the main text) were selected for this purpose. These compounds contain an additional amide moiety between the linker and the electrophilic warhead, a spacer functionalized in the *meta* or *para* position and a chain of variable length connecting it to the salicylaldehyde. They served as ideal examples for evaluating the impact of these structural differences (common to the other compounds as well) on the interaction with the target lectin domain.

It is worth noting that CovDock scores (defined as the average of the initial pre-reaction and post-reaction in-place Glide scores) display a trend that confirms our selection procedure. The less promising ligands, such as **A12** (**Table SI-1**), which fails both filters (see **Figure SI-2**), B1-B3 (**Table SI-2**) failing Filter 2 or C12-C19 (**Table SI-3**) missing some additional interactions, showed less favorable docking scores compared to the more promising ligands, which often reach the best docking scores (e.g. ligands C30-C33).

As a validation of the workflow, compound **A12** (**Table SI-1**) was synthesized and tested by MALDI-MS analysis (see below **Figure SI-12**) showing that, as opposed to **2-5**, no covalent adduct is formed.

Table SI-1. Compounds A1-A20 - did not pass Filter 1.



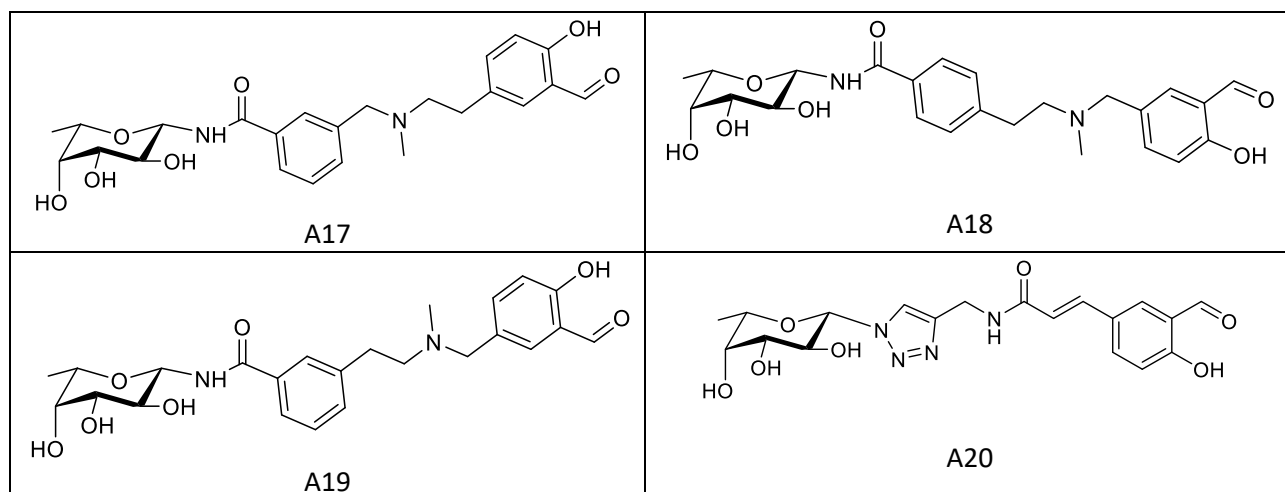


Table SI-2. Compounds B1-B3 - passed Filter 1, but not Filter 2.

The range of CovDock affinity score is reported for each compound (in kcal/mol).

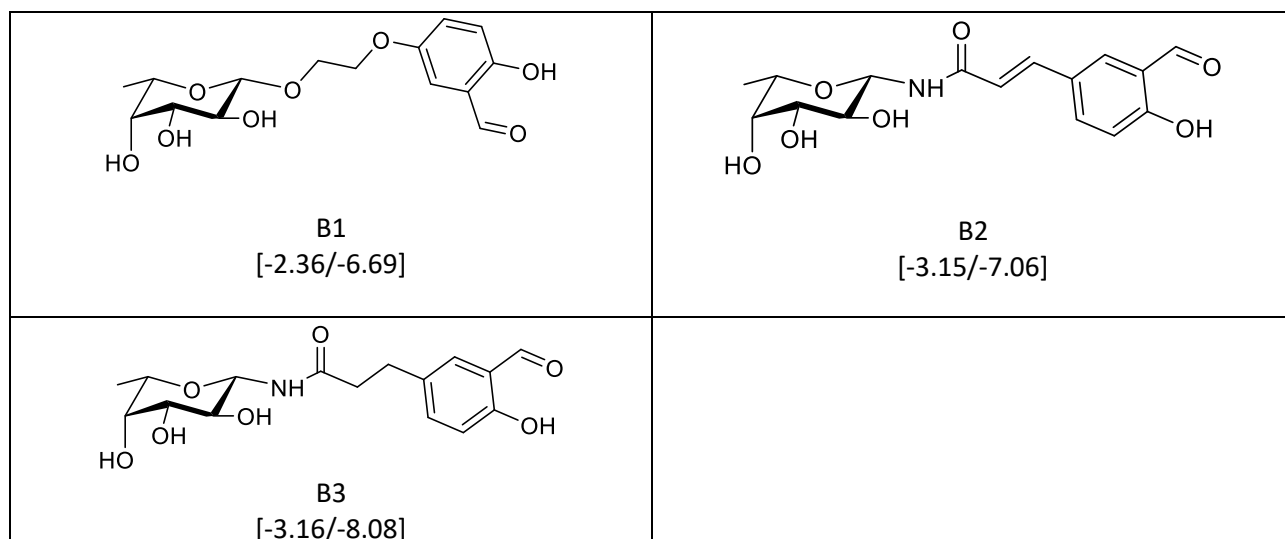
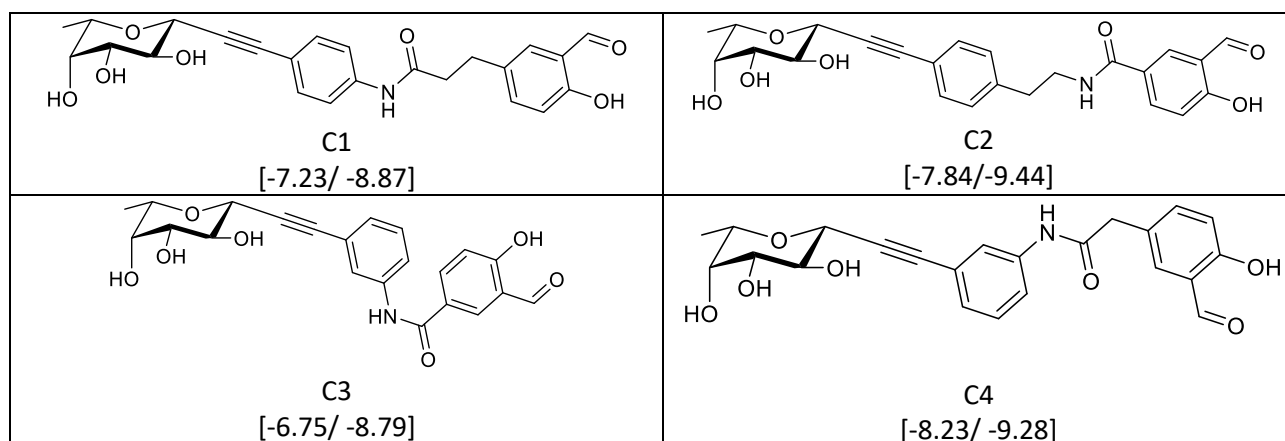
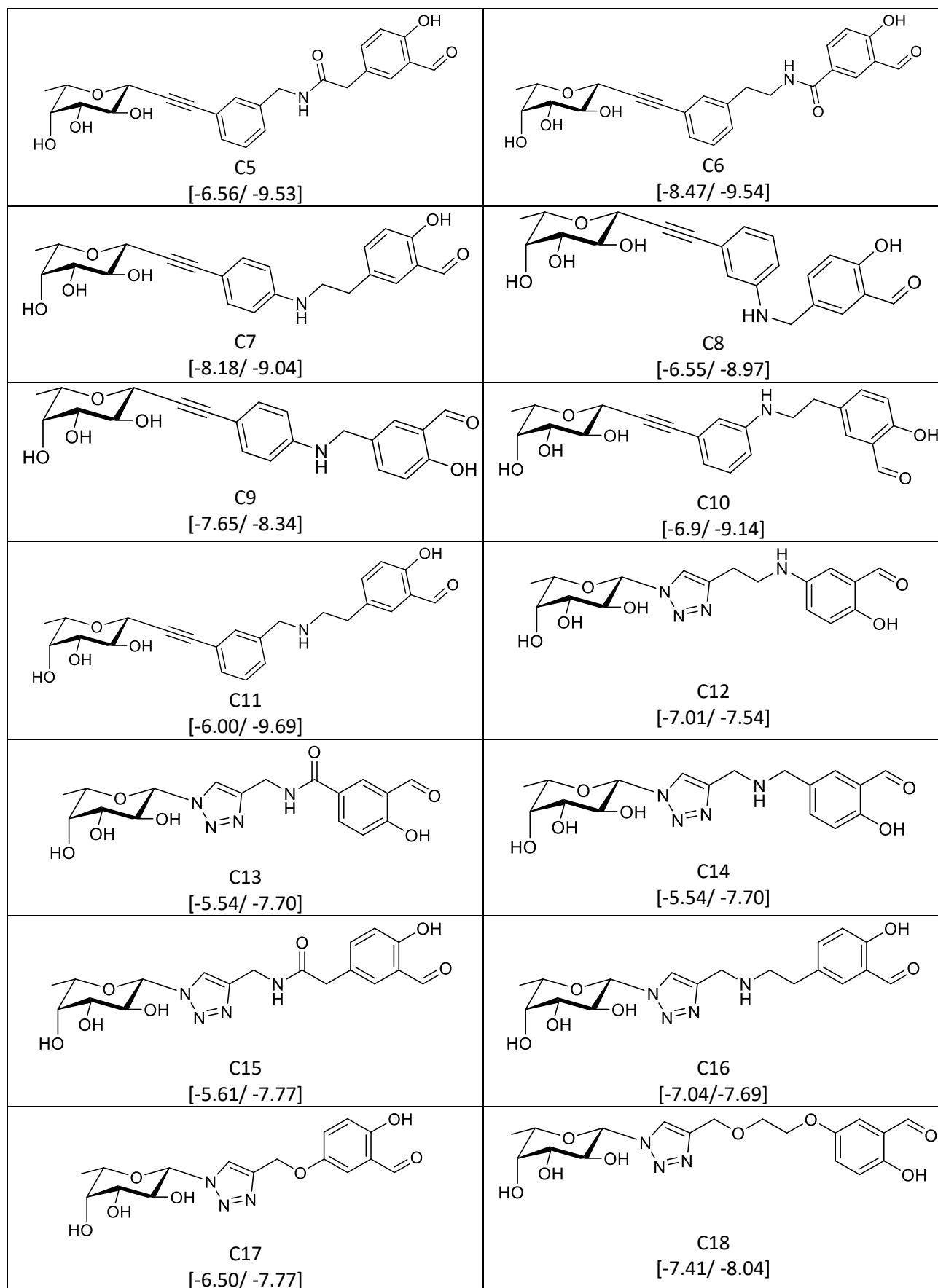
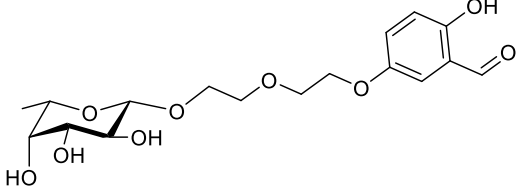
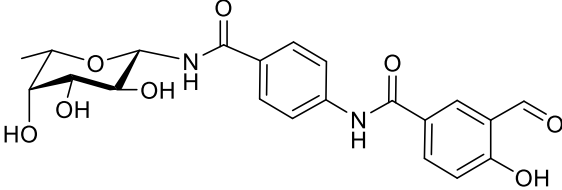
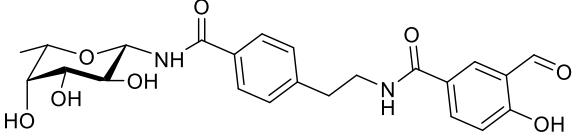
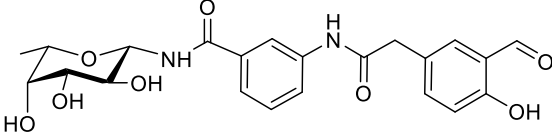
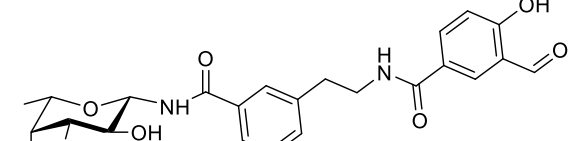
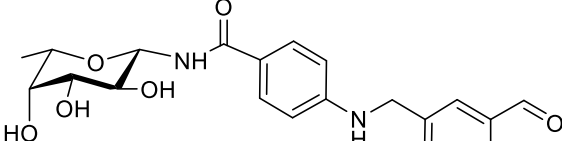
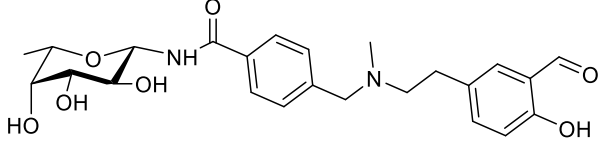
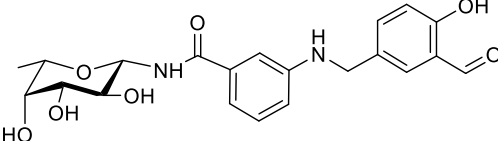
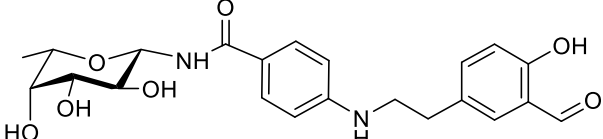
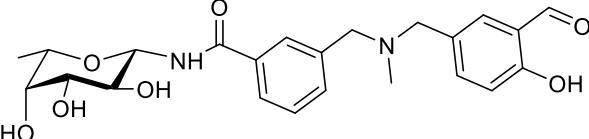
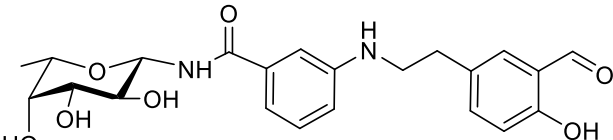
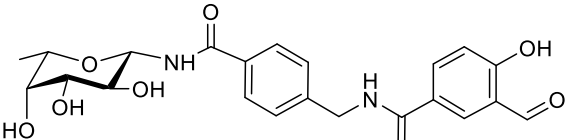
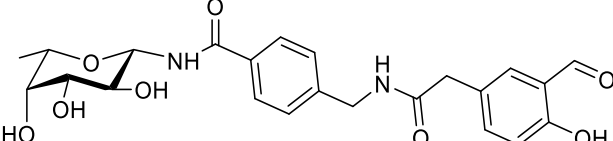
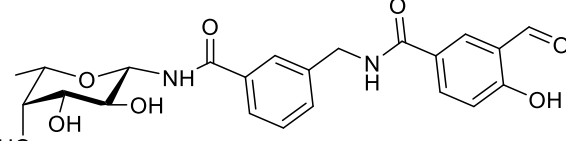


Table SI-3. Compounds C1-C33 - passed both Filter 1 and Filter 2.

The range of CovDock affinity score is reported for each compound (in kcal/mol).





 <p style="text-align: center;">C19 [-7.03/-7.65]</p>	 <p style="text-align: center;">C20 [-6.85/-7.93]</p>
 <p style="text-align: center;">C21 [-8.65/-9.26]</p>	 <p style="text-align: center;">C22 [-7.88/-9.02]</p>
 <p style="text-align: center;">C23 [-7.77/-9.68]</p>	 <p style="text-align: center;">C24 [-7.77/-8.24]</p>
 <p style="text-align: center;">C25 [-7.66/-9.27]</p>	 <p style="text-align: center;">C26 [-7.64/-8.63]</p>
 <p style="text-align: center;">C27 [-7.80/-8.62]</p>	 <p style="text-align: center;">C28 [-6.58/-8.84]</p>
 <p style="text-align: center;">C29 [-7.83/-9.09]</p>	 <p style="text-align: center;">C30 (2) [-8.09/-9.25]</p>
 <p style="text-align: center;">C31 (3) [-8.31/-9.48]</p>	 <p style="text-align: center;">C32 (4) [-7.54/-9.68]</p>

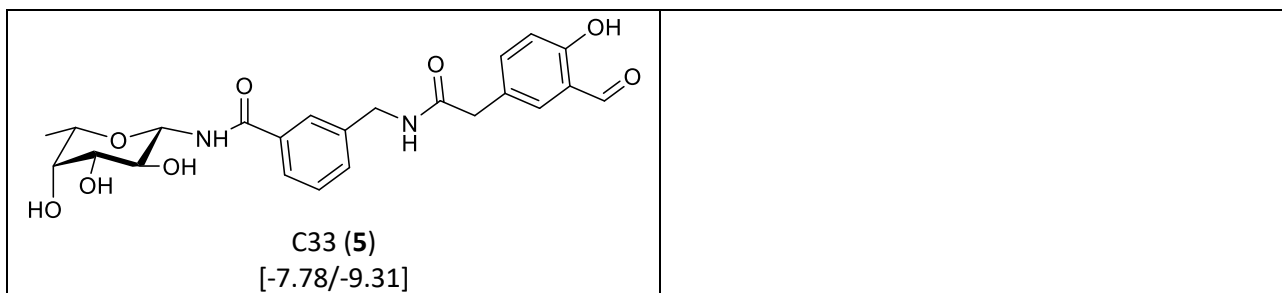
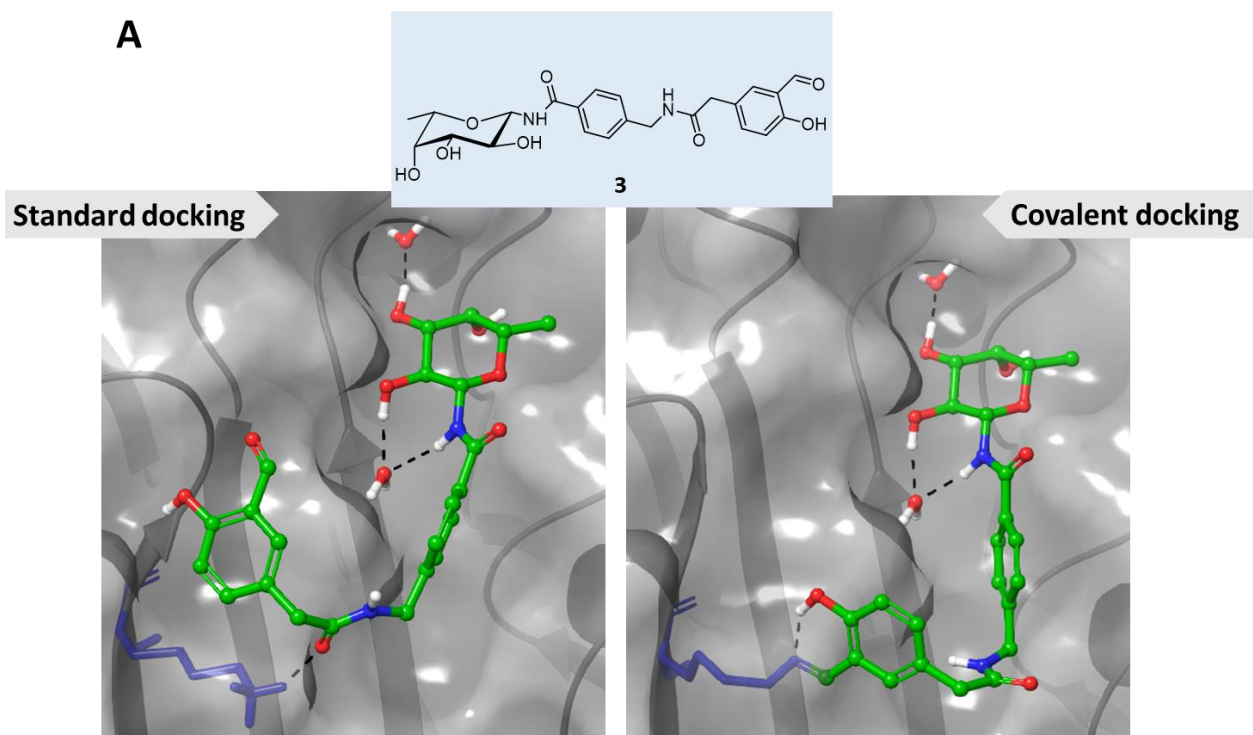


Figure SI-1. Standard and Covalent Docking poses of compounds 3-5



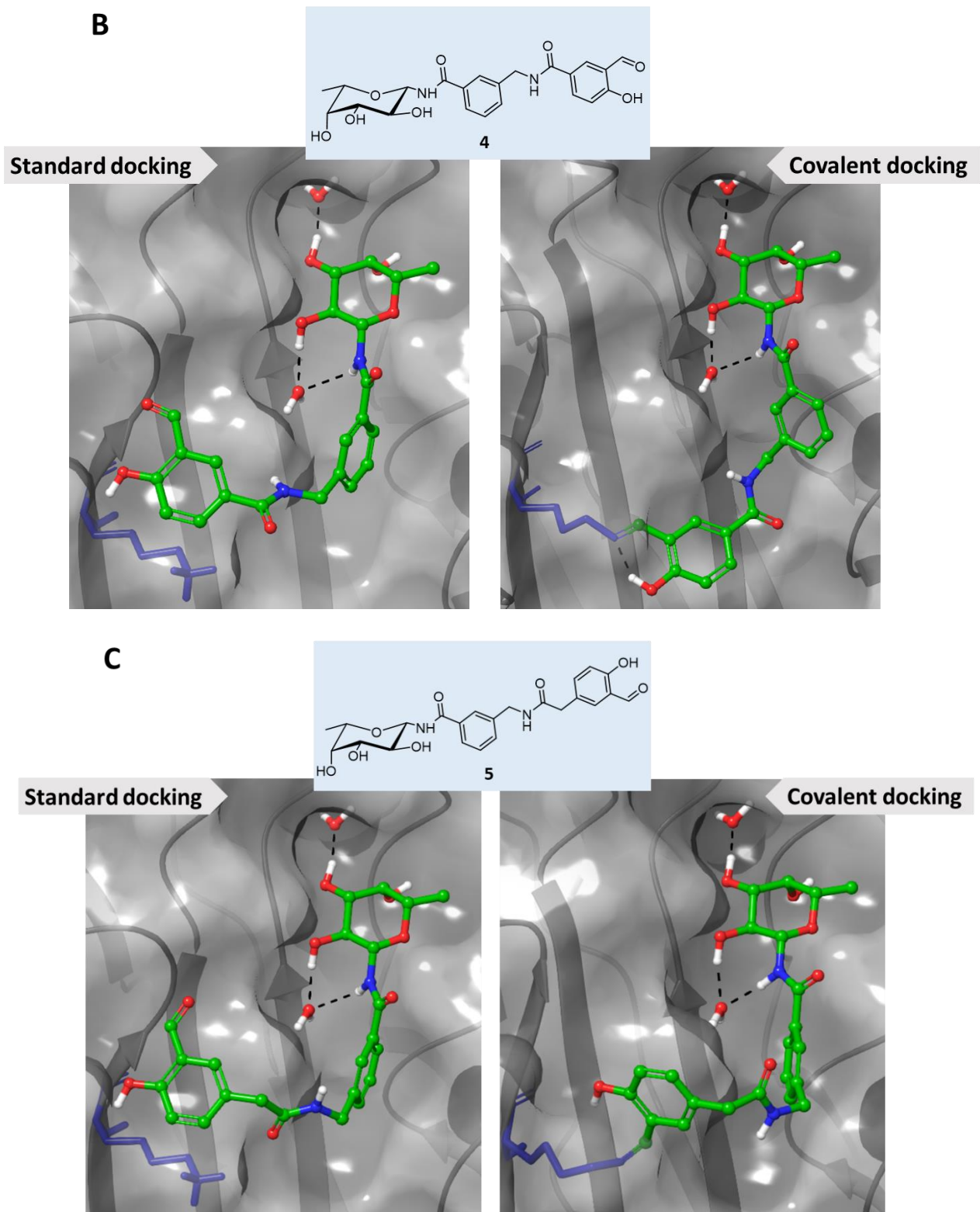


Figure SI-1. One pose obtained from standard docking and one from covalent docking (PDB ID: 2WQ4) are shown for the designed compounds A) 3, B) 4 and C) 5. Two highly conserved water molecules are retained in docking calculations; H-bond interactions are depicted as a black dashed line. Lys108 residue is coloured in blue.

Figure SI-2. Standard and Covalent Docking poses of compound A12 from **Table SI-1**

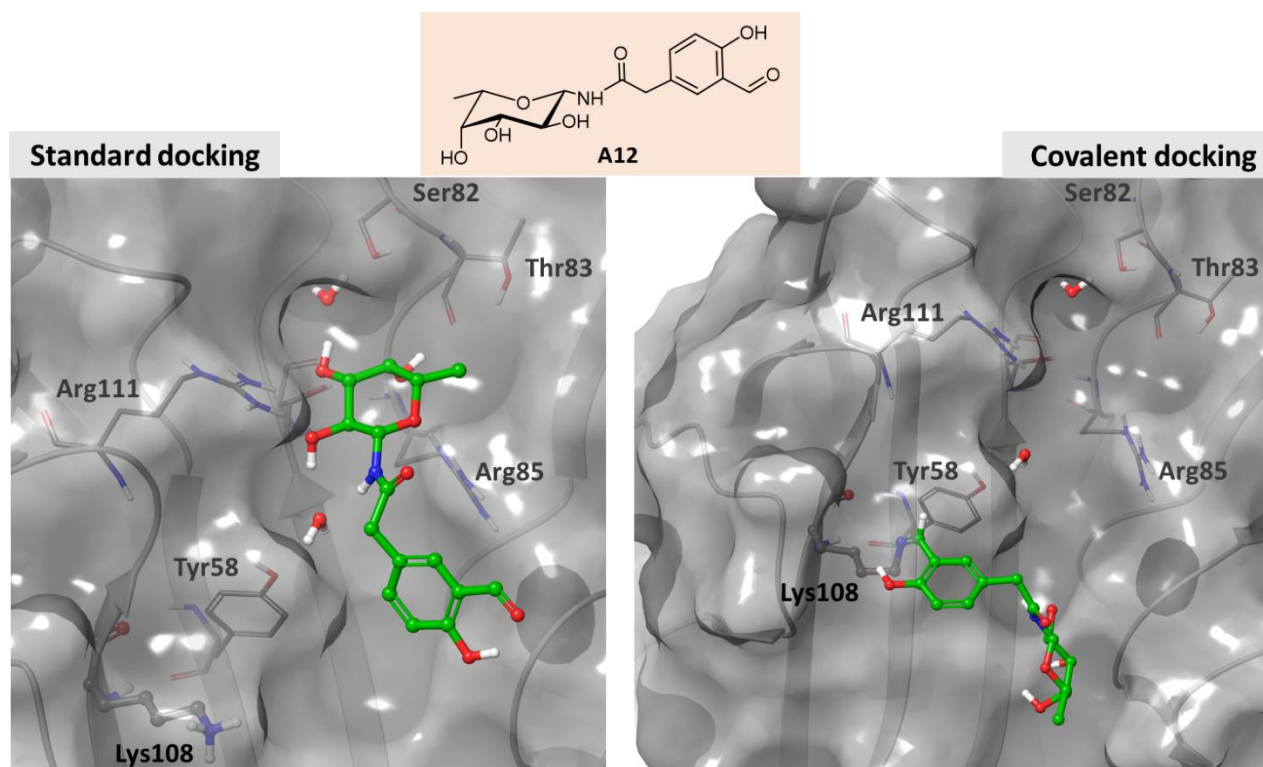
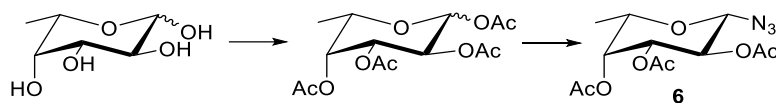


Figure SI-2. One pose obtained from standard docking and one from covalent docking (PDB ID: 2WQ4) are shown for the designed compound A12, which did not pass Filter 1 and 2 during *in silico* screening. In standard docking, the distance between the aldehyde carbonyl and Lys108 amino group is $> 10 \text{ \AA}$ in all the poses, while in covalent docking the fucose core did not maintain the proper position within the binding site (CovDock scores: $-2.50/-5.95 \text{ kcal/mol}$). The two highly conserved water molecules retained in docking calculations are reported.

2. Synthesis

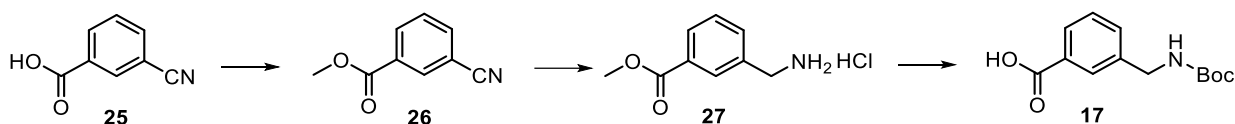
2.1 Synthesis of (1,2,3,4-tri-*O*-acetyl β -L-fucopyranosyl) azide **6**



L-fucose (0.92 g, 5.6 mmol, 1 eq) was dissolved in pyridine (5.29 mL) and cooled to 0 °C. Acetic anhydride (5.29 mL, 56 mmol, 10 eq) was added dropwise and the reaction mixture was stirred at room temperature overnight. The solvent was removed under reduced pressure by co-evaporation with toluene. The crude 1,2,3,4-Tetra-*O*-acetyl-L-fucopyranose (65:35 mixture of α/β pyranoside and traces of furanoside form) was used for the next reaction without further purification. Y = quant., R_f (n-Hex/AcOEt 1:1) = 0.72. Characterization data in agreement with those reported in literature.⁶ ¹H NMR (400 MHz, CDCl₃) α -anomer δ 6.34 (d, J = 2.72 Hz, 1H, H-1), 5.37 - 5.29 (mult., 3H, H-2 + H-3 + H-4), 4.27 (q, J = 6.5 Hz, 1H, H-5), 2.20 - 1.98 (s, 12H, OAc), 1.16 (d, J = 6.5 Hz, 3H, H-6); β -anomer δ = 5.68 (d, J = 8.3 Hz, 1H, H-1), 5.27 (dd, J = 3.34 Hz, J = 0.8 Hz, 1H, H-4), 5.07 (dd, J = 10.4 Hz, J = 3.5 Hz, 1H, H-3), 4.00-3.93 (m, 1H, H-5), 2.20 - 1.98 (m, 12H, OAc), 1.23 (d, J = 6.4 Hz, 3H, H-6).

1,2,3,4-Tetra-*O*-acetyl-L-fucopyranose (1.86 g, 5.6 mmol, 1 eq) was dissolved in anhydrous CH₂Cl₂ (14 mL) and cooled to 0 °C under N₂ atmosphere. Trimethylsilyl azide (TMSN₃, 11.2 mmol, 2 eq) and trimethylsilyl triflate (TMSOTf, 2.24 mmol, 0.4 eq) were added to the solution, and the reaction mixture was stirred at room temperature overnight. The reaction was diluted with dichloromethane and washed with a sat. aqueous solution of NaHCO₃ (2x10 mL) and water (10 mL), dried over anhydrous Na₂SO₄, filtered and concentrated under reduced pressure. The residue was suspended in isopropyl ether (4 mL) and the precipitate was filtered under vacuum, giving **6** as the pure β -anomer in 63% yield. R_f (n-Hex/AcOEt 2:1) = 0.52. Characterization data in agreement with those reported in the literature.⁷ ¹H NMR (400 MHz, CDCl₃) δ 5.27 (dd, J = 3.3 Hz, J = 0.8 Hz, 1H, H-4), 5.14 (dd, J = 10.3 Hz, J = 8.8 Hz, 1H, H-2), 5.03 (dd, J = 10.3 Hz, J = 3.4 Hz, 1H, H-3), 4.57 (d, J = 8.6 Hz, 1H, H-1), 3.90 (dq, J = 1.2 Hz, J = 6.4 Hz, 1H, H-5), 2.19 (s, 3H, OAc), 2.09 (s, 3H, OAc), 1.99 (s, 3H, OAc), 1.25 (d, J = 6.4 Hz, 3H, H-6).

2.2 Synthesis of acid 17



Synthesis of methyl 3-cyanobenzoate 26 - To a solution of 3-cyanobenzoic acid **25** (1.01 g, 6.86 mmol, 1 eq), in anhydrous methanol (13.7 mL), under inert atmosphere, conc. H₂SO₄ (10% v/v, 1.37 mL) was added, and the reaction mixture was stirred at reflux temperature overnight. Then, the mixture was concentrated under reduced pressure, and the residue was diluted with H₂O and extracted with dichloromethane (3 x 10 mL). The combined organic layers were washed with a sat. aqueous solution of NaHCO₃ (30 mL), brine (30 mL), dried over anhydrous Na₂SO₄, filtered and the solvents evaporated under reduced pressure affording **26** as a white solid. Y = 90%. R_f (n-Hex/AcOEt 1:1 + 0.1% FA) = 0.81. Characterization data in agreement with those reported in literature.⁸ ¹H NMR (400 MHz, CDCl₃) δ 8.33 (s, 1H, H-2), 8.27 (d, J = 7.9 Hz, 1H, H-6), 7.83 (d, J = 7.8 Hz, 1H, H-4), 7.59 (t, J = 7.8 Hz, 1H, H-5), 3.96 (s, 3H, OCH₃).

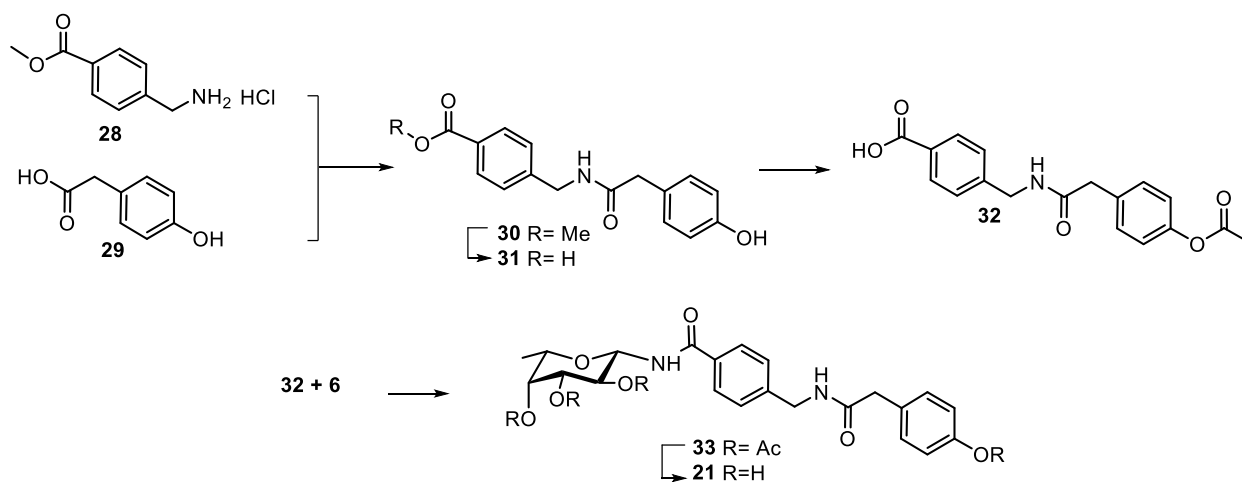
Synthesis of methyl 3-(aminomethyl)benzoate hydrochloride 27 - Methyl 3-cyanobenzoate **26** (446 mg, 2.77 mmol, 1 eq), was dissolved in anhydrous THF under N₂ and cooled to 0°C. Then BH₃·THF was added as a 1 M solution (final conc. of methyl 3-cyanobenzoate in THF = 0.15M), and the mixture was stirred at 60°C overnight. After 18h, the mixture was concentrated at half the volume under reduced pressure, and the residue was acidified with 6 N HCl until pH=2. The solvent completely was removed by evaporation at reduced pressure, and the solid obtained was suspended in n-Hex and filtered, affording **27** as a white solid. Y = 96%. R_f (CH₂Cl₂/MeOH 9:1) = 0.10. Characterization data in agreement with those reported in literature.⁹ ¹H NMR (400 MHz, CD₃OD) δ 8.16 (s, 1H, H-2), 8.07 (d, J = 7.8 Hz, 1H, H-6), 7.72 (d, J = 7.7 Hz, 1H, H-4), 7.58 (t, J = 7.8 Hz, 1H, H-5), 4.20 (s, 2H, Ph-CH₂), 3.93 (s, 3H, OCH₃).

Synthesis of 3-((tert-butoxycarbonyl)amino)methylbenzoic acid 17 - To a solution of methyl 3-(aminomethyl)benzoate hydrochloride **27** (222 mg, 1.1 mmol, 1 eq) and di-tert-butyl dicarbonate (Boc₂O, 360 mg, 1.65 mmol, 1.5 eq) in anhydrous THF (11 mL) under N₂ and at 0°C, Et₃N (0.46 mL, 3.3 mmol, 3 eq) was added and the mixture was stirred overnight at room temperature. The mixture was concentrated under reduced pressure, and the residue was diluted with H₂O and extracted with CH₂Cl₂ (3 x 10 mL). The combined organic phases were washed with brine (30 mL), dried over Na₂SO₄, filtered and concentrated to dryness. The crude was purified by flash chromatography on silica gel (n-Hex/AcOEt 7:3) to give the Boc-protected intermediate as a white solid. Y = 74%. R_f (n-Hex/AcOEt 7:3) = 0.34. Characterization data in agreement with those reported in literature.¹⁰ ¹H

NMR (400 MHz, CDCl₃) δ 7.98-7.90 (m, 2H, H-2 + H-6), 7.49 (d, J = 7.5 Hz, 1H, H-4), 7.41 (t, J = 7.6 Hz, 1H, H-5), 4.90 (bs, 1H, NHBoc), 4.36 (d, J = 5.3 Hz, 2H, Ph-CH₂), 3.92 (s, 3H, OCH₃), 1.46 (s, 9H, Boc).

The Boc-protected intermediate methyl 3-(((tert-butoxycarbonyl)amino)methyl)benzoate (197 mg, 0.74 mmol, 1 eq) was dissolved in a 3:1 mixture of THF/H₂O (conc. = 0.25 M), and then lithium hydroxide monohydrate (LiOH·H₂O, 124 mg, 2.96 mmol, 4 eq) was added and the mixture was stirred at room temperature overnight. The THF was evaporated under reduced pressure, and the residue was treated with 1 N HCl (until pH=2) and extracted with AcOEt (3 x 7 mL). The combined organic layers were washed with brine (20 mL), dried over Na₂SO₄, filtered and concentrated under reduced pressure affording **17** as a white solid. Y = 89%. R_f (CH₂Cl₂ /MeOH 95:5) = 0.28. Characterization data in agreement with those reported in literature.¹¹ ¹H NMR (400 MHz, CDCl₃) δ 8.01 (d, J = 7.7 Hz, 2H, H-2 + H-6), 7.54 (d, J = 6.9 Hz, 1H, H-4), 7.44 (t, J = 7.7 Hz, 1H, H-5), 4.94 (bs, 1H, NHBoc), 4.38 (d, J = 5.1 Hz, 2H, Ph-CH₂), 3.92 (s, 3H, OCH₃), 1.47 (s, 9H, Boc).

2.3 Synthesis of negative control **21**



Synthesis of methyl 4-((2-(4-hydroxyphenyl)acetamido)methyl)benzoate 30 - To a suspension of **28** (208 mg, 1.03 mmol, 1 eq), EDC·HCl (257 mg, 1.34 mmol, 1.3 eq), and HOBT (181 mg, 1.34 mmol, 1.3 eq) in anhydrous DMF (3.43 mL) under N₂ atmosphere, iPr₂EtN (0.54 mL, 3.09 mmol, 3 eq) was added, obtaining a clear solution. Then **29** (157 mg, 1.03 mmol, 1 eq) was added, and the reaction mixture was stirred at room temperature for 24 h. The solvent was evaporated in vacuo, the residue was diluted with CH₂Cl₂ (10 mL) and washed with sat. solution of NH₄Cl (10 mL), sat. solution of NaHCO₃ (10 mL) and brine (8 mL). The organic phase was dried over anhydrous Na₂SO₄ and concentrated under reduced pressure. The crude was purified by flash chromatography on silica gel (n-Hex/AcOEt 7:3) affording **30** as a white foam. Y = 76%. R_f (n-Hex/AcOEt 3:7) = 0.26. MS (ESI)

calcd for $C_{17}H_{17}NO_4$ $[M-H]^-$ m/z : 298.11; found: 298.77. 1H NMR (400 MHz, CD_3OD) δ 7.94 (d, J = 8.4 Hz, 2H, Ph-H-2 + Ph-H-6), 7.32 (d, J = 8.5 Hz, 2H, Ph-H-3 + Ph-H-5), 7.12 (d, J = 8.6 Hz, 2H, Ph'-H-2 + Ph'-H-6), 6.74 (d, J = 8.6 Hz, 2H, Ph'-H-3 + Ph'-H-5), 4.42 (s, 2H, Ph- CH_2 -N), 3.89 (s, 3H, OCH_3), 3.46 (s, 2H, Ph'- CH_2 -CO). ^{13}C chemical shifts extrapolated from HSQC exp.: δ 129.7 (Ph'-C-2 + Ph'-C-6), 129.3 (Ph-C-2 + Ph-C-6), 127.0 (Ph-C-3 + Ph-C-5), 115.0 (Ph'-C-3 + Ph'-C-5), 51.1 (OCH_3), 42.4 (Ph- CH_2 -N), 41.7 (Ph'- CH_2 -CO).

Synthesis of 4-((2-(4-Acetoxyphenyl)acetamido)methyl)benzoic acid 32 - Compound **30** (170 mg, 0.57 mmol, 1 eq) was dissolved in a 3:1 mixture of THF/ H_2O (0.25 M), and then LiOH. H_2O (71.5 mg, 1.7 mmol, 3 eq) was added and the mixture was stirred at room temperature for 3 h. The mixture was acidified with 1 N HCl (until pH=2) and extracted with AcOEt (3 x 7 mL). The combined organic layers were dried over anhydrous Na_2SO_4 and concentrated under reduced pressure. The crude acid **31** was used in the following step. Y = 94%. Rf ($CH_2Cl_2/MeOH$ 9:1) = 0.16. MS (ESI) calcd for $C_{16}H_{15}NO_4$ $[M-H]^-$ m/z : 284.09; found: 284.80. 1H NMR (400 MHz, CD_3OD) δ 7.94 (d, J = 8.3 Hz, 2H, Ph-H-2 + Ph-H-6), 7.31 (d, J = 8.4 Hz, 2H, Ph-H-3 + Ph-H-5), 7.12 (d, J = 8.5 Hz, 2H, Ph'-H-2 + Ph'-H-6), 6.74 (d, J = 8.6 Hz, 2H, Ph'-H-3 + Ph'-H-5), 4.42 (s, 2H, Ph- CH_2 -N), 3.46 (s, 2H, Ph'- CH_2 -CO). ^{13}C chemical shifts extrapolated from HSQC exp.: δ 124.9 (Ph'-C-2 + Ph'-C-6), 124.7 (Ph-C-2 + Ph-C-6), 122.0 (Ph-C-3 + Ph-C-5), 110.2 (Ph'-C-3 + Ph'-C-5), 37.6 (Ph- CH_2 -N), 36.7 (Ph'- CH_2 -CO).

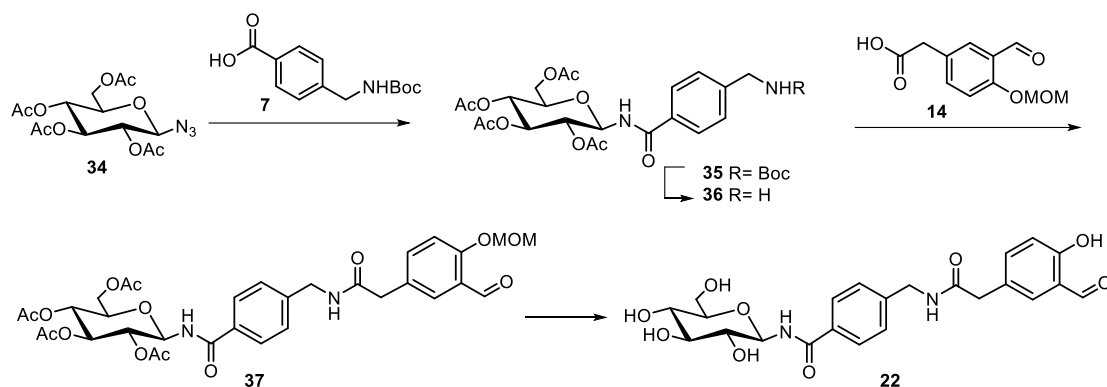
To a solution of **31** (45 mg, 0.16 mmol, 1 eq) in anhydrous pyridine (0.32 mL), acetic anhydride (0.051 mL, 0.54 mmol, 3.4 eq) was added dropwise and the mixture was stirred at room temperature overnight. After 18 h, the mixture was concentrated under reduced pressure, the residue was diluted with 1 N HCl (2 mL) and extracted with AcOEt (2 x 2 mL). The organic layers were combined, dried over anhydrous Na_2SO_4 and concentrated under reduced pressure affording **32** as a white foam. Y = 89%. Rf (n-Hex/AcOEt 3:7) = 0.51. MS (ESI) calcd for $C_{18}H_{17}NO_5$ $[M-H]^-$ m/z : 326.10; found: 326.21. 1H NMR (400 MHz, CD_3OD) δ 8.58 (bs, 1H, $NHCO$), 7.95 (d, J = 8.3 Hz, 2H, Ph-H-2 + Ph-H-6), 7.35-7.32 (m, 4H, Ph-H-3 + Ph-H-5 + Ph'-H-2 + Ph'-H-6), 7.05 (d, J = 8.5 Hz, 2H, Ph'-H-3 + Ph'-H-5), 4.43 (d, J = 5.8 Hz, 2H, Ph- CH_2 -N), 3.58 (s, 2H, Ph'- CH_2 -CO), 2.27 (s, 3H, OAc). ^{13}C chemical shifts extrapolated from HSQC exp.: δ 129.7 (Ph'-C-2 + Ph'-C-6), 129.5 (Ph-C-2 + Ph-C-6), 126.9 (Ph-C-3 + Ph-C-5), 121.5 (Ph'-C-3 + Ph'-C-5), 42.6 (Ph- CH_2 -N), 41.7 (Ph'- CH_2 -CO), 19.4 (OAc).

Synthesis of (4-((2-(4-hydroxyphenyl)acetamido)methyl)benzamido)- β -L-fucopyranose **21**

Staudinger ligation of azide **6** (48.5 mg, 0.154 mmol, 1.1 eq) with acid **32** (46.3 mg, 0.14 mmol, 1 eq), following the general procedure for Staudinger ligation afforded **33**, which was purified by flash chromatography on silica gel (n-Hex/AcOEt 6:4 to 2:8) to a white foam. Y = 63%. Rf (n-Hex/AcOEt 3:7) = 0.54. MS (ESI) calcd C₃₀H₃₄N₂O₁₁ [M+H]⁺ *m/z*: 599.22; found: 599.17. ¹H NMR (400 MHz, CDCl₃) δ 7.70 (d, *J* = 8.2 Hz, 2H, Ph-H-2 + Ph-H-6), 7.30-7.24 (m, 4H, Ph-H-3 + Ph-H-5 + Ph'-H-2 + Ph'-H-6), 7.09 (d, *J* = 8.5 Hz, 2H, Ph'-H-3 + Ph'-H-5), 7.04 (d, *J* = 8.8 Hz, 1H, LFuc-NHCO), 5.77 (t, *J* = 5.1 Hz, 1H, Ph-NHCO-Ph'), 5.39-5.33 (m, 2H, H-1 + H-4), 5.24-5.18 (m, 2H, H-2 + H-3), 4.45 (d, *J* = 5.8 Hz, 2H, Ph-CH₂), 4.01 (q, *J* = 6.3 Hz, 1H, H-5), 3.69 (s, 2H, Ph'-CH₂), 2.30 (s, 3H, OAc) 2.19 (s, 3H, Fuc-OAc), 2.03 (s, 3H, Fuc-OAc), 2.02 (s, 3H, Fuc-OAc), 1.21 (d, *J* = 6.4 Hz, 3H, H-6). ¹³C chemical shifts extrapolated from HSQC exp.: δ 130.3 (Ph'-C-2 + Ph'-C-6), 127.6 (Ph-C-3 + Ph-C-5), 127.5 (Ph-C-2, Ph-C-6), 122.2 (Ph'-C-3, Ph'-C-5), 78.7 (C-1), 71.0 (C-3), 70.9 (C-5), 70.3 (C-4), 68.6 (C-2), 43.15 (Ph-CH₂), 43.1 (Ph'-CH₂), 21.0-20.5 (OAc), 16.0 (C-6).

33 (70.6 mg, 0.127 mmol, 1eq) was dissolved in anhydrous methanol (0.63 mL) under N₂, and a freshly prepared 0.1 M solution of sodium methoxide in anhydrous methanol (0.06 mL) was added (final conc. of methoxide = 0.01 M). The resulting mixture was stirred at room temperature until full conversion (3.5 h). The reaction was quenched by adding Amberlite IRA 120 H⁺ to pH 7, then the resin was filtered out and the solvent was removed under vacuum. The crude product was purified by automatic inverse phase flash chromatography (SFAR C18 D, H₂O/MeOH 9:1 to 5:5) to give **21** as a white amorphous solid. Y = 66%. Rf (H₂O/MeOH 1:1) = 0.73. Samples for interaction studies were further purified by semi-preparative RP-HPLC (H₂O + 0.1% TFA/CH₃CN) with gradient: 0-1 min, 10%; 1-10 min, 10-45%; 10-13 min, 45-100%. tr = 6.90 min. HRMS (ESI) calcd for C₂₂H₂₆N₂O₇ [M-H]⁻ *m/z*: 429.1664; found 429.1662. ¹H NMR (400 MHz, DMSO d₆) δ 9.22 (s, 1H, Ph'-OH), 8.75 (d, *J* = 8.8 Hz, 1H, LFuc-NHCO), 8.48 (t, *J* = 5.9 Hz, 1H, NHCO), 7.85 (d, *J* = 8.2 Hz, 2H, Ph-H-2 + Ph-H-6), 7.27 (d, *J* = 8.2 Hz, 2H, Ph-H-3 + Ph-H-5), 7.07 (d, *J* = 8.4 Hz, 2H, Ph'-H-2 + Ph'-H-6), 6.68 (d, *J* = 8.4 Hz, 2H, Ph'-H-3 + Ph'-H-5), 4.88 (t, *J* = 8.9 Hz, 1H, H-1), 4.75-4.71 (m, 2H, Lfuc-OH-2 + Lfuc-OH-3), 4.46 (d, *J* = 3.9 Hz, 1H, Lfuc-OH-4), 4.30 (d, *J* = 5.9 Hz, 2H, Ph-CH₂), 3.63-3.56 (m, 2H, H-2 + H-5), 3.48 (t, *J* = 3.4 Hz, 1H, H-4), 3.41-3.39 (m, 1H, H-3), 3.35 (s, 2H, Ph'-CH₂), 1.11 (d, *J* = 6.4 Hz, 3H, H-6). ¹³C NMR (100 MHz, DMSO d₆) δ 171.4 (NHCO), 167.0 (NHCO), 156.4 (Ar quat), 143.6 (Ar quat.), 133.1 (Ar quat), 130.4 (Ph'-C-2 + Ph'-C-6), 128.1 (Ph-C-2 + Ph-C-6), 127.1 (Ph-C-3 + Ph-C-5), 126.9 (Ar quat.), 115.5 (Ph'-C-3 + Ph'-C-5), 81.1 (C-1), 74.8 (C-3), 72.1 (C-5), 71.7 (C-4), 69.5 (C-2), 42.3 (Ph-CH₂), 42.0 (Ph'-CH₂), 17.3 (C-6).

2.4 Synthesis of glucose negative control 22



Synthesis of (4-(aminomethyl)benzamido)-2,3,4,6-tetra-O-acetyl-β-D-glucopyranose 36

Staudinger ligation of glucosyl azide **34** (0.743 g, 1.99 mmol, 1 eq) and acid **7** (0.5 g, 1.99 mmol, 1 eq) according to the general procedure for Staudinger ligation afforded (4-(((tert-butoxycarbonyl)amino)methyl)benzamido)-2,3,4,6-tetra-O-acetyl-β-D-glucopyranose **35**, which was purified by flash chromatography on silica gel (n-Hex/AcOEt 7:3 to 5:5) to a white solid. Y = 53%. R_f (n-Hex/AcOEt 4:6) = 0.46. MS (ESI) calcd C₂₇H₃₆N₂O₁₂ [M+Na]⁺ m/z: 603.22; found: 603.22. ¹H NMR (400 MHz, CDCl₃) δ 7.72 (d, *J* = 8.2 Hz, 2H, Ph-H-2 + Ph-H-6), 7.36 (d, *J* = 8.1 Hz, 2H, Ph-H-3 + Ph-H-5), 7.01 (d, *J* = 8.5 Hz, 1H, NHCO), 5.45-5.37 (m, 2H, H-1 + H-3), 5.14-5.03 (m, 2H, H-2 + H-4), 4.91 (brs, 1H, NHBoc), 4.38-4.34 (m, 3H, H-6' + Ph-CH₂), 4.11 (dd, *J* = 12.4 Hz, *J* = 4.1 Hz, 1H, H-6), 3.91 (dd, *J* = 10.0 Hz, *J* = 1.9 Hz, 1H, H-5), 2.08 (s, 3H, OAc), 2.05 (s, 6H, 2x OAc), 2.04 (s, 3H, OAc), 1.47 (s, 9H, Boc).

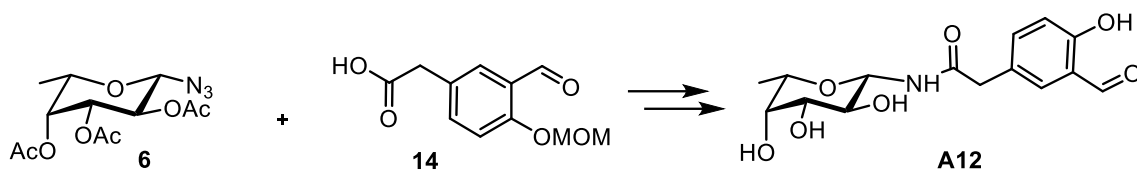
Boc deprotection of **35** according to the general procedure for Boc removal afforded **36** (400 mg) as a yellowish foam. Y = 79%. R_f (CH₂Cl₂/MeOH 95:5) = 0.20. MS (ESI) calcd C₂₃H₃₀N₂O₁₀ [M+H]⁺ m/z: 481.18; found: 481.21. ¹H NMR (400 MHz, CDCl₃) δ 7.73 (d, *J* = 8.2 Hz, 2H, Ph-H-2 + Ph-H-6), 7.40 (d, *J* = 8.2 Hz, 2H, Ph-H-3 + Ph-H-5), 6.98 (d, *J* = 9.3 Hz, 1H, NHCO), 5.49-5.37 (m, 2H, H-1 + H-3), 5.14-5.03 (m, 2H, H-2 + H-4), 4.35 (dd, *J* = 12.5 Hz, *J* = 4.3 Hz, 1H, H-6), 4.11 (dd, *J* = 12.5 Hz, *J* = 2.1 Hz, 1H, H-6'), 3.94-3.89 (m, 3H, Ph-CH₂ + H-5), 2.08-2.05-2.03 (4s, 4x3H, OAc). ¹³C chemical shifts extrapolated from HSQC exp.: δ 127.6 (Ph-C-2, Ph-C-6), 127.4 (Ph-C-3, Ph-C-5), 78.9 (C-1), 73.8 (C-5), 72.9 (C-3), 70.6 (C-2), 68.2 (C-4), 61.8 (C-6), 45.8 (Ph-C), 20.6-20.4 (OAc).

Synthesis of (4-((2-(3-Formyl-4-(methoxymethoxy)phenyl)acetamido)methyl)benzamido)-2,3,4,6-tetra-O-acetyl-β-D-glucopyranose 37 - The amine **36** (60.1 mg, 0.126 mmol, 1 eq) and the acid **14** (28.2 mg, 0.126 mmol, 1 eq) were coupled according to the general procedure for coupling and the product was purified by flash chromatography on silica gel (n-Hex/Acetone 7:3 to 5:5) affording **37** as a yellow oil. Y = 25%. R_f (n-Hex/Acetone 1:1) = 0.37. MS (ESI) calcd C₃₃H₃₈N₂O₁₄ [M+Na]⁺ m/z: 709.22; found 709.10. ¹H NMR (400 MHz, CDCl₃) δ 10.45 (s, 1H, COH), 7.68 (m, 3H, Ph-H-2 + Ph-

H-6 + Ph(SA)-H-2), 7.50 (dd, $J = 8.6$ Hz, $J = 2.3$ Hz, 1H, Ph(SA)-H-6), 7.25 – 7.19 (m, 2H, Ph-H-3 + Ph-H-5 + Ph(SA)-H-5), 7.14 (d, $J = 9.0$ Hz, 1H, Fuc-NHCO), 6.03 (brs, 1H, NHCO), 5.46 – 5.31 (m, 2H, H-1 + H-3), 5.29 (s, 2H, OCH₂ MOM), 5.07 (m, 2H, H-2 + H-4), 4.45 (d, $J = 5.9$ Hz, 2H, Ph(SA)-CH₂), 4.31 (dd, $J = 12.5$ Hz, $J = 4.3$ Hz, 1H, H-6), 4.09 (dd, $J = 12.5$ Hz, $J = 1.7$ Hz, 1H, H-6'), 3.91 – 3.84 (m, 1H, H-5), 3.58 (s, 2H, Ph-CH₂), 3.51 (s, 3H, OCH₃ MOM), 2.06 (s, 3H, OAc), 2.04 (s, 3H, OAc), 2.03 (s, 3H, OAc), 2.01 (s, 3H, OAc). ¹³C chemical shifts extrapolated from HSQC exp.: 136.8 (Ph(SA)-C-6), 128.5 (Ph(SA)-C-2), 127.7 (Ph-C-2, Ph-C-6), 127.6 (Ph-C-3, Ph-C-5), 115.8 (Ph(SA)-C-5), 94.4 (OCH₂ MOM), 78.7 (C-1), 72.6 (C-3), 73.4 (C-5), 70.8 (C-4), 68.2 (C-2), 61.4 (C-6), 56.5 (OCH₃ MOM), 43.1 (Ph-CH₂), 42.5 (Ph(SA)-CH₂), 20.6-20.4 (OAc).

Synthesis of (4-((2-(3-formyl-4-(methoxymethoxy)phenyl)acetamido)methyl)benzamido)- β -D-glucopyranose 22 - Compound **37** (41.2 mg, 0.06 mmol) was dissolved in a 4:1 mixture of 96% ethanol and CHCl₃, and conc. HCl (10 eq) was added (EtOH/CHCl₃/HCl 4:1:1). The reaction mixture was stirred at 40°C until complete deprotection, as verified by TLC (CH₂Cl₂/MeOH 95:5). The solvents were removed under reduced pressure, and the residue was subjected to flash column chromatography to afford **22**, which was purified by automatic RP flash chromatography (SFAR C18 D, from 100% H₂O to H₂O/CH₃CN 1:1). Y = 40%. R_f (H₂O/CH₃CN 1:1) = 0.57. Samples for interaction studies were further purified by semi-preparative RP-HPLC (H₂O + 0.1% TFA/CH₃CN) with gradient: 0-1 min, 10-20%; 1-10 min, 20-50%, 10-13 min, 50-100%. tr = 8.22 min. HRMS (ESI) calcd for C₂₃H₂₆N₂O₉ [M+Na]⁺ m/z: 497.1536; found: 497.1537. ¹H NMR (400 MHz, DMSO d₆) δ 10.26 (s, 1H, COH), 8.76 (d, $J = 8.9$ Hz, 1H, Glc-NHCO), 8.59 (brs, 1H, NHCO), 7.85 (d, $J = 7.9$ Hz, 2H, Ph-H-2 + Ph-H-6), 7.59 (s, 1H, Ph(SA)-H-2), 7.44 (d, $J = 8.5$ Hz, 1H, Ph(SA)-H-6), 7.30 (d, $J = 8.0$ Hz, 2H, Ph-H-3 + Ph-H-5), 6.95 (d, $J = 8.4$ Hz, 1H, Ph(SA)-H-5), 5.02 – 4.85 (m, 4H, H-1 + 3xOH), 4.49 (m, 1H, OH), 4.33 (d, $J = 5.9$ Hz, 2H, Ph-CH₂), 3.68 (dd, $J = 11.5$ Hz, $J = 5.4$ Hz, 1H, H-6), 3.45 (m, 3H, Ph(SA)-CH₂ + H-6'), 3.35-3.33 (H-2, under H₂O peak, extrapolated from COSY and HSQC) 3.27 – 3.07 (m, 3H, H-3 + H-4 + H-5). ¹³C NMR (100 MHz, DMSO d₆) δ 191.8 (COH), 170.8 (NHCO), 166.8 (NHCO), 159.9 (Ar quat), 143.5 (Ar quat.), 137.6 (Ph(SA)-C-6), 133.1 (Ar quat.), 129.5 (Ph(SA)-C-2), 128.1 (Ph-C-2, Ph-C-6), 127.8 (Ar quat.), 127.2 (Ph-C-3, Ph-C-5), 117.6 (Ph(SA)-C-5), 80.7 (C-1), 79.2 (C-3), 78.1 (C-5), 72.6 (C-2), 70.6 (C-4), 61.5 (C-6), 42.3 (Ph-CH₂), 41.5 (Ph(SA)-CH₂).

2.5 Synthesis of compound **A12** (Table SI-1)



Synthesis of (2-(3-formyl-4-hydroxyphenyl)acetamido)- β -L-fucopyranose **A12**

Staudinger ligation of fucosyl azide **6** (69.3 mg, 0.22 mmol, 1 eq) and acid **14** (49.3 mg, 0.22 mmol, 1 eq) according to the general procedure for Staudinger ligation afforded the fully protected coupling product, which was purified by flash chromatography on silica gel (CH₂Cl₂/AcOEt 9:1 to 7:3) to a white foam. Y = 40%. R_f (n-Hex/AcOEt 1:1) = 0.23. MS (ESI) calcd C₂₃H₂₉NO₁₁ [M+Na]⁻ m/z: 494.16; found: 494.41. ¹H NMR (400 MHz, CDCl₃) δ 10.48 (s, 1H, COH), 7.66 (d, *J* = 2.1 Hz, 1H, Ph-H-2), 7.42 (dd, *J* = 8.6 Hz, *J* = 2.2 Hz, 1H, Ph-H-6), 7.22 (d, *J* = 8.6 Hz, 1H, Ph-H-5), 6.30 (d, *J* = 8.9 Hz, 1H, NHCO), 5.30 (s, 2H, OCH₂ MOM), 5.25 (d, *J* = 3.4 Hz, 1H, H-4), 5.18 – 4.97 (m, 3H, H-1 + H-2 + H-3), 3.91 (q, *J* = 6.3 Hz, 1H, H-5), 3.51 (m, 6H, Ph-CH₂ + OCH₃ MOM), 2.14 (s, 3H, OAc), 1.96 (s, 3H, OAc), 1.93 (s, 3H, OAc), 1.17 (d, *J* = 6.3 Hz, 3H, H-6).

The protected intermediate was dissolved in a 4:1 mixture of 96%-ethanol and CHCl₃, and conc. HCl (10 eq) was added (EtOH/CHCl₃/HCl 4:1:1). The reaction mixture was stirred at room temperature until complete deprotection, as verified by TLC (CH₂Cl₂/MeOH 9:1). The solvents were removed under reduced pressure, and the residue was subjected to flash column chromatography on silica gel (CH₂Cl₂/MeOH 90:10 to 85:15) to afford **A12**. Y = 61%. R_f (CH₂Cl₂/MeOH 9:1) = 0.27. MS (ESI) calcd C₁₅H₁₉NO₇ [M+Na]⁻ m/z: 324.32; found: 324.28. ¹H NMR (400 MHz, DMSO d₆) δ 10.23 (s, 1H, COH), 8.56 (d, *J* = 9.0 Hz, 1H, NHCO), 7.52 (d, *J* = 2.2 Hz, 1H, Ph-H-2), 7.39 (dd, *J* = 8.5 Hz, *J* = 2.3 Hz, 1H, Ph-H-6), 6.91 (d, *J* = 8.5 Hz, 1H, Ph-H-5), 4.62 (t, *J* = 8.8 Hz, 1H, H-1), 3.65 – 3.16 (m, 6H, H-4 + H-5 + H-2 + H-3 + Ph-CH₂), 1.05 (d, *J* = 6.4 Hz, 1H, H-6). ¹³C NMR (100 MHz, DMSO d₆) δ 191.9 (COH), 171.0 (NHCO), 137.8 (Ph-C-6), 129.7 (Ph-C-2), 127.2 (Ar quat.), 122.40 (Ar quat.), 117.7 (Ph-C-5), 80.4 (C-1), 74.7 (C-3), 71.92 (C-5), 71.6 (C-4), 69.8 (C-2), 41.4 (Ph-CH₂), 17.2 (C-6).

3. Thermal Shift Assays

Figure SI-3. First derivatives of fluorescence curves obtained from TSA experiments

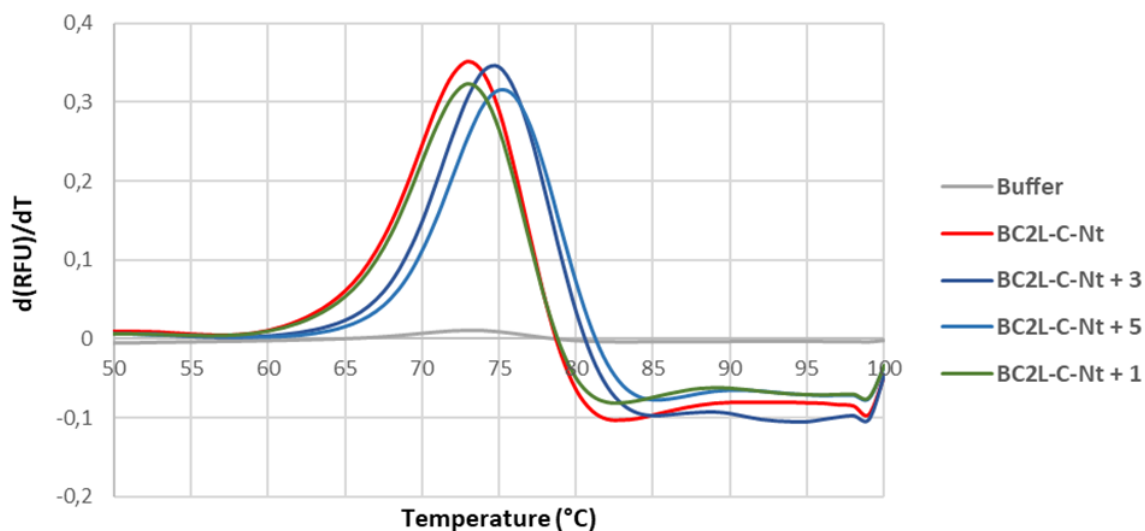


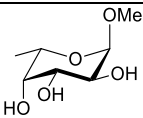
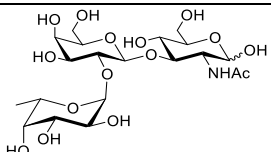
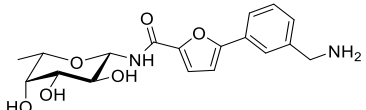
Figure SI-3. First derivatives of fluorescence curves obtained from TSA experiments. Data were obtained by measuring SYPRO Orange dye fluorescence over a temperature range of 20 to 100°C. RFU = relative fluorescence unit.

The thermal stability of BC2L-C-Nt in the presence of **1**, **3** and **5** was analyzed by TSA using a MiniOpticon real-time PCR system (Bio-Rad Ltd). The measurements were performed in 96-well PCR microplates with 25 μ L of mix containing 0.6 mg/mL of Bc2L-C-Nt, 10 \times Sypro Orange dye (Merk Sigma-Aldrich) and 0.21 mM ligand in 25mM Hepes pH 8.0 and 150 mM NaCl after centrifugation at 1000g for 2 min. Samples were incubated at room temperature for 2 h before running the experiments. A temperature gradient from 20 to 100 $^{\circ}$ C was applied with a heating rate of 1 $^{\circ}$ C/min and fluorescence intensity was measured with Ex/Em: 490/530 nm. The data processing was performed with the CFX Manager software.

The addition of the non-covalent ligand **1** produced no variation of the protein denaturation temperature (\sim 73 $^{\circ}$ C for both the protein alone (red curve) and in the presence of **1** (green curve)). In the presence of **3** or **5**, a positive shift of about 2 $^{\circ}$ C was observed (curves in blue, with Tm \sim 75 $^{\circ}$ C), suggesting a strong and stabilizing interaction, which may correspond to the presence of a covalent bond between ligand and protein.

4. Validation of SPR competition assays: comparison with ITC experiments

Table SI-4. K_D values from ITC experiments for compounds 1, 23 and 24

Entry	Ligand	K_D (μM)	
		SPR	ITC
1	α-methyl-L-fucoside  24	----	2700 ± 700^a
2	H-type 1  23	19.9 ± 0.31^b	25.4 ± 4.5^c
3	1 	103 ± 5^b	159 ± 7^a

a. From ref 4⁴; b. This work; c. from ref 12.¹²

5. SPR competition assays – sensorgrams and inhibition curves

Figure SI-4. BC2L-C-Nt titration over the fucosylated surface

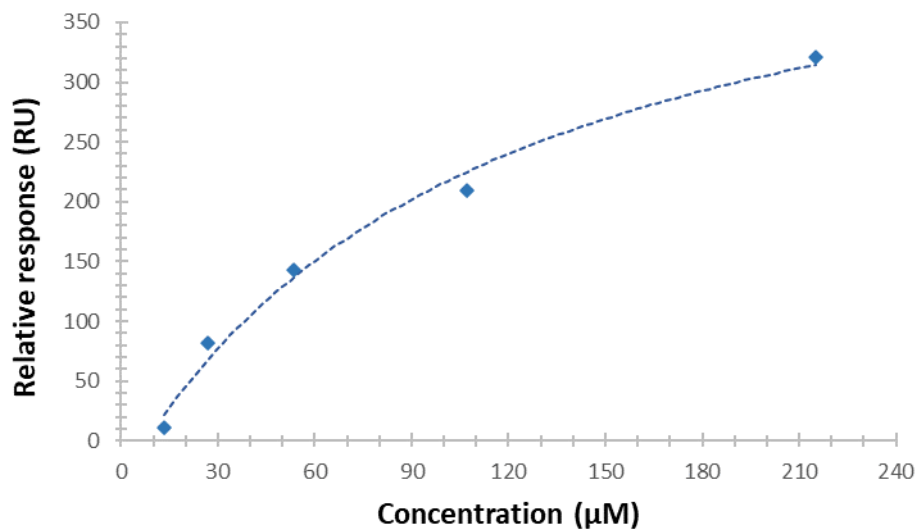


Figure SI-4. BC2L-C-Nt titration over the fucosylated chip used in the SPR competition experiments.

Figure SI-5. SPR sensorgrams

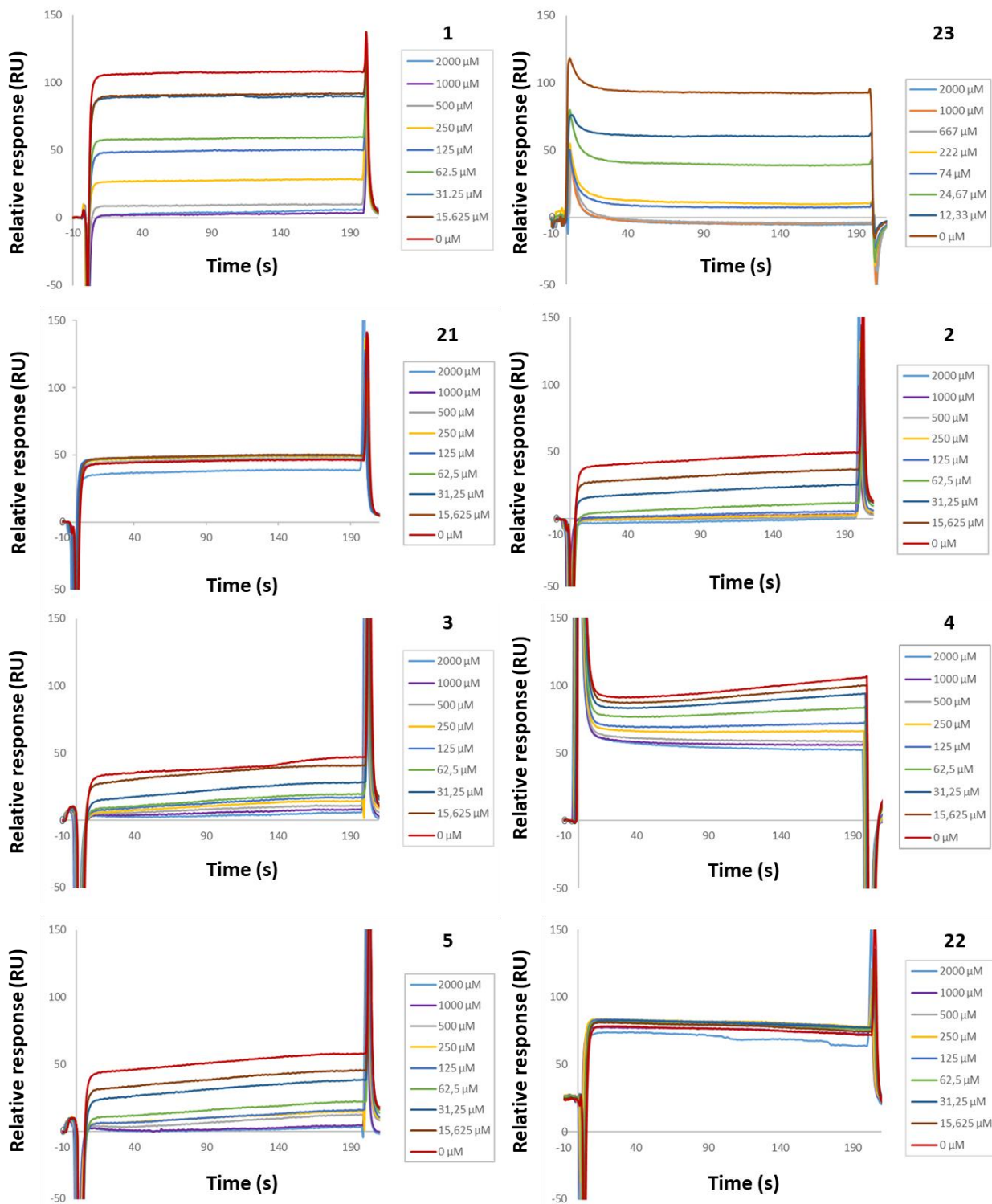


Figure SI-5. Sensorgrams of covalent ligands 2-5, non-covalent compound 1, trisaccharide H-type 1 23 and negative controls 21 and 22.

Figure SI-6. Inhibition curves

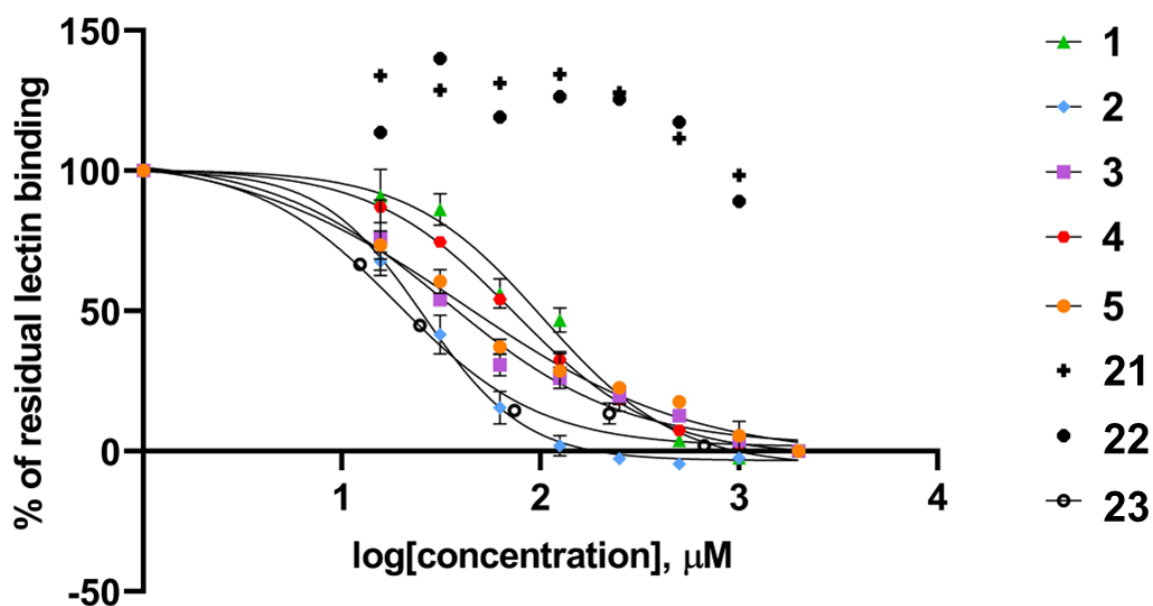


Figure SI-6. Inhibition curves of covalent ligands 2-5, non-covalent compound 1, H-type 1 trisaccharide 23 and negative controls 21 and 22. For each compound analyses were performed in duplicate, and errors are reported as bars for each point. For the negative controls 21 and 22, the 100% of relative inhibition was not reached and the estimated IC_{50} value is higher than 2 mM. The curves were obtained with the GraphPad Prism program (version 8.0.2) by fitting the data to a variable slope 4 parameter fit.

6. Mass MALDI-TOF analysis – additional spectra

Figure SI-7. MALDI-TOF spectra of a 1:10 mixture of protein and ligand 2

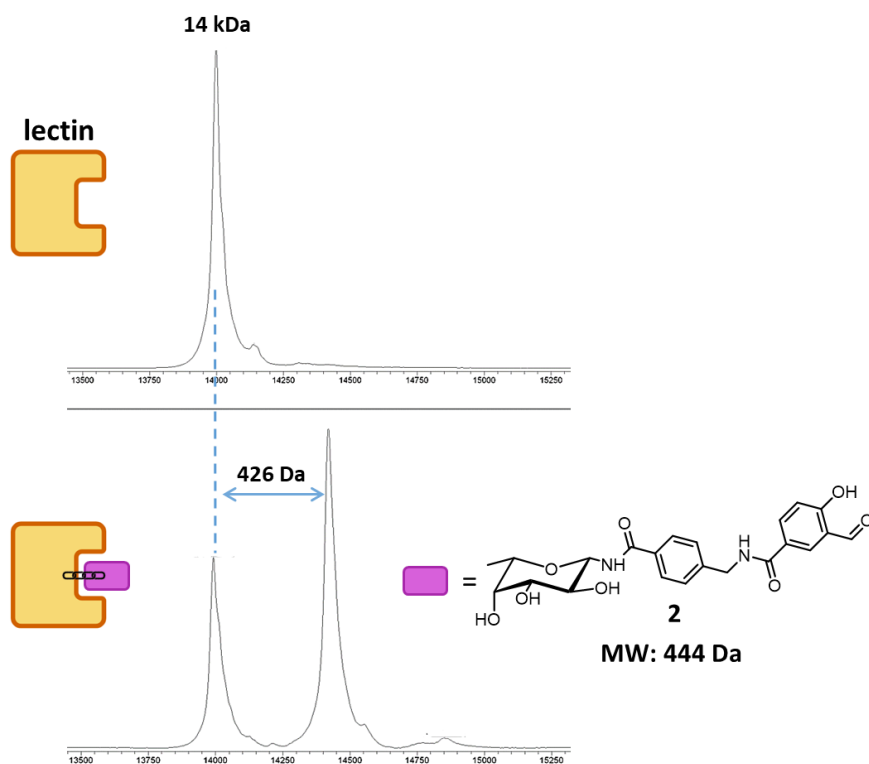


Figure SI-7. Enlarged section of MALDI-TOF spectra of protein alone (top) and in the presence of ligand 2 (bottom) with protein:ligand ratio = 1:10.

Figure SI-8. MALDI-TOF spectra of a 1:4 mixture of protein and ligand 4

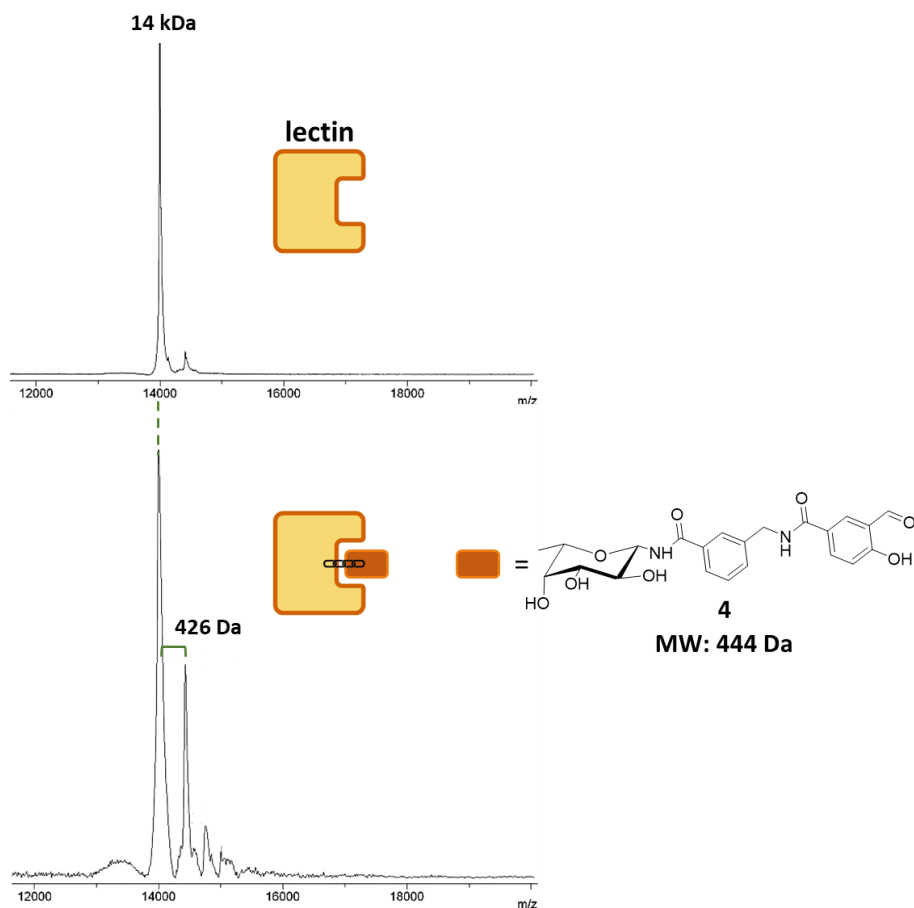


Figure SI-8. Enlarged section of MALDI-TOF spectra of protein alone (top) and in the presence of ligand 4 (bottom) with protein:ligand ratio = 1:4.

Figure SI-9. MALDI-TOF spectra of a 1:200 mixture of protein and ligand 5

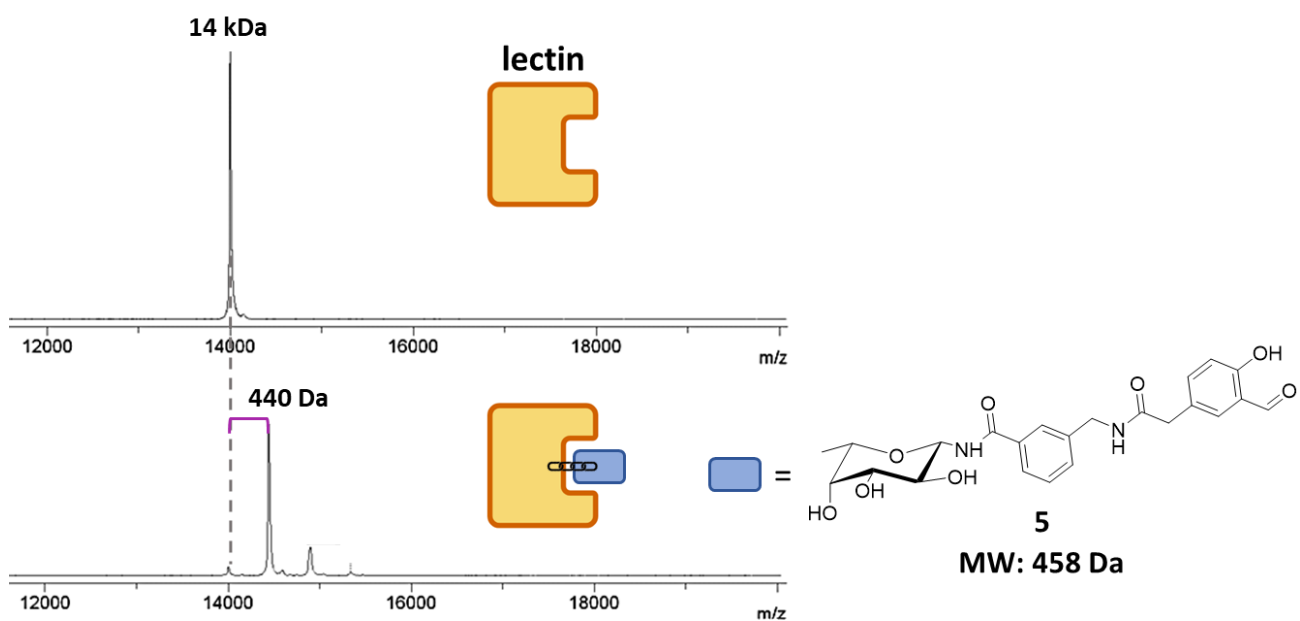


Figure SI-9. Enlarged section of MALDI-TOF spectra of protein alone (top) and in the presence of ligand 5 (bottom) with protein:ligand ratio = 1:200.

Figure SI-10. MALDI-TOF spectra of a 1:10 mixture of protein and ligand **3** after 2 h incubation

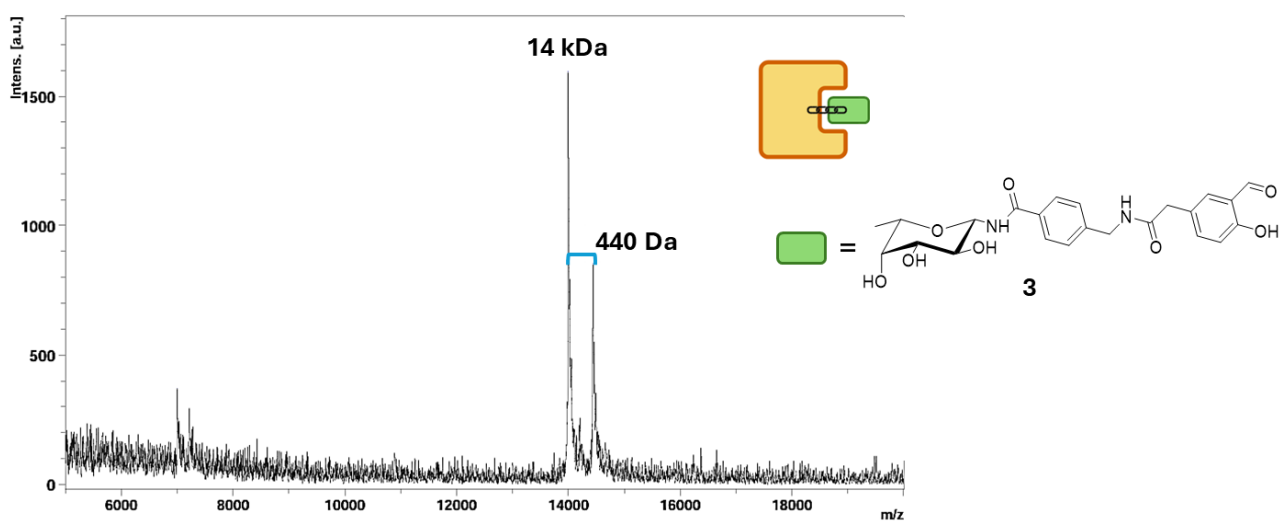


Figure SI-10. MALDI-TOF spectra of protein in the presence of ligand **3** with protein:ligand ratio = 1:10, after 2 h of incubation.

Figure SI-11. MALDI-TOF spectra of a 1:200 mixture of protein and negative control **22**

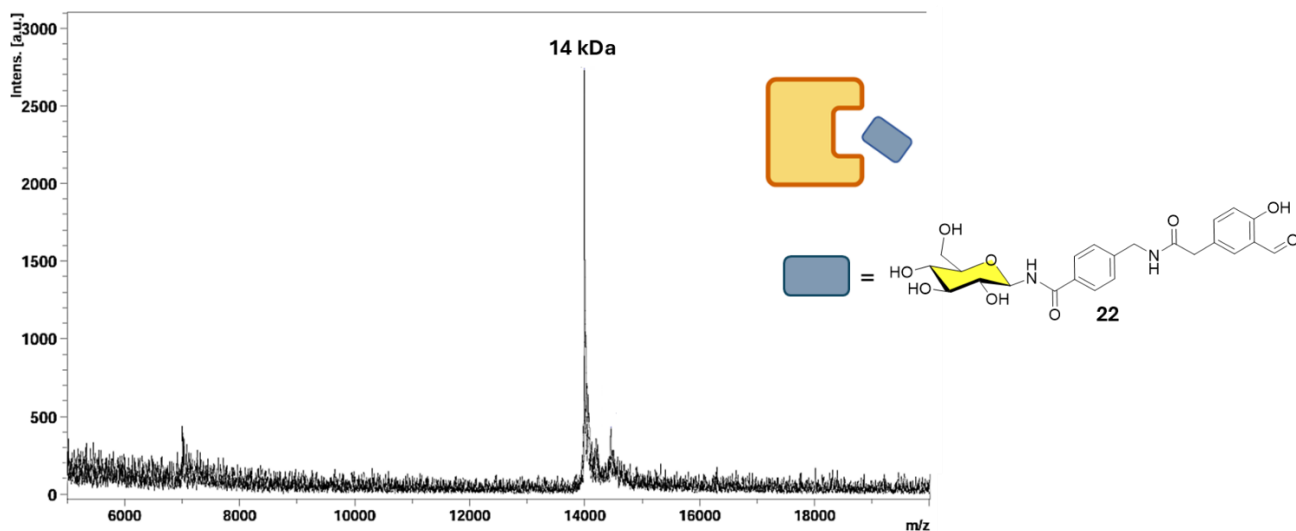


Figure SI-11. MALDI-TOF spectra of protein in the presence of negative control **22** with protein:ligand ratio = 1:200, after 24 h of incubation. It shows no evident additional peak other than that of the protein alone, indicating no covalent adduct formation.

Figure SI-12. MALDI-TOF spectra of a 1:200 mixture of protein and A12 (Table SI-1)

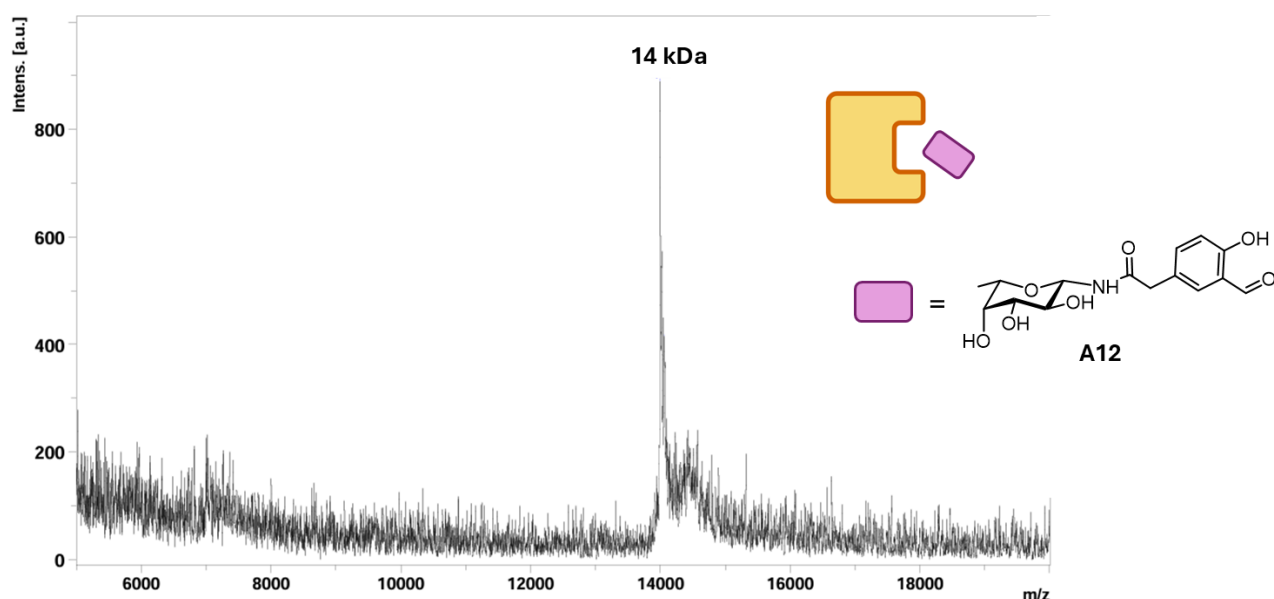


Figure SI-12. MALDI-TOF spectra of protein in the presence of negative control A12 with protein:ligand ratio = 1:200, after 24 h of incubation. It shows no evident additional peak other than that of the protein alone, indicating no covalent adduct formation.

7. LC-MS analysis of BC2L-C-Nt:2 complex after NaBH₄ reduction and Trypsin digestion

In the absence of ligand, trypsin digestion of the protein produced a large peptide fragment (79-104, VPESTGRMPFTLVATIDVGSQVTFVK) just upstream of Lys 108. Two additional short sequences were detected, GQW**K** (105-108, t_R 10.10 min, m/z 259.6397 ($z=2$)) and GQW**K**SVR (105-111, t_R 12.57 min, m/z 287.4961 ($z=3$)), both containing the target residue (in bold) (Figure SI-9). After incubation with **2** and NaBH₄ reduction, we found both these peptides modified by a mass shift of 428 Da, as GQW**K** (105-108 + C₂₂H₂₄N₂O₇; t_R 22.01 min, m/z 473.7195 ($z=2$)) and GQW**K**SVR (105-111 + C₂₂H₂₄N₂O₇; t_R 21.16 min, m/z 430.2161 ($z=3$)) (Figure SI-10), thus proving that the ligand is covalently linked to Lys108.

7.1 **Figure SI-13.** LC-MS analysis of the protein

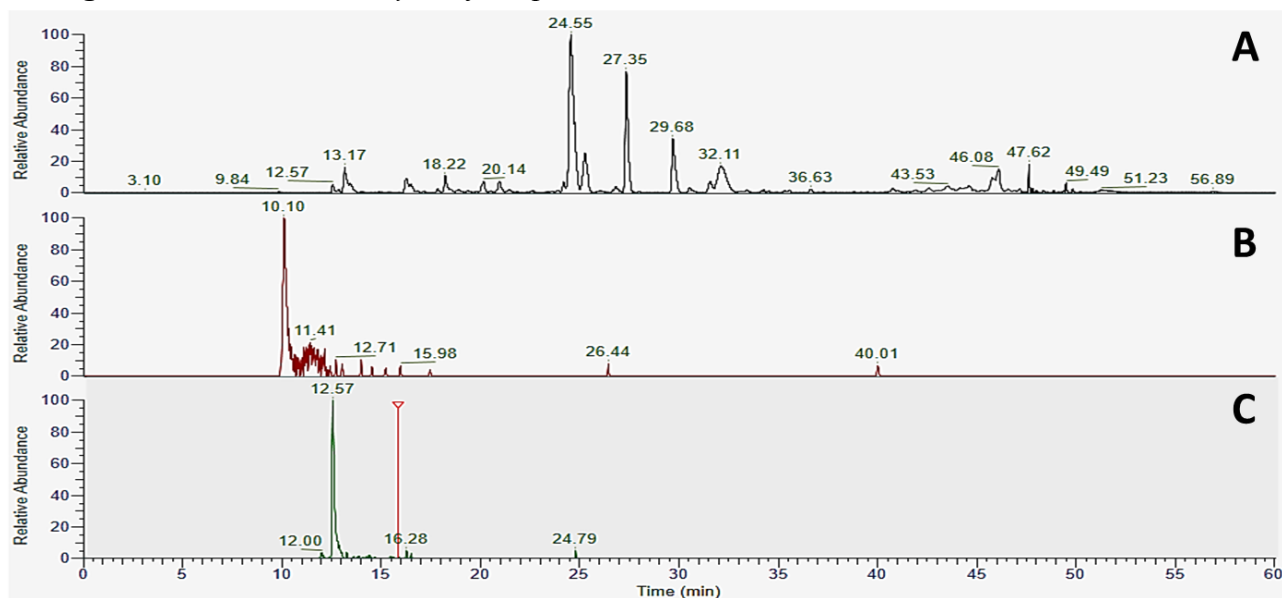


Figure SI-13. A) LC chromatogram of the protein alone after treatment with NaBH_4 and Trypsin. B) Extracted-ion chromatogram (XIC) at t_R 10.10 min. with m/z 259.6397 ($z=2$) corresponding to tetrapeptide **GQWK**. C) XIC at t_R 12.57 min. with m/z 287.4961 ($z=3$) corresponding to heptapeptide **GQWKSVR**.

7.2 **Figure SI-14.** LC-MS analysis of protein:2 mixture

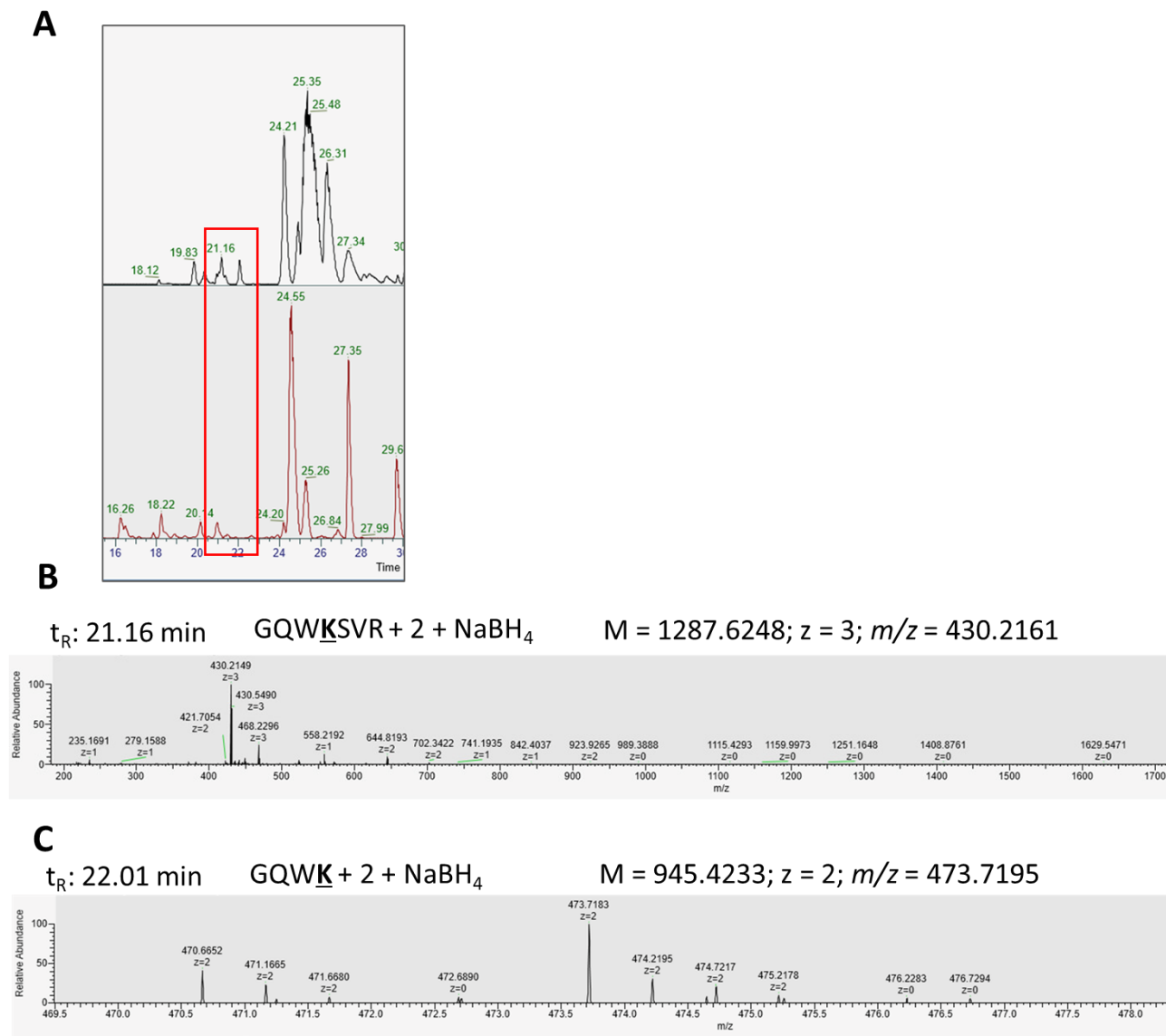
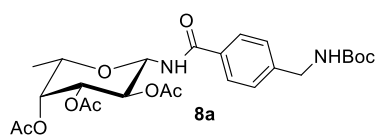
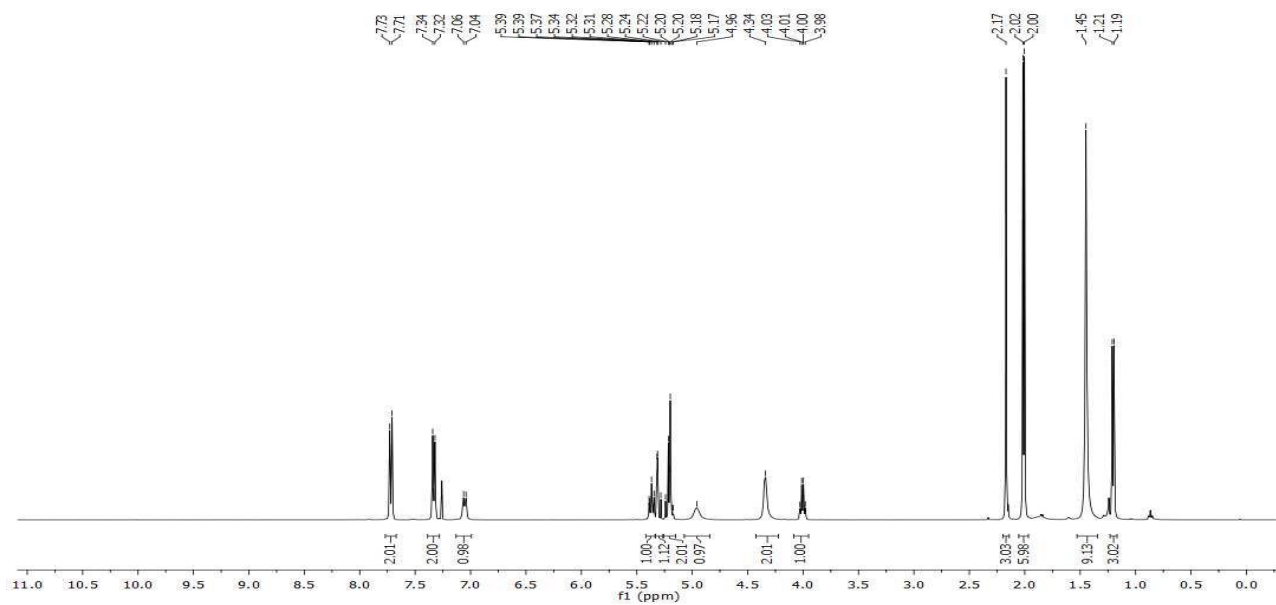


Figure SI-14. A) extracted portion of LC chromatogram of the protein:2 mixture (upper) and protein alone (lower) after treatment with NaBH_4 and Trypsin. The region where the modified tetrapeptide $\text{GQW}\underline{\text{K}}$ and heptapeptide $\text{GQW}\underline{\text{K}}\text{SVR}$ were detected is highlighted in red box. B) MS spectra of peak with $t_R = 21.16$ min., which corresponds to $\text{GQW}\underline{\text{K}}\text{SVR} + 2$; C) MS spectra of peak with $t_R = 22.01$ min., which corresponds to $\text{GQW}\underline{\text{K}} + 2$.

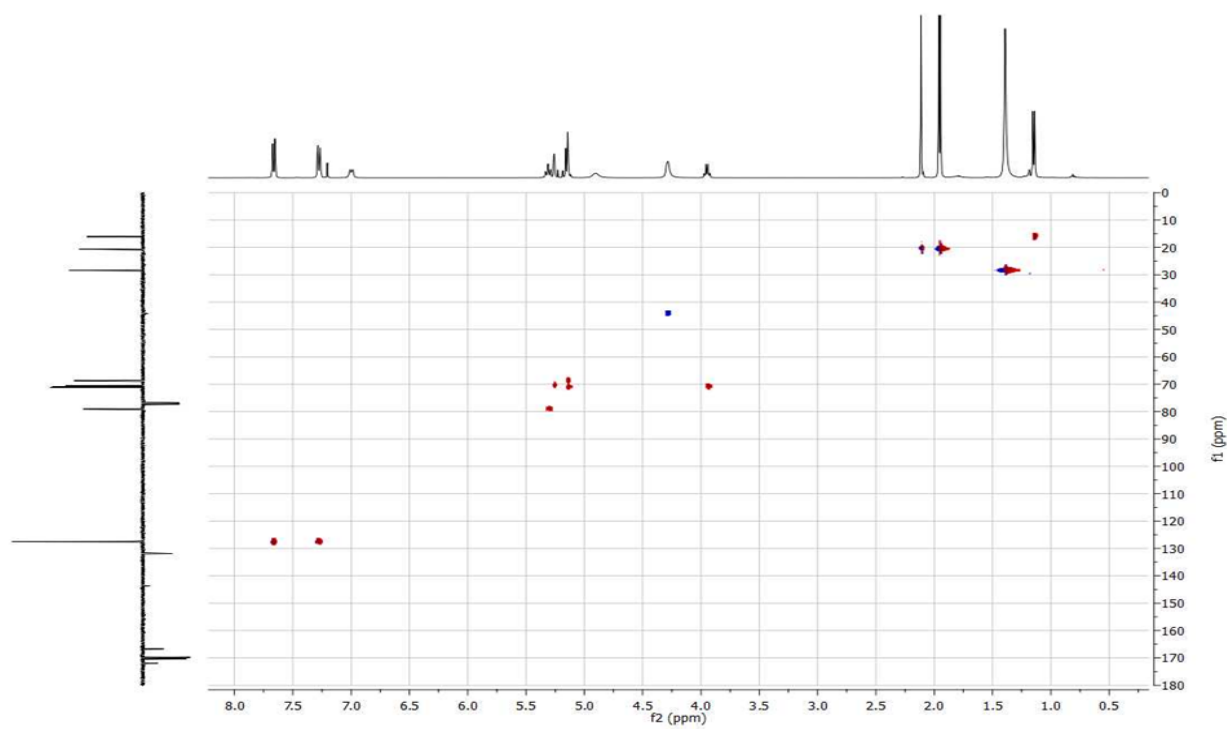
8. NMR spectra

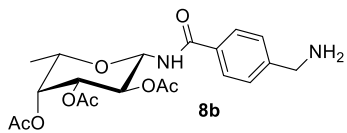


^1H NMR, 400 MHz, CDCl_3

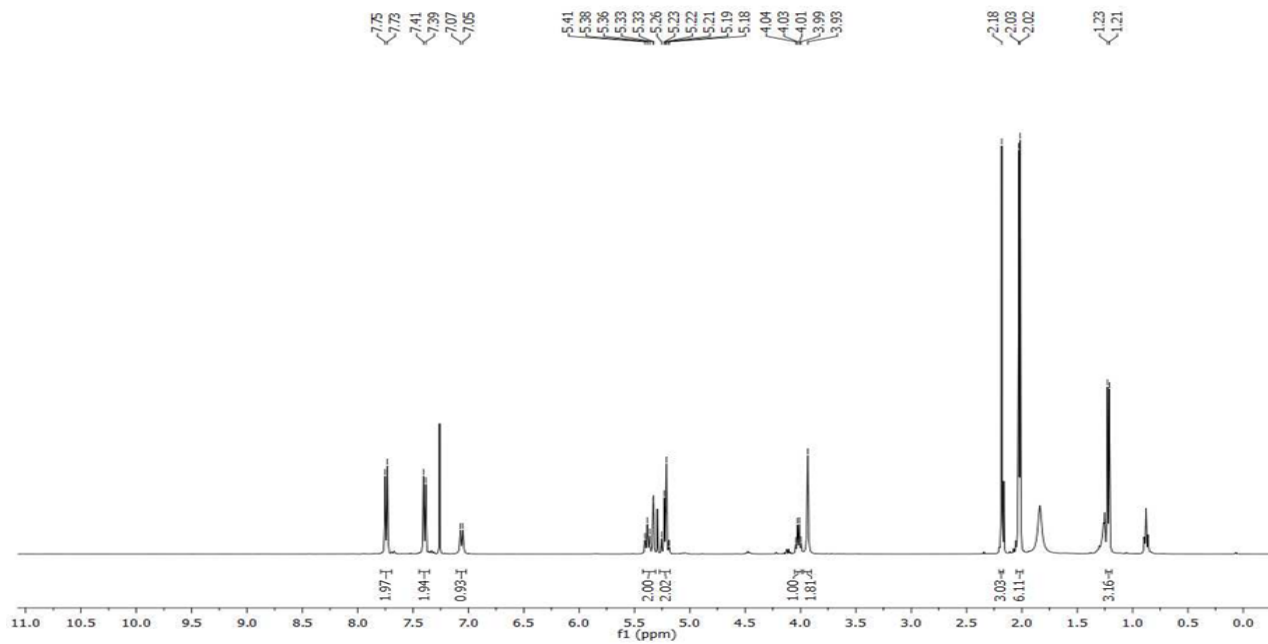


^1H - ^{13}C HSQC, CDCl_3

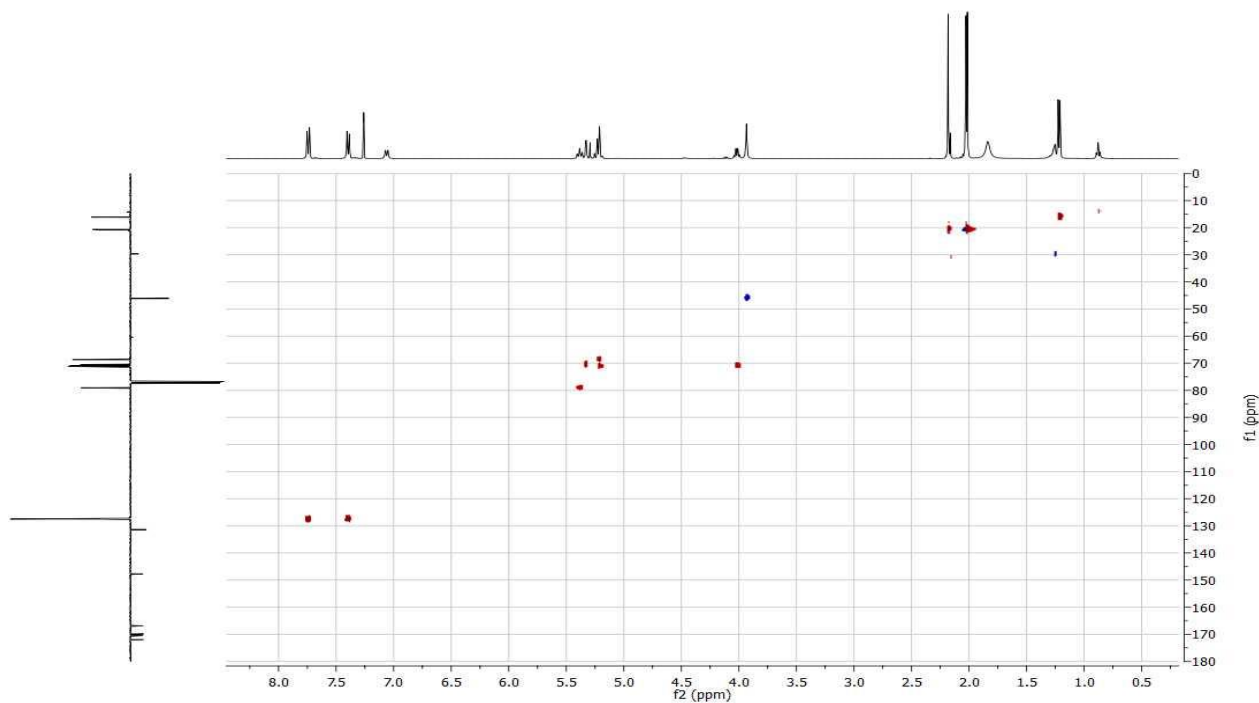


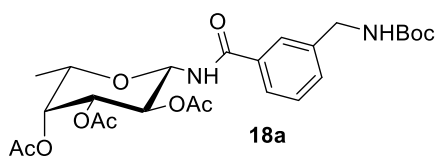


^1H NMR, 400 MHz, CDCl_3

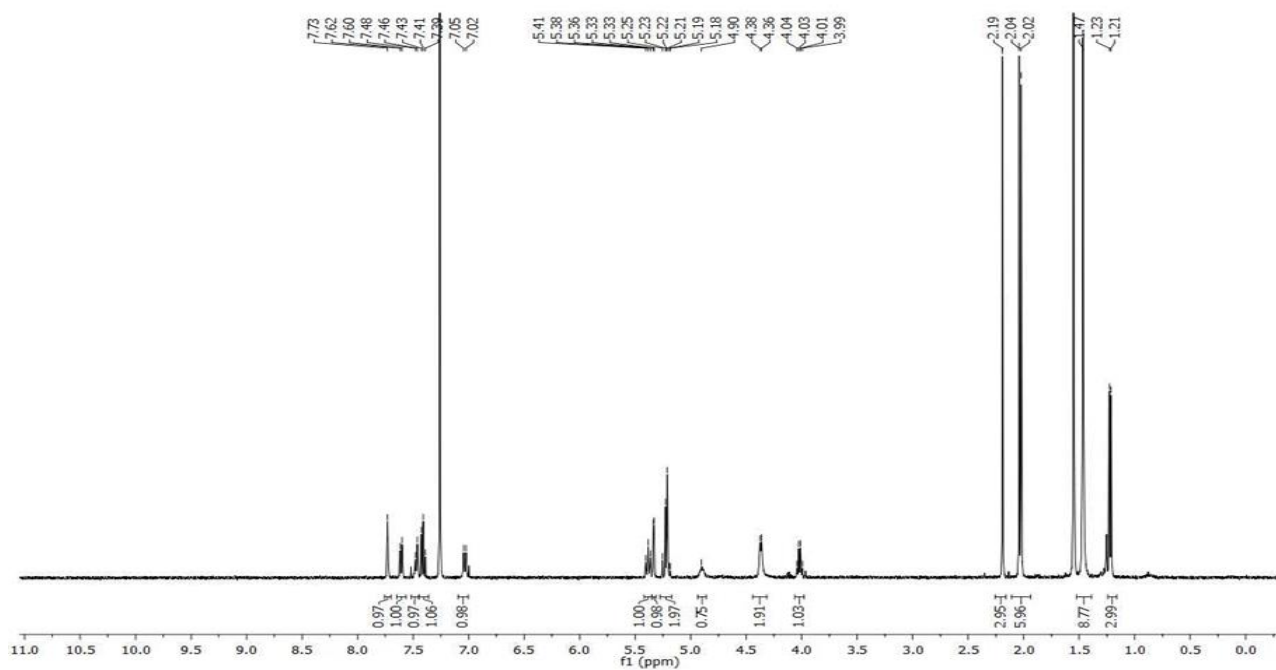


^1H - ^{13}C HSQC, CDCl_3

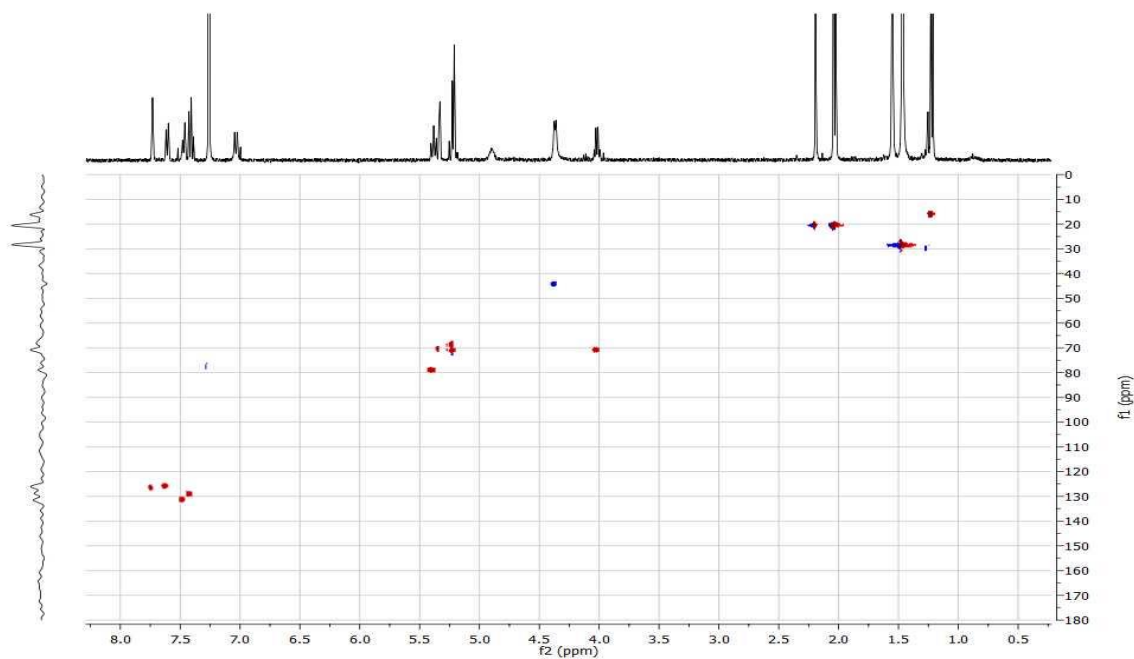


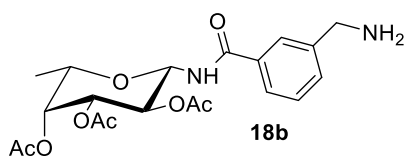


^1H NMR, 400 MHz, CDCl_3

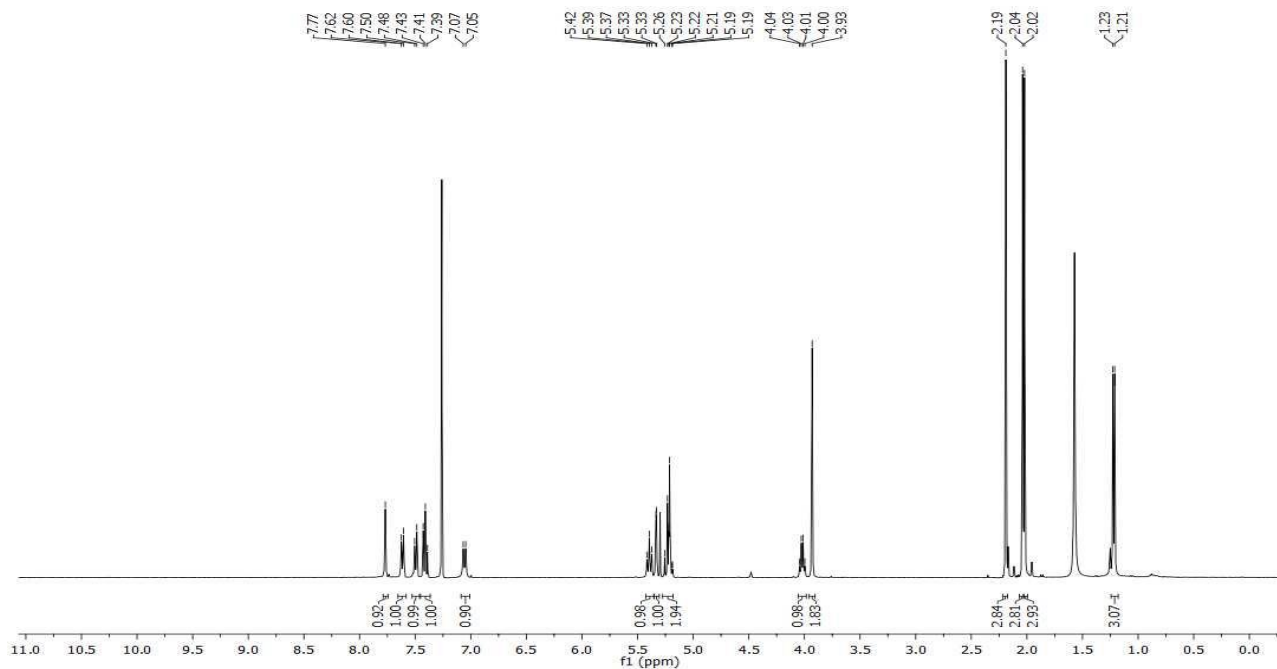


^1H - ^{13}C HSQC, CDCl_3

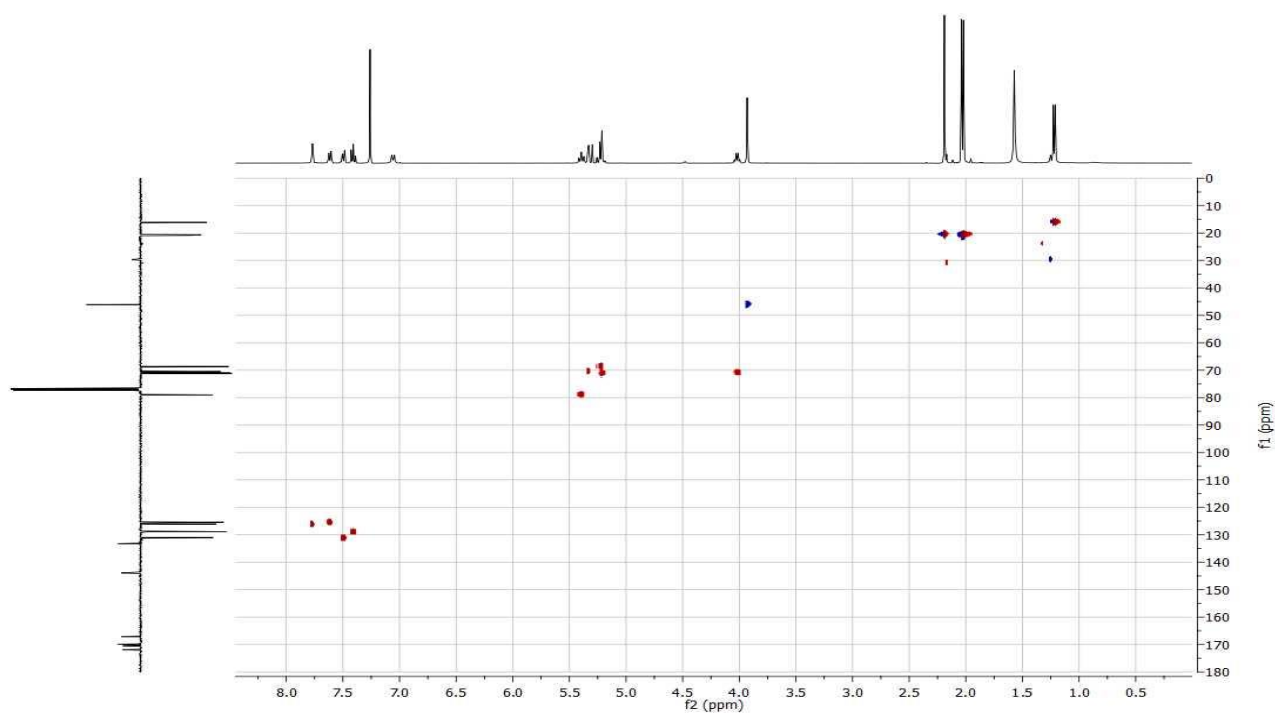


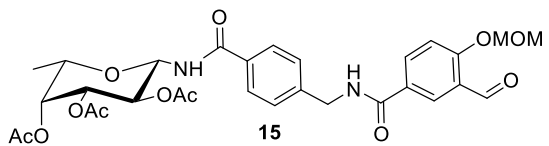


^1H NMR, 400 MHz, CDCl_3

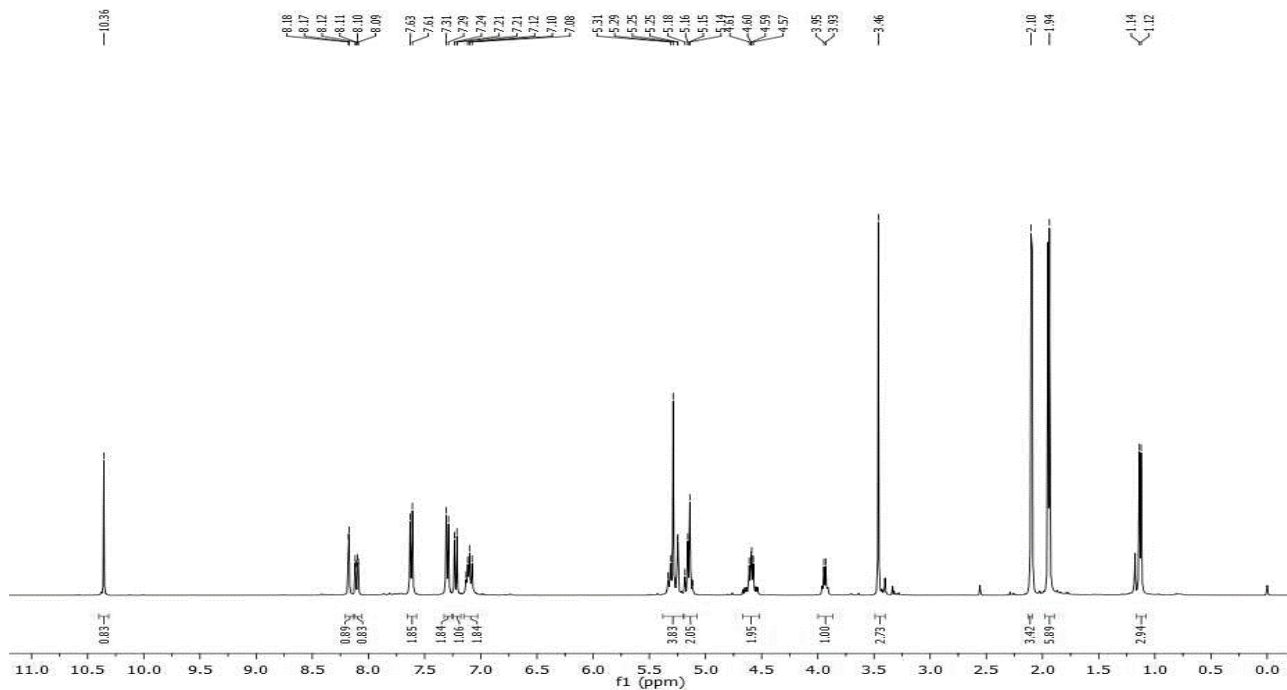


^1H - ^{13}C HSQC, CDCl_3

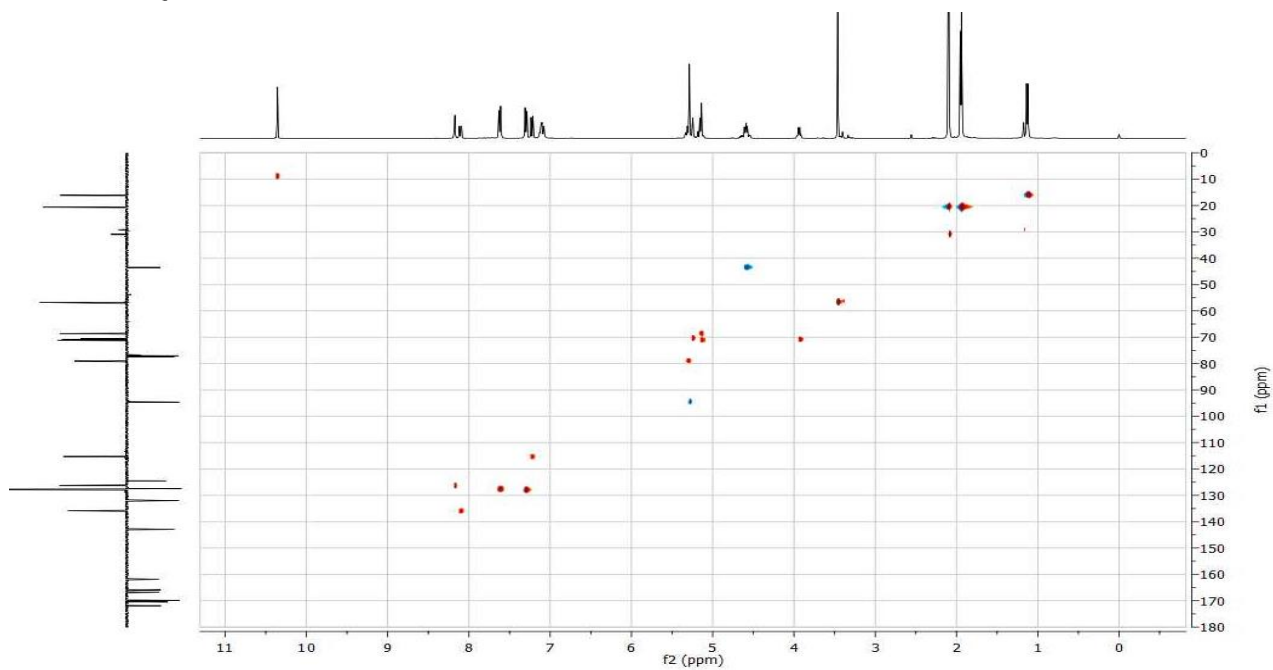


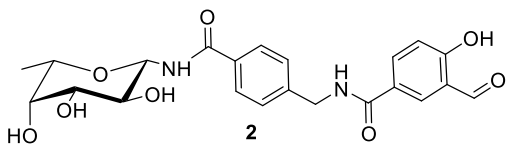


^1H NMR, 400 MHz, CDCl_3

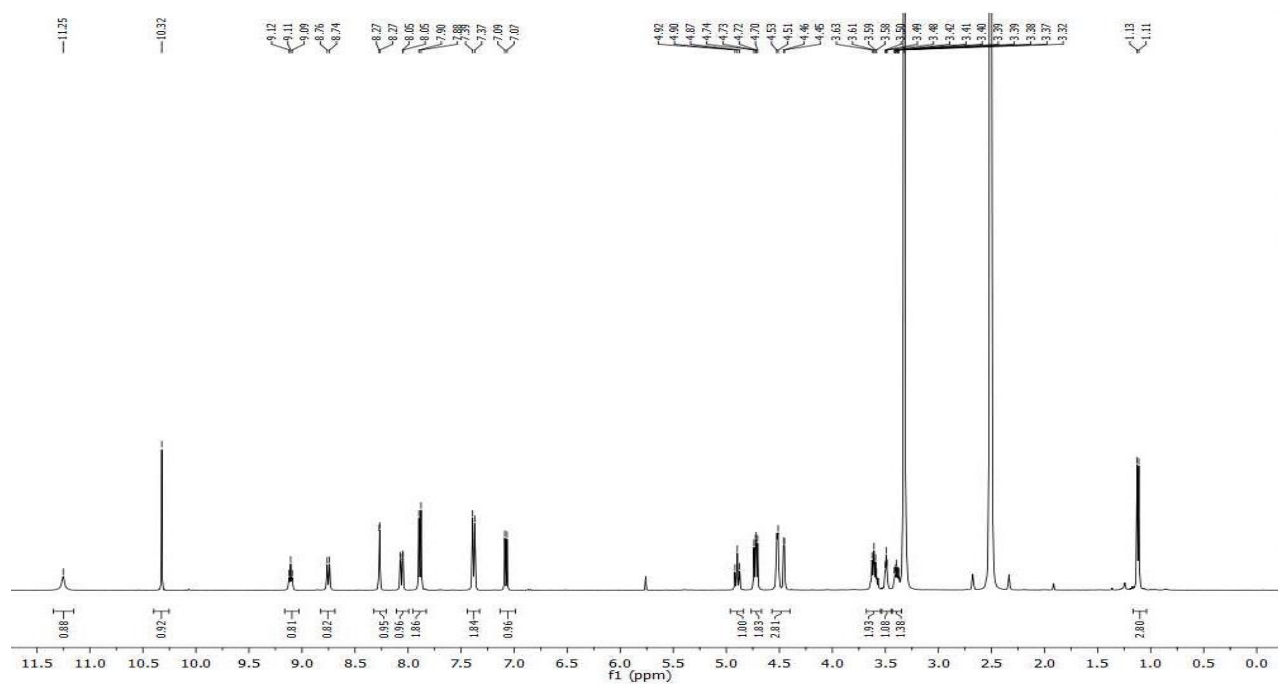


^1H - ^{13}C HSQC, CDCl_3

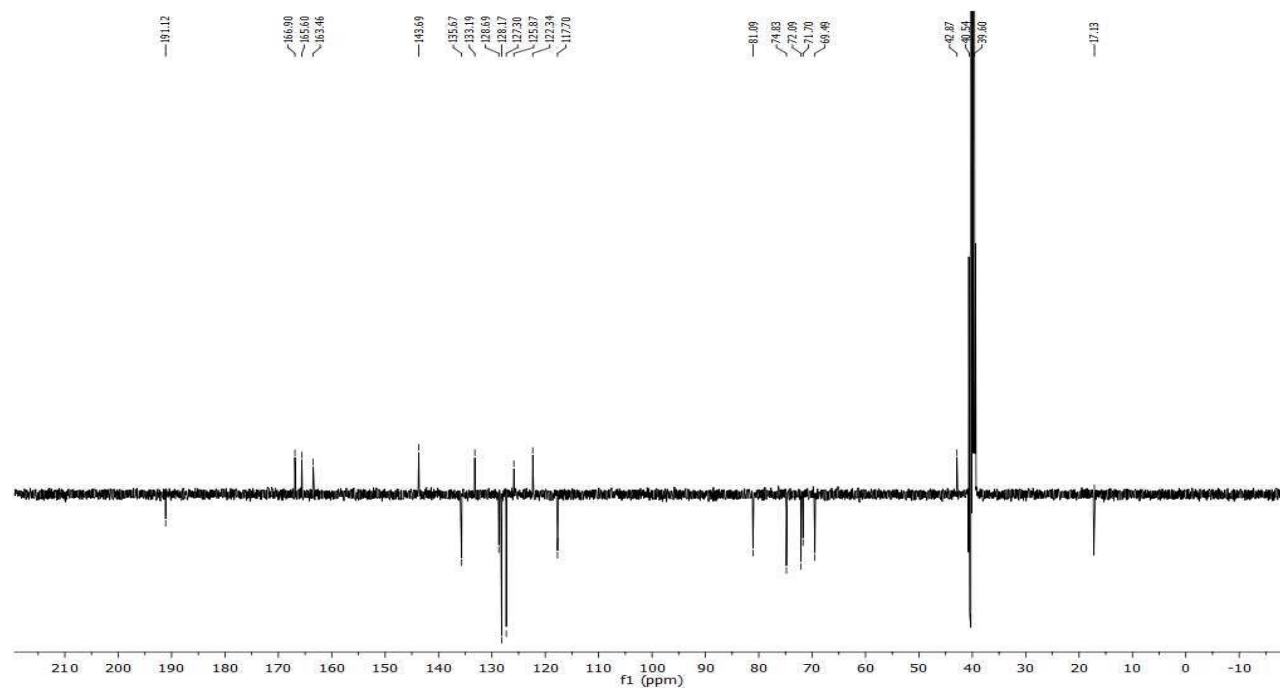


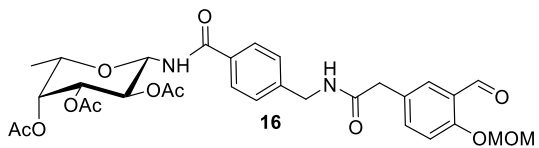


$^1\text{H NMR}$, 400 MHz, DMSO d_6

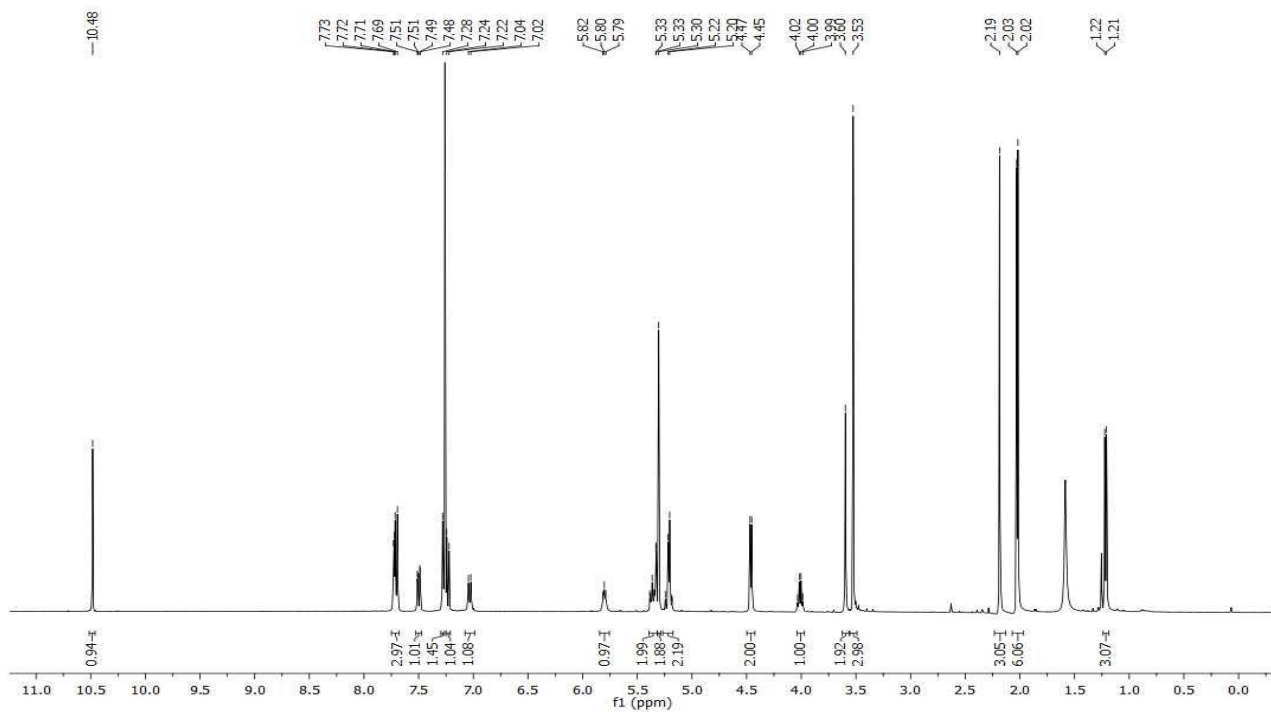


$^{13}\text{C NMR}$, 100 MHz, DMSO d_6

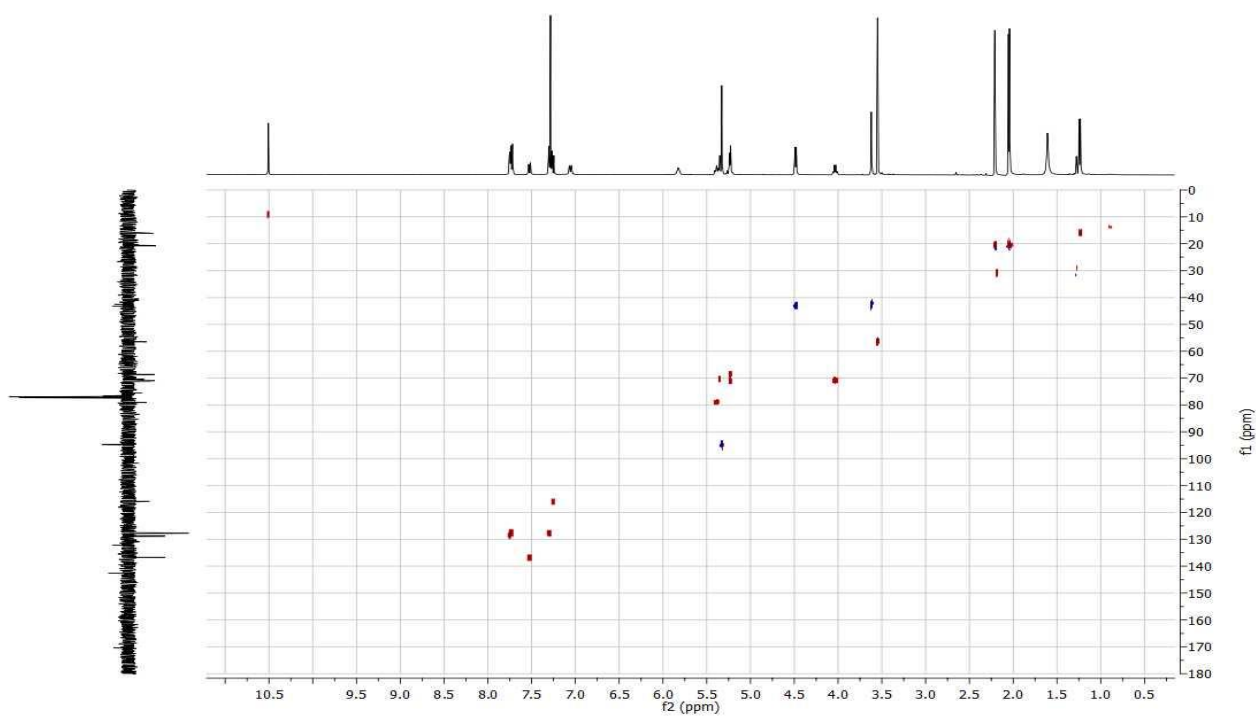


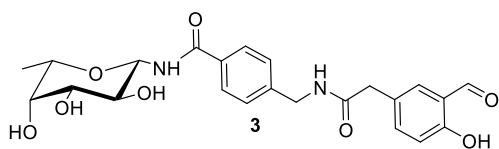


^1H NMR, 400 MHz, CDCl_3

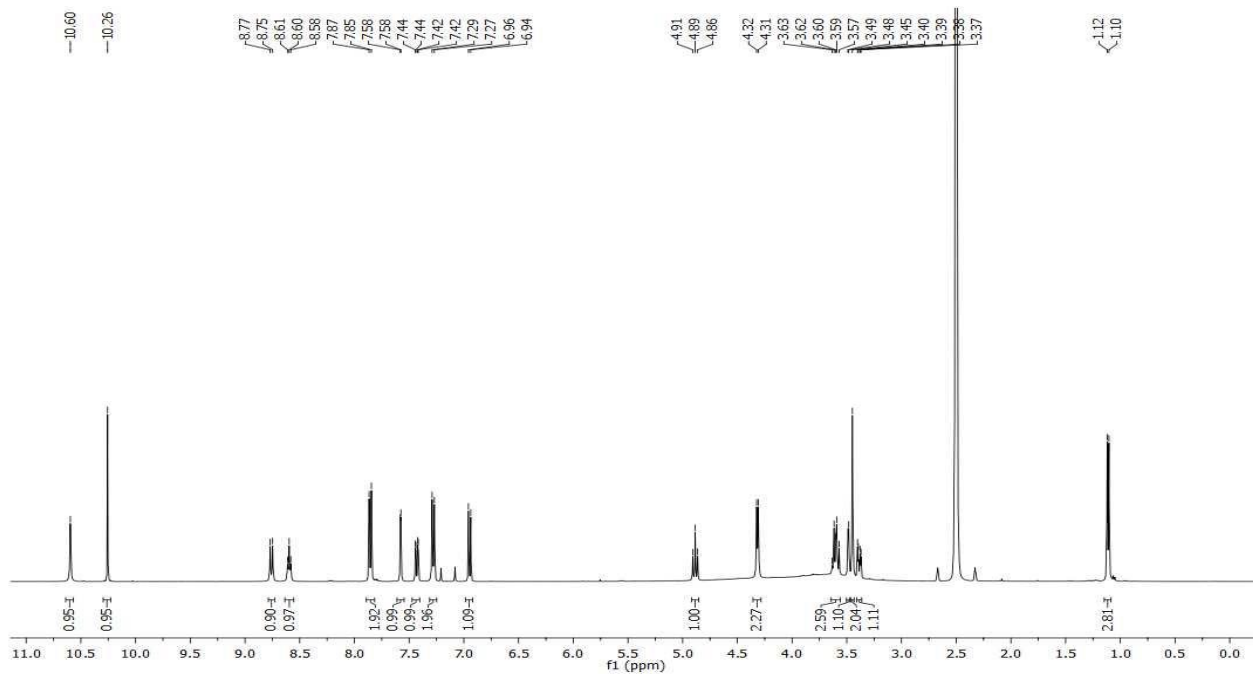


^1H - ^{13}C HSQC, CDCl_3

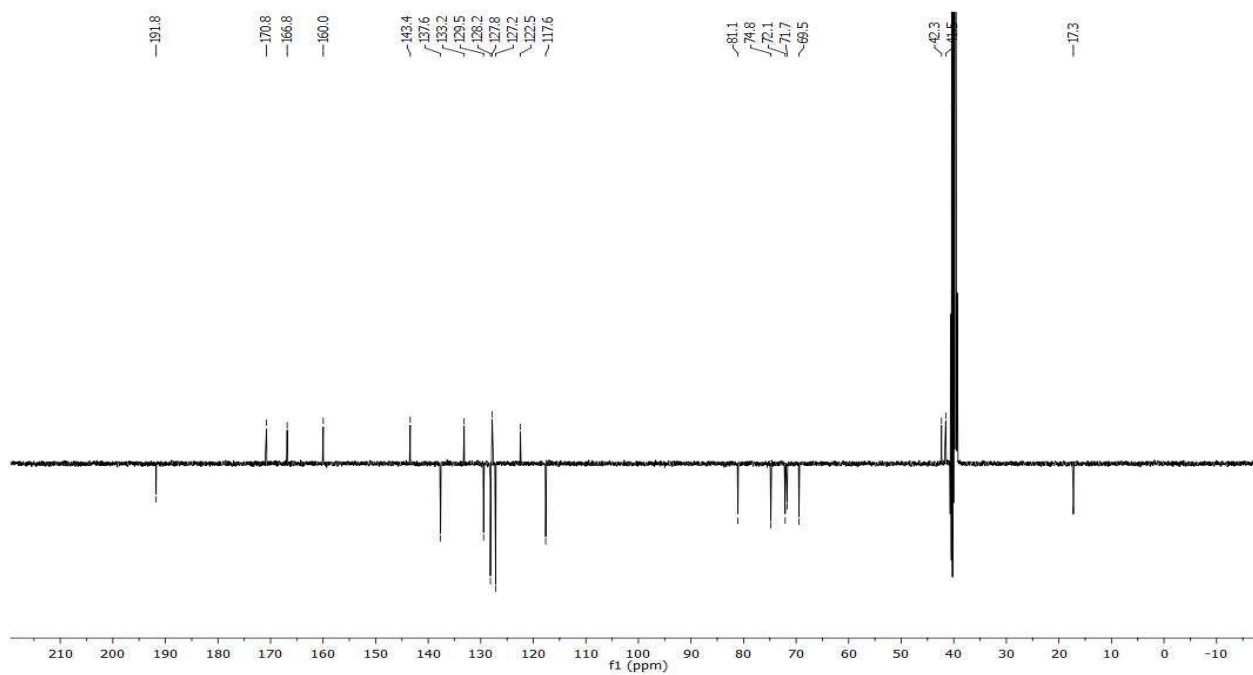


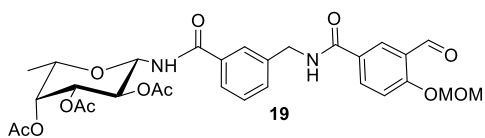


$^1\text{H NMR}$, 400 MHz, DMSO d_6

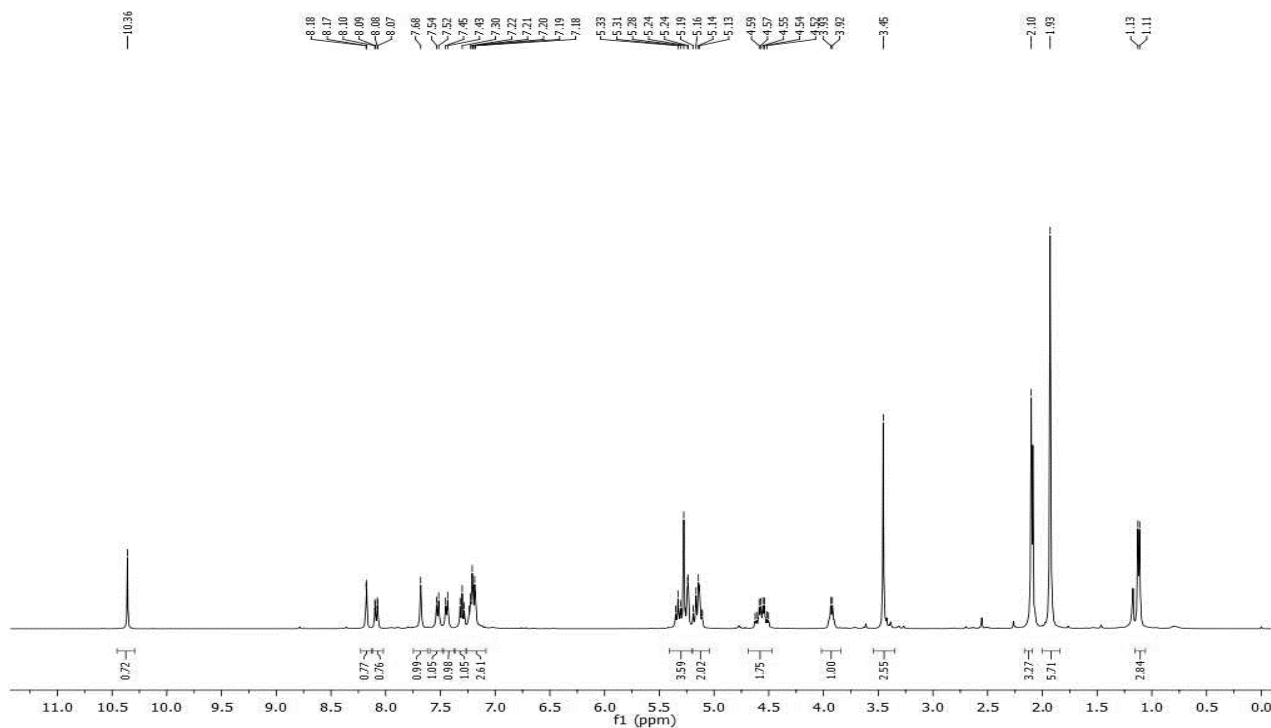


$^{13}\text{C NMR}$, 100 MHz, DMSO d_6

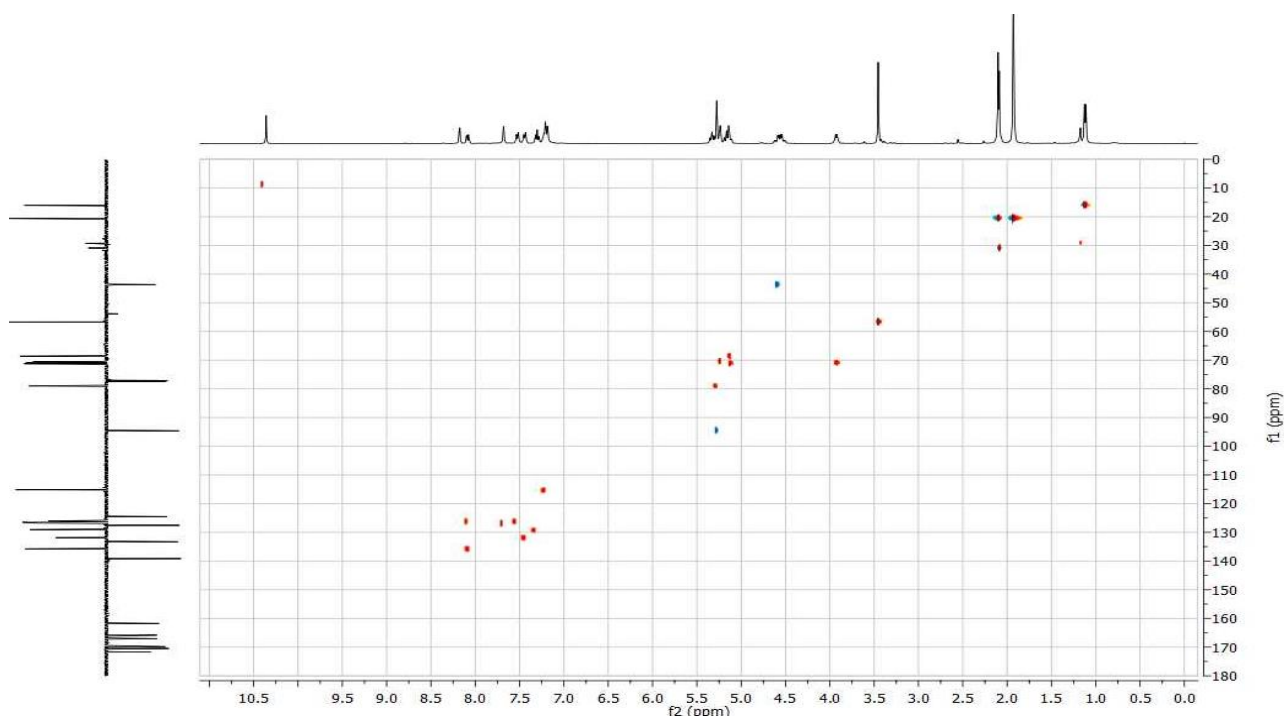


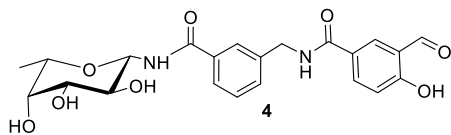


^1H NMR, 400 MHz, CDCl_3

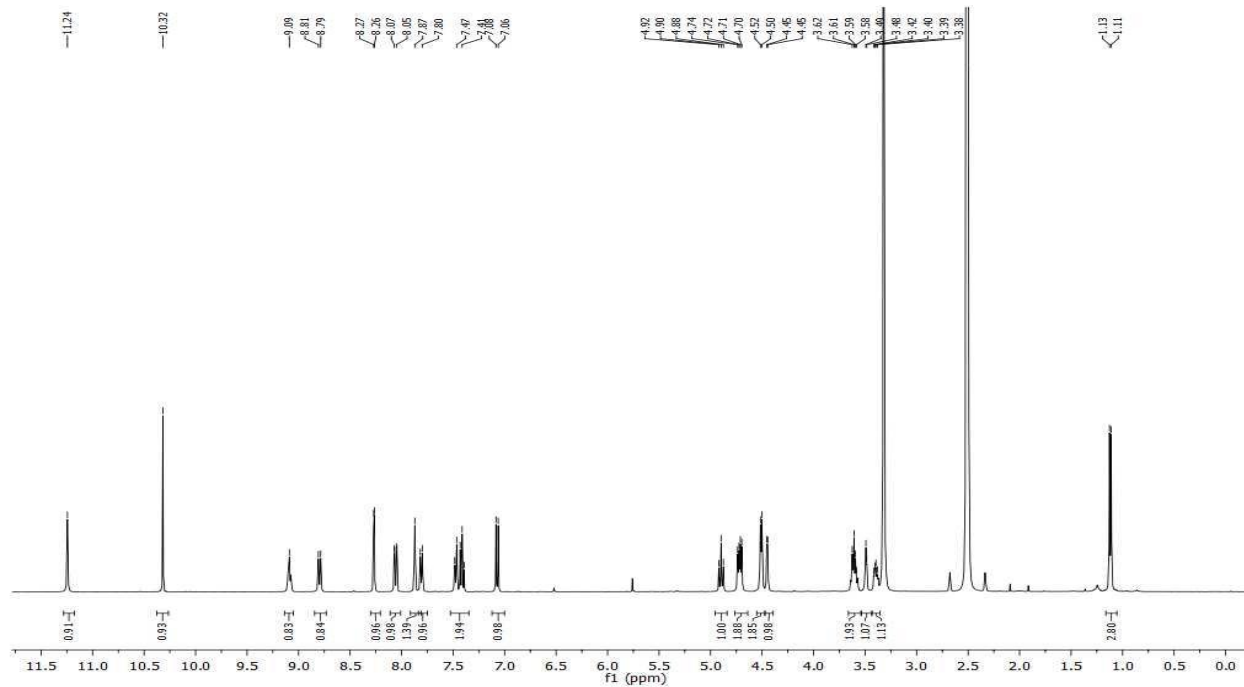


^1H - ^{13}C HSQC, CDCl_3

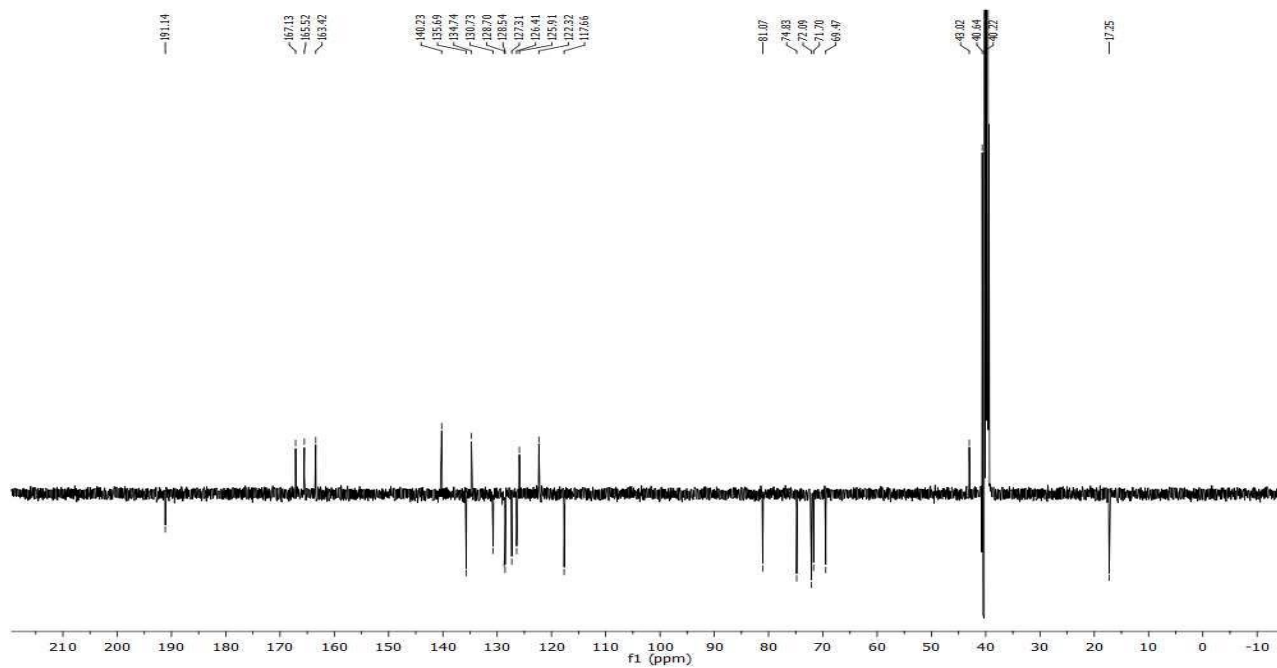


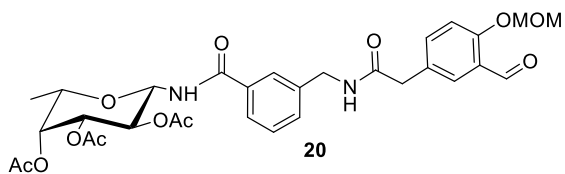


$^1\text{H NMR}$, 400 MHz, DMSO d_6

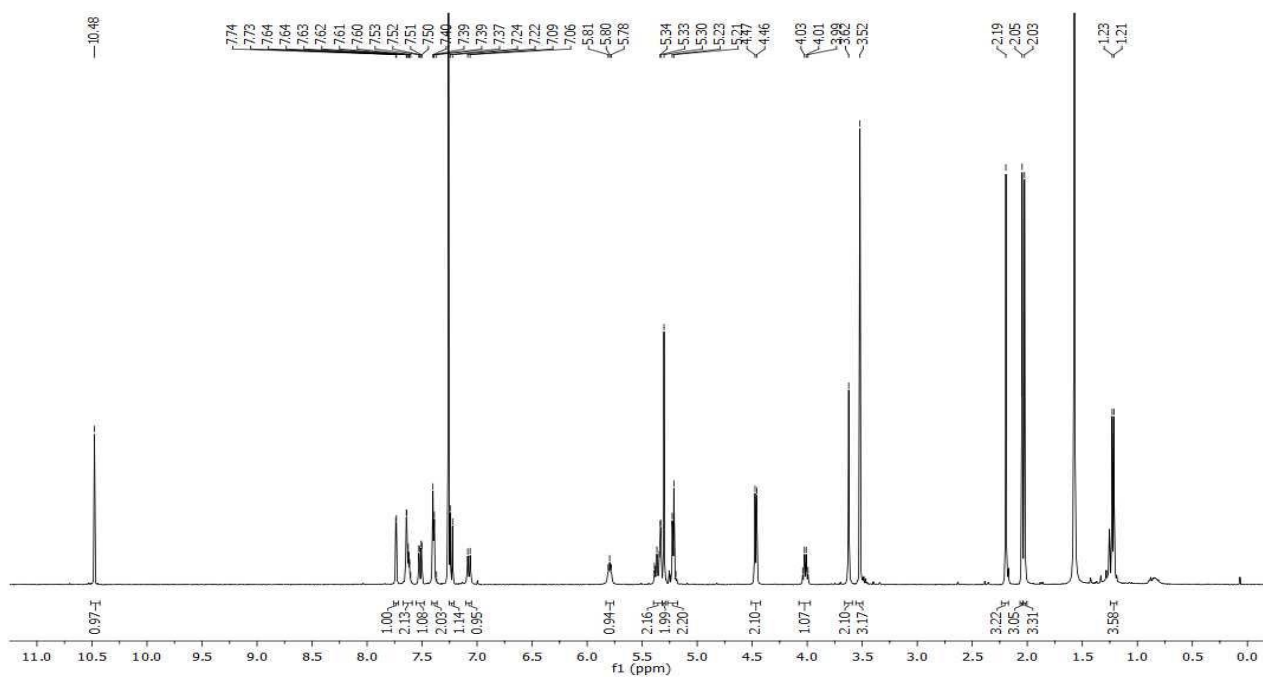


$^{13}\text{C NMR}$, 100 MHz, DMSO d_6

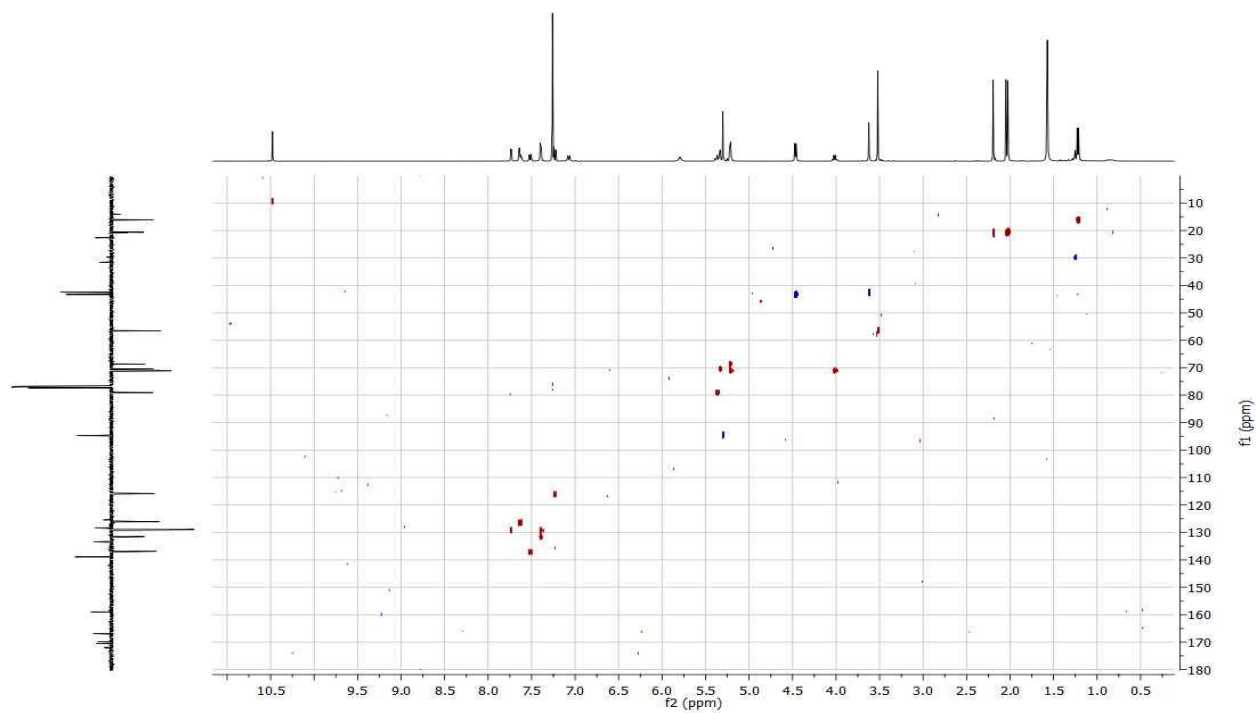


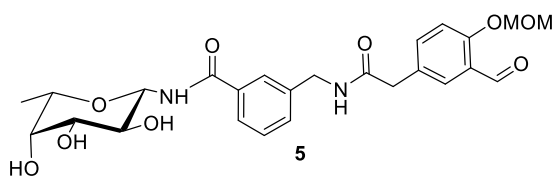


^1H NMR, 400 MHz, CDCl_3

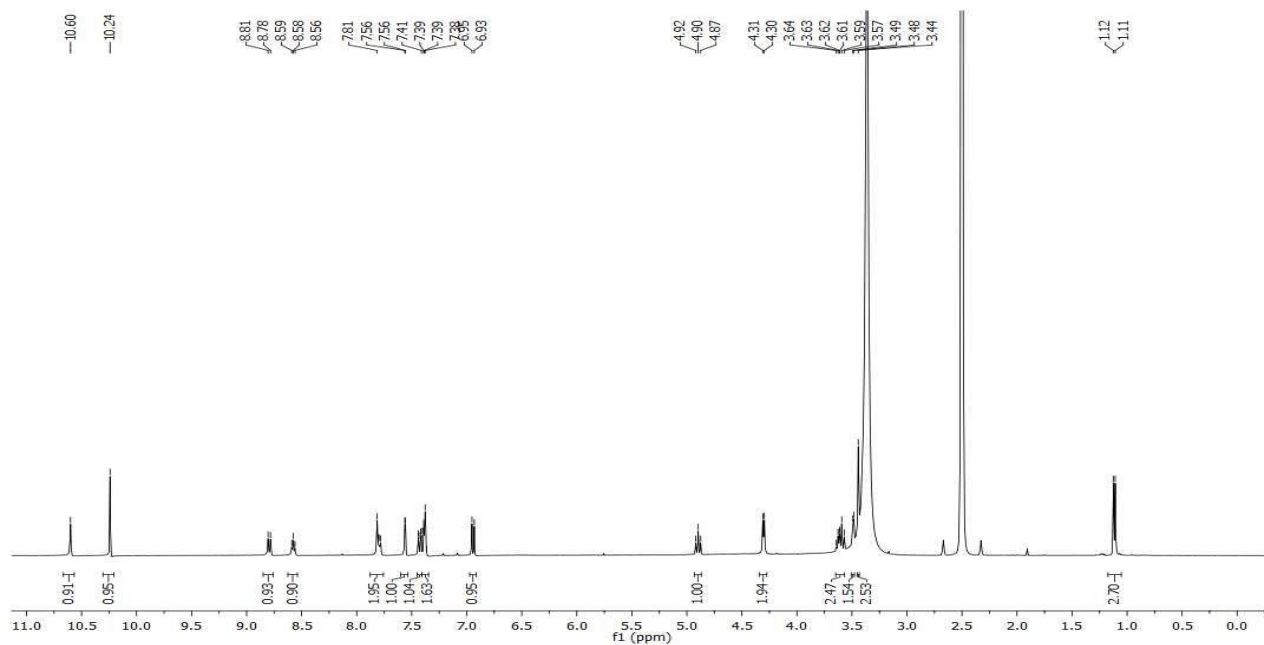


^1H - ^{13}C HSQC, CDCl_3

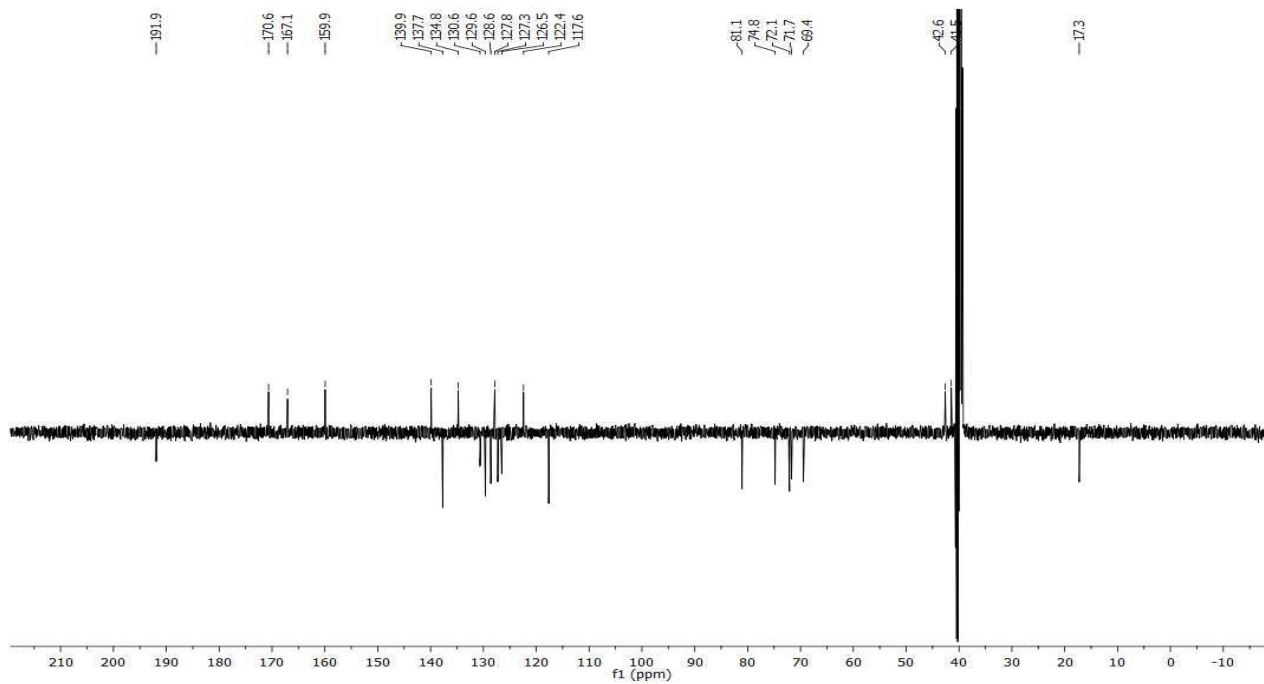


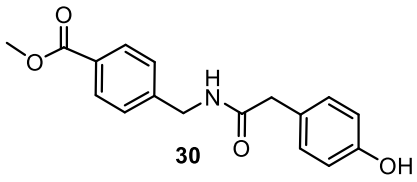


^1H NMR, 400 MHz, DMSO d_6

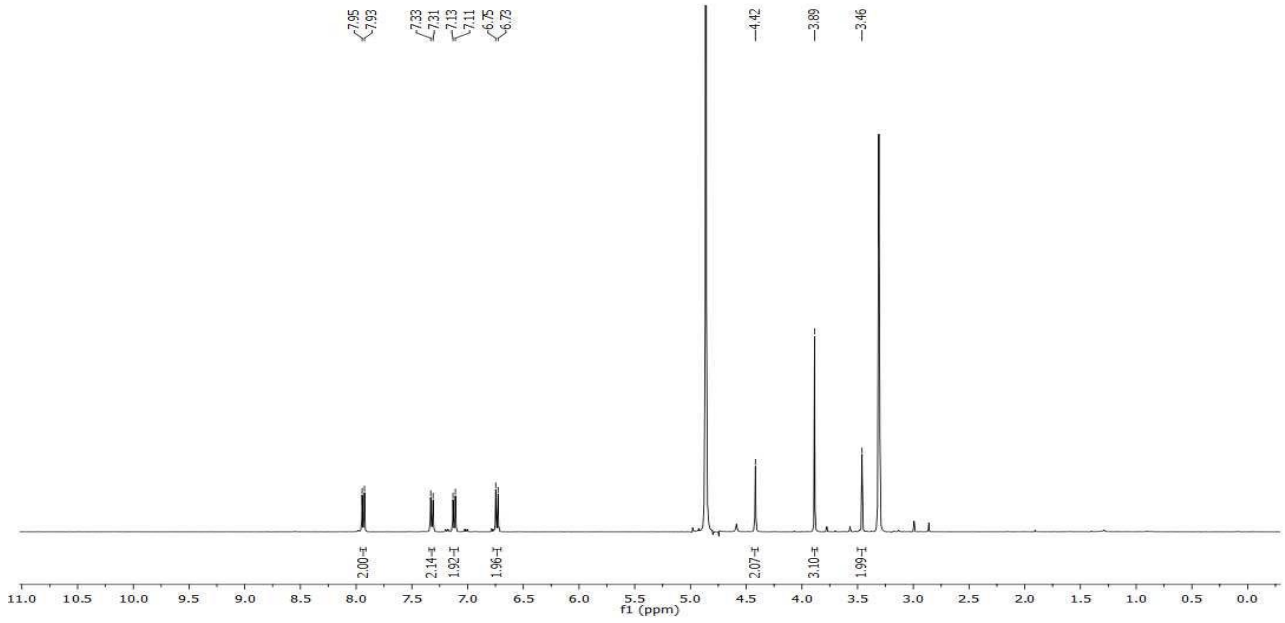


^{13}C NMR, 100 MHz, DMSO d_6

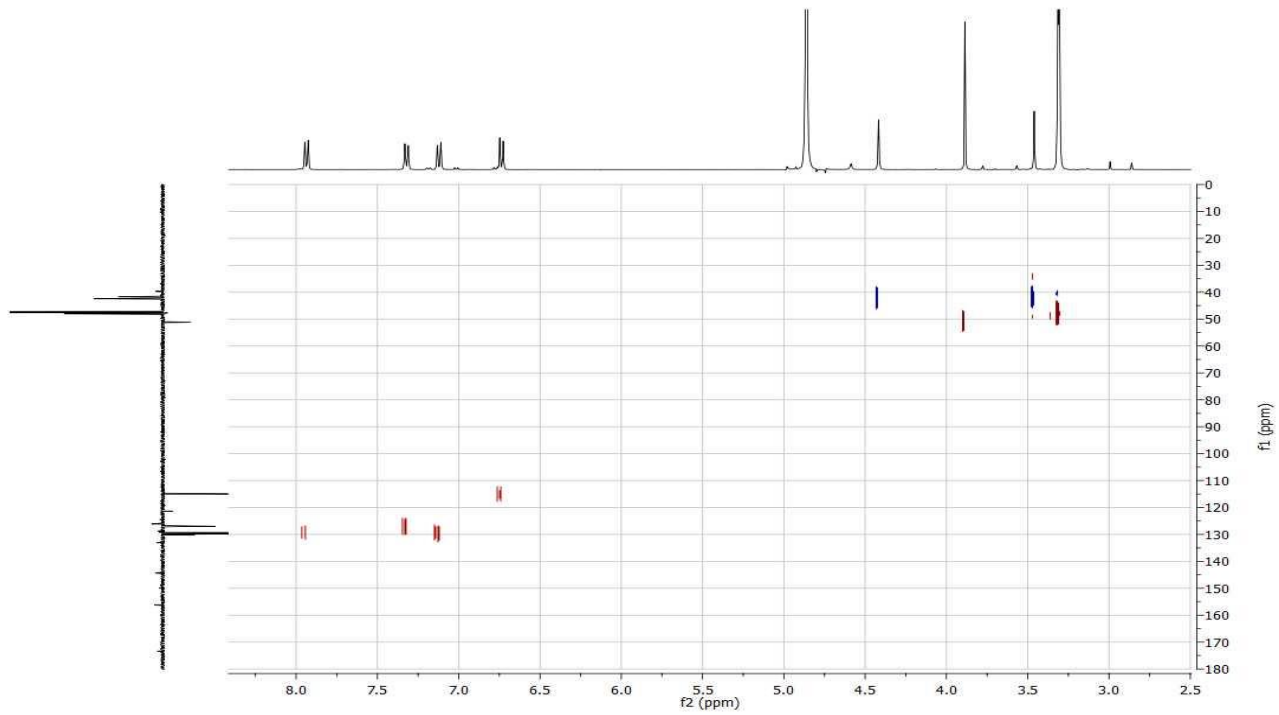


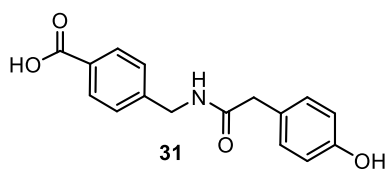


^1H NMR, 400 MHz, CD_3OD

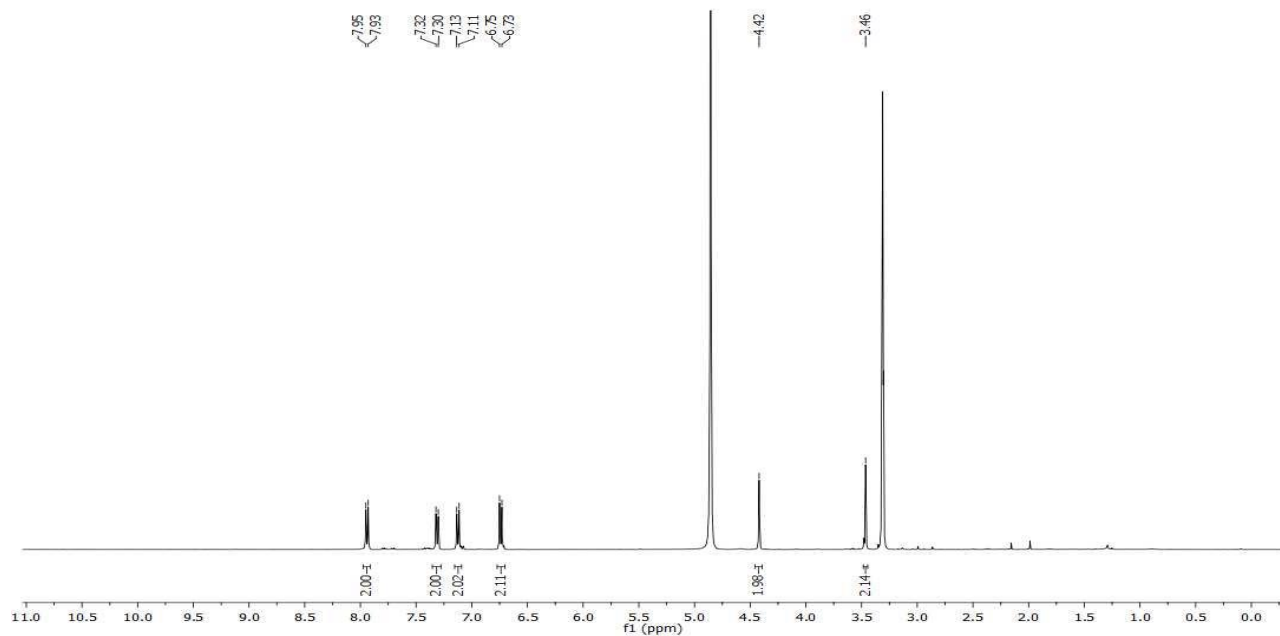


^1H - ^{13}C HSQC, CD_3OD

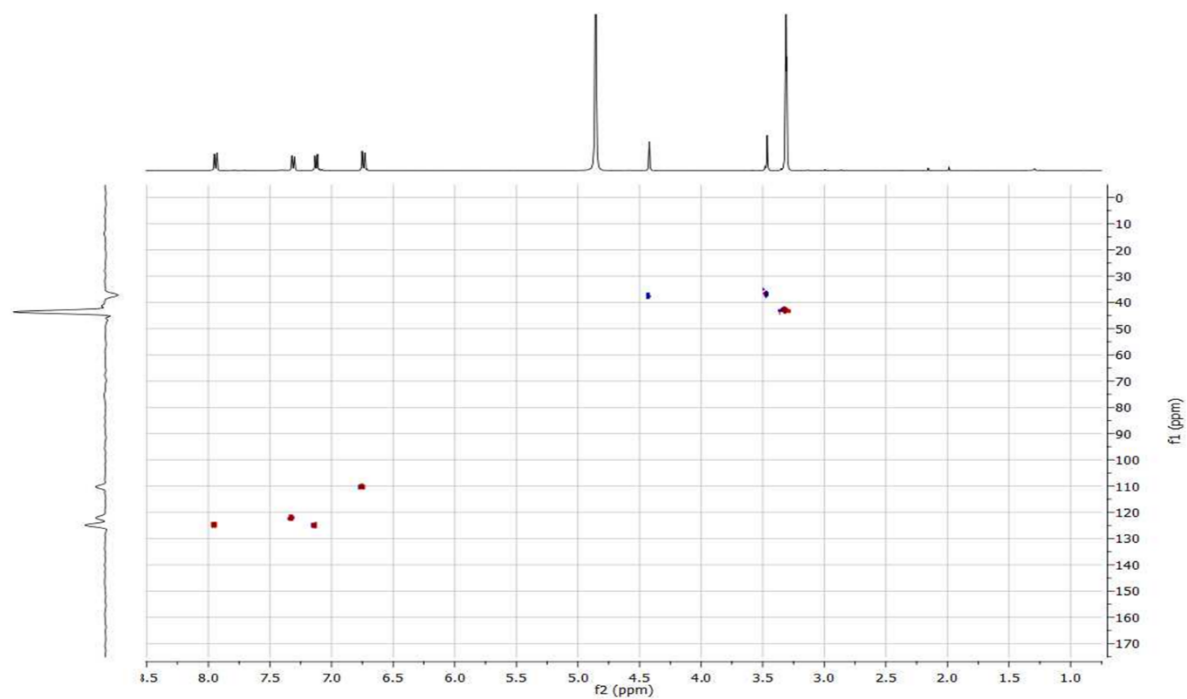


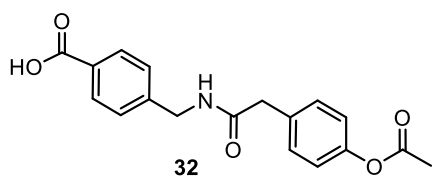


^1H NMR, 400 MHz, CD_3OD

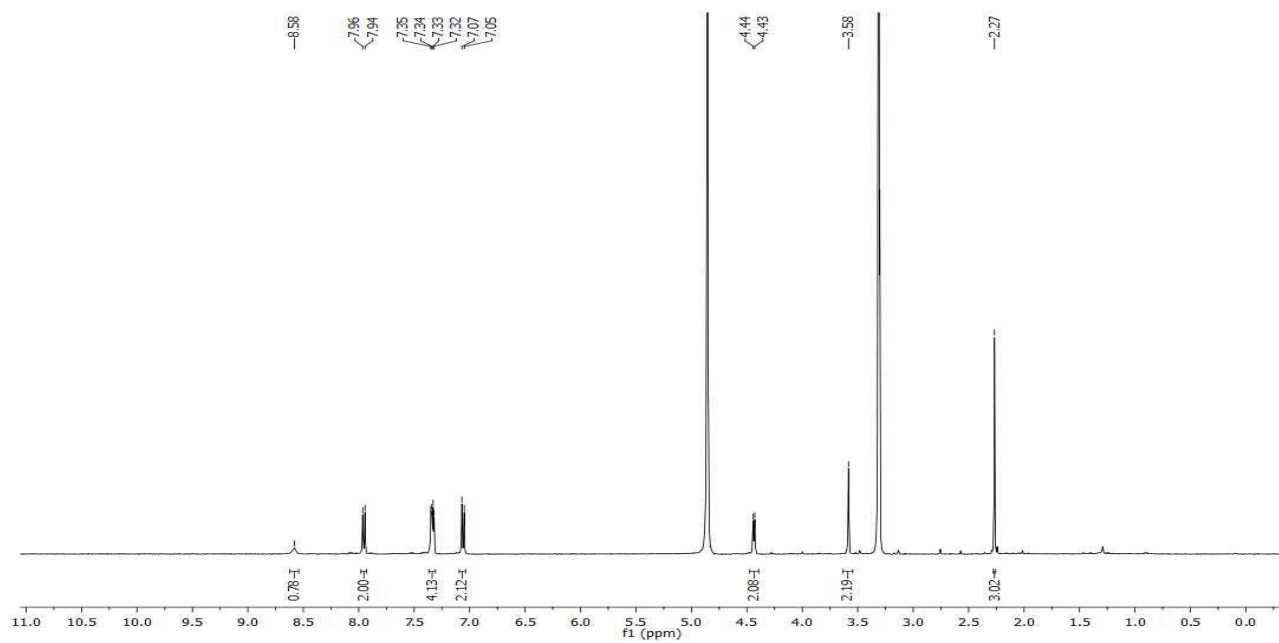


^1H - ^{13}C HSQC, CD_3OD

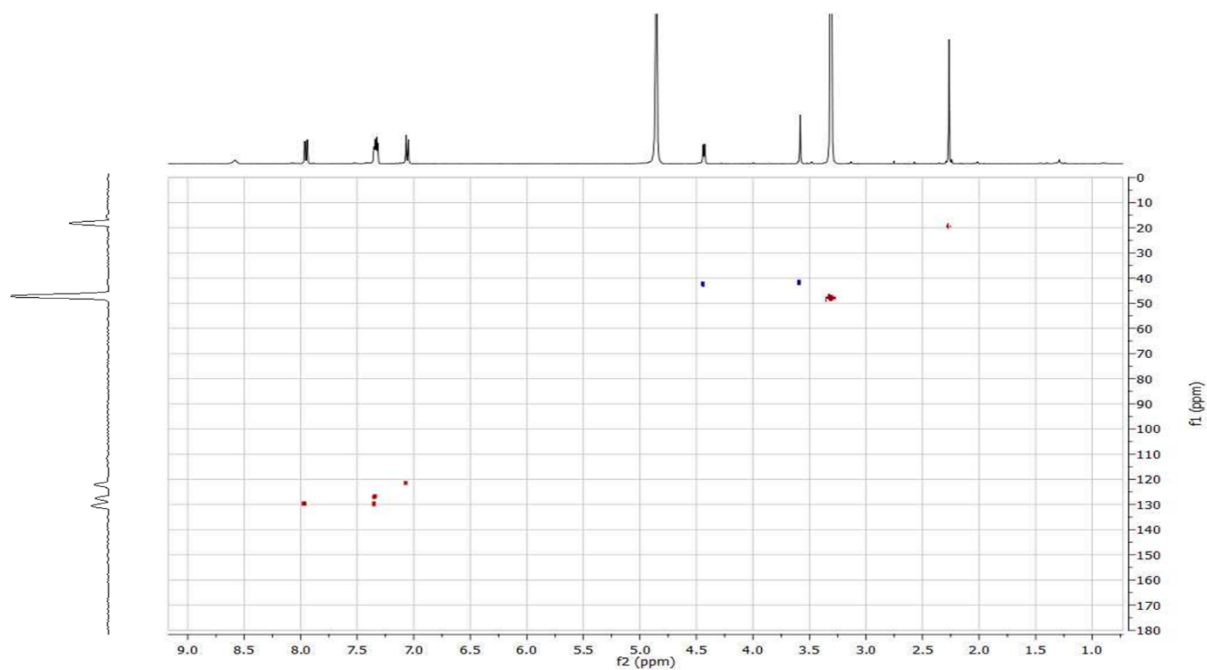


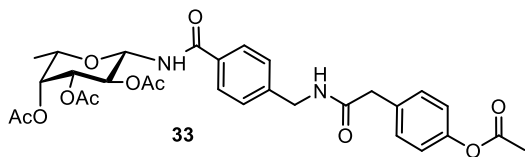


^1H NMR, 400 MHz, CD_3OD

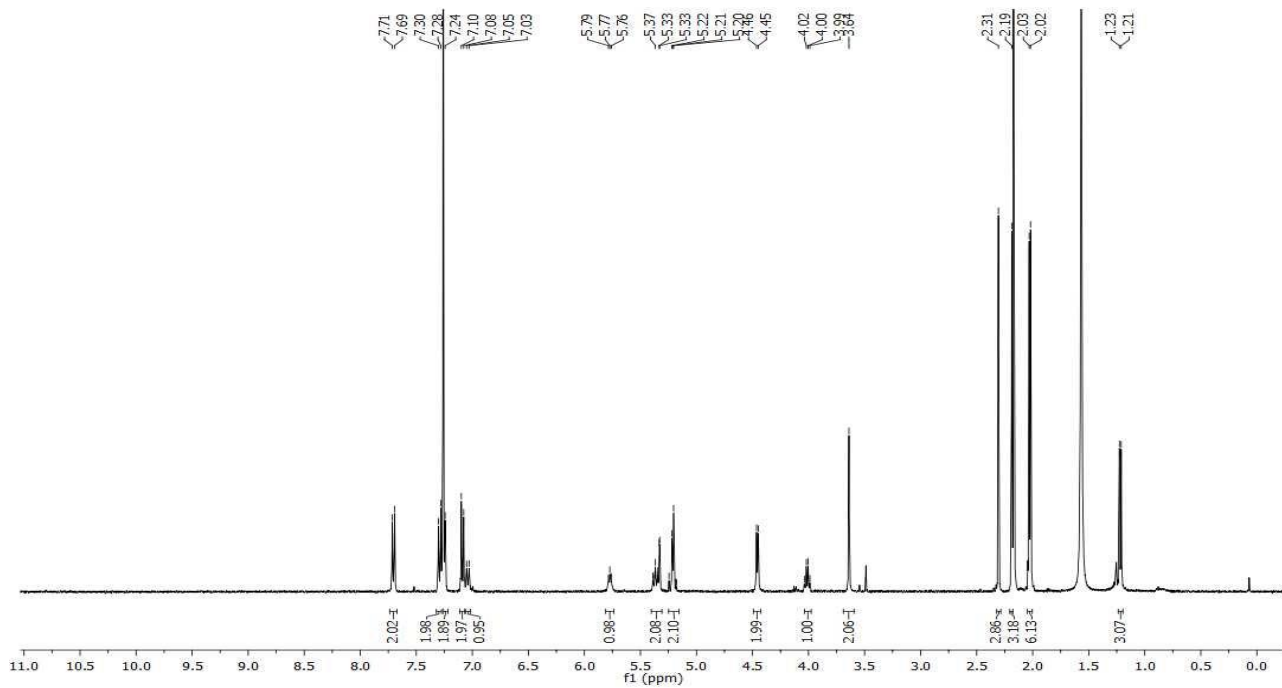


^1H - ^{13}C HSQC, CD_3OD

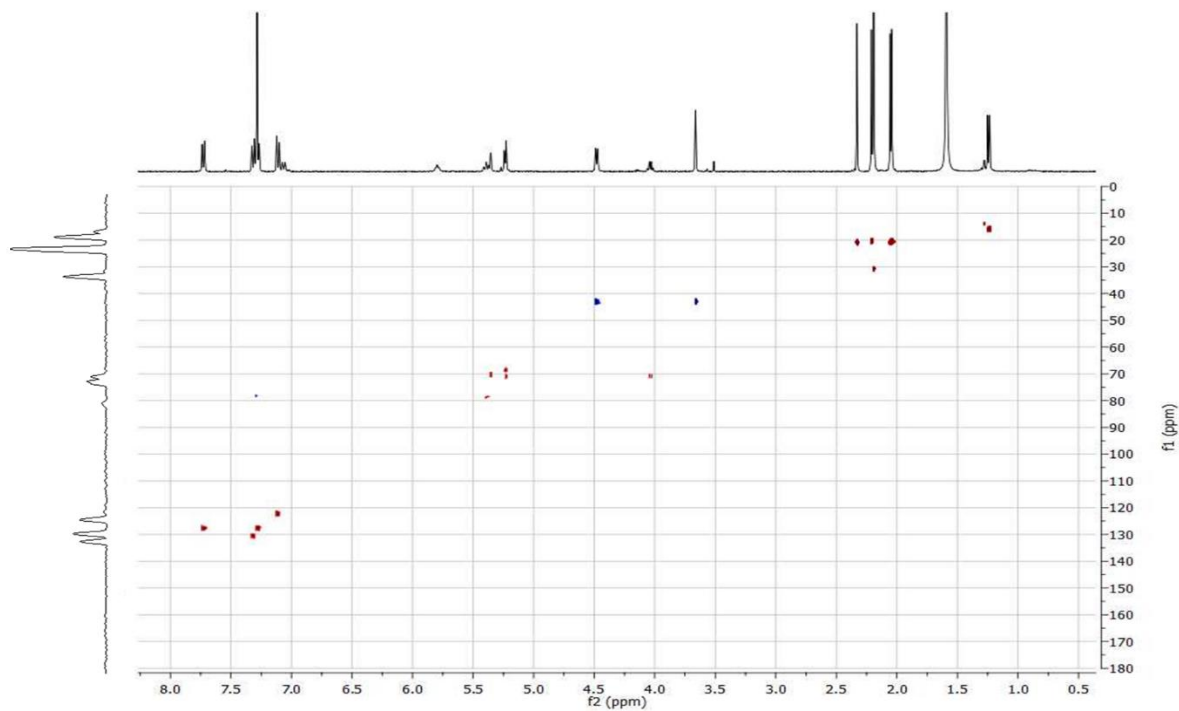


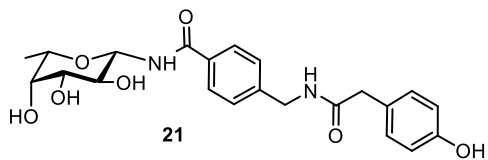


^1H NMR, 400 MHz, CDCl_3

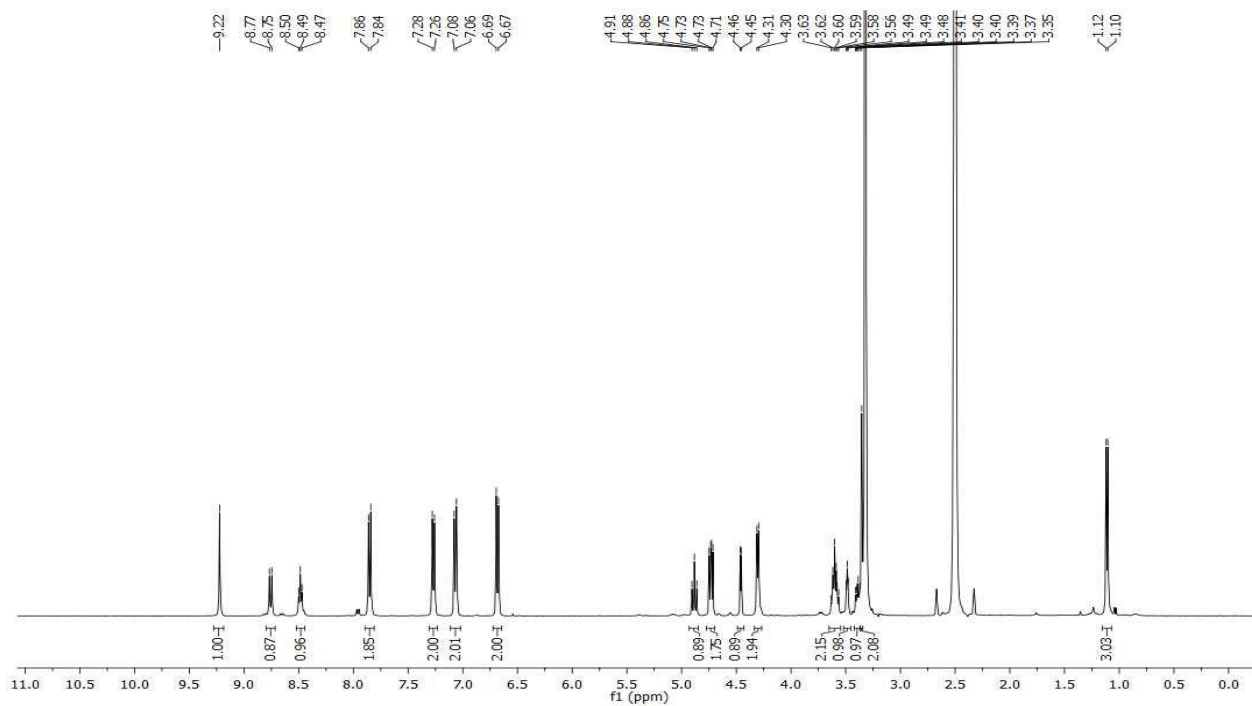


^1H - ^{13}C HSQC, CDCl_3

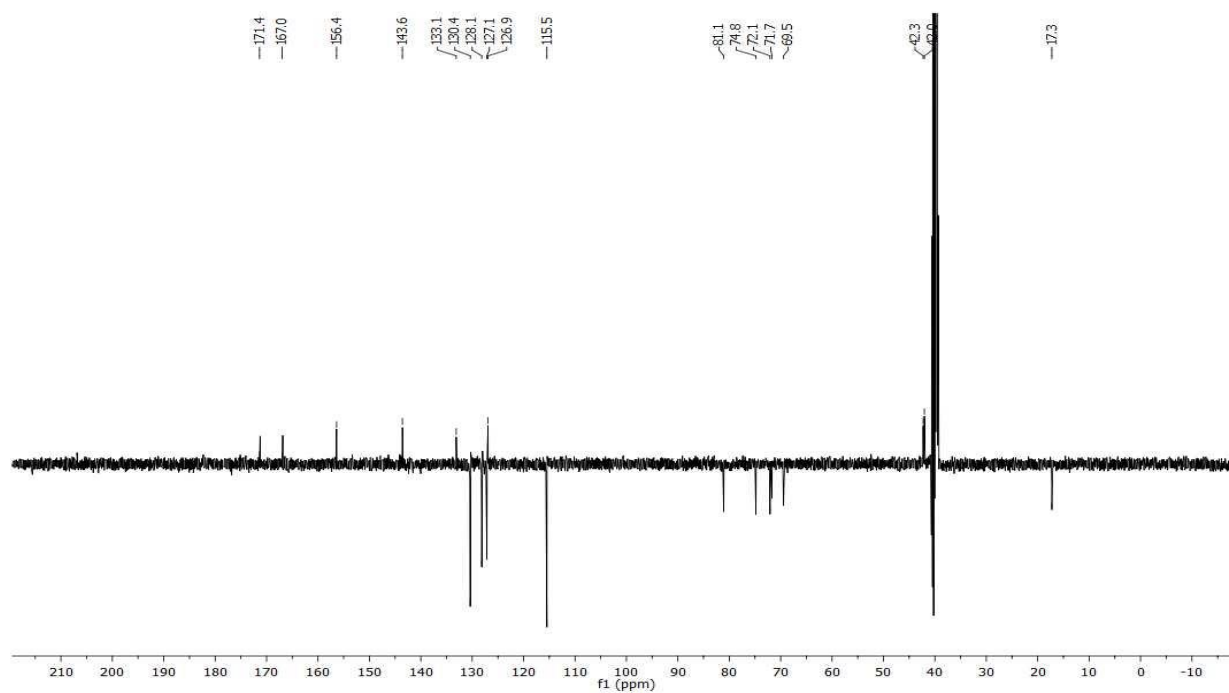


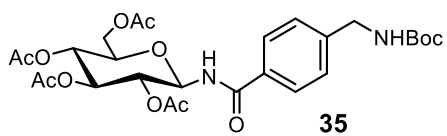


^1H NMR, 400 MHz, DMSO d_6

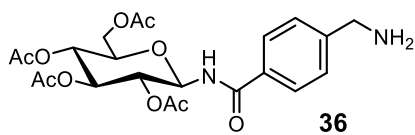
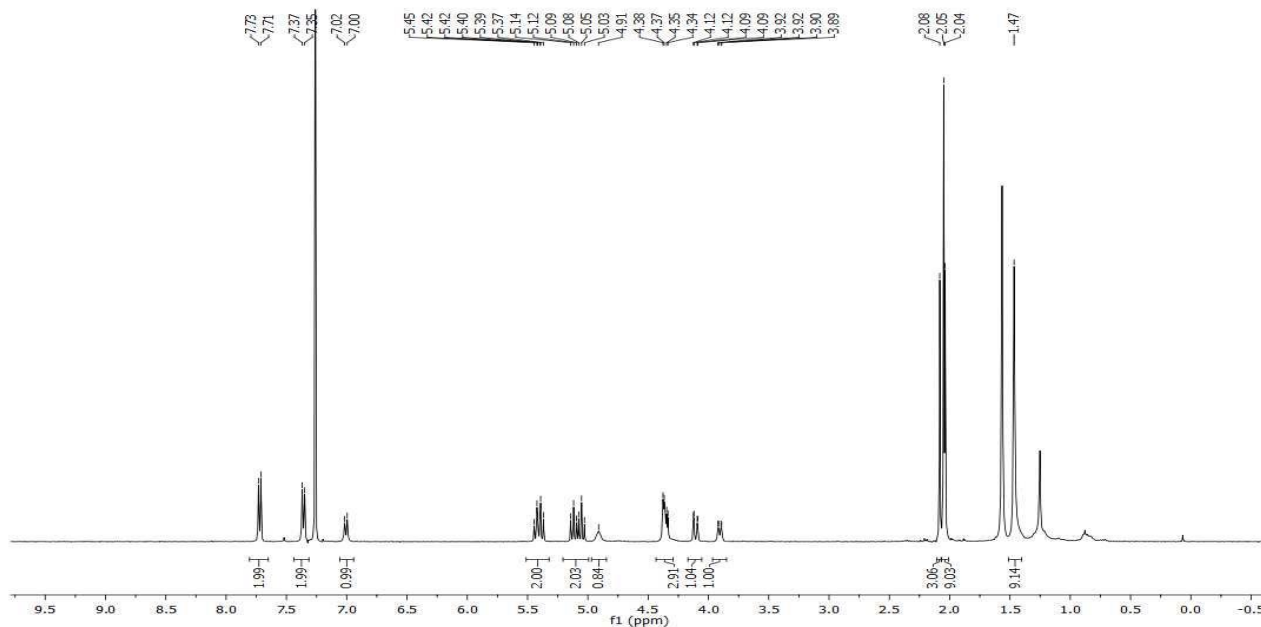


^{13}C NMR, 100 MHz, DMSO d_6

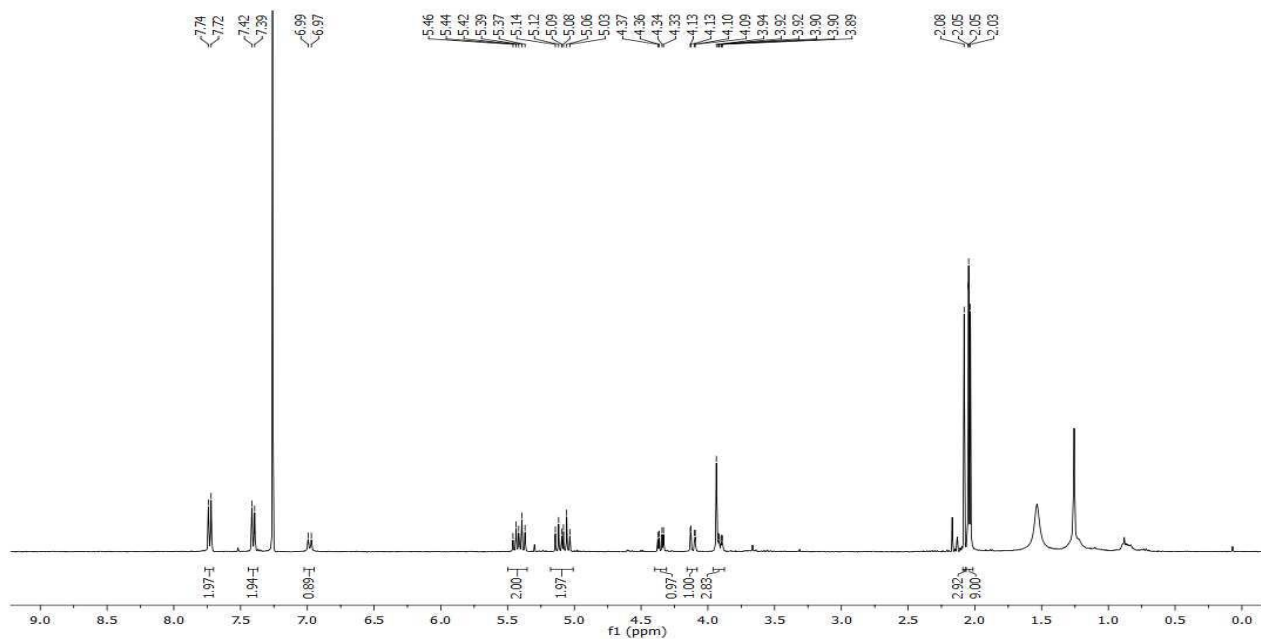


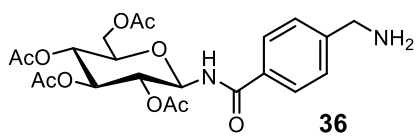


$^1\text{H NMR}$, 400 MHz, CDCl_3

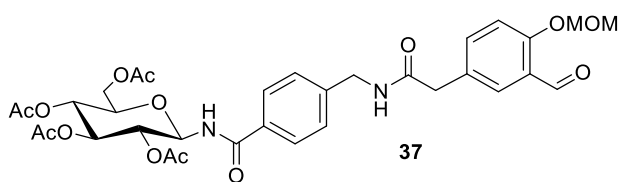
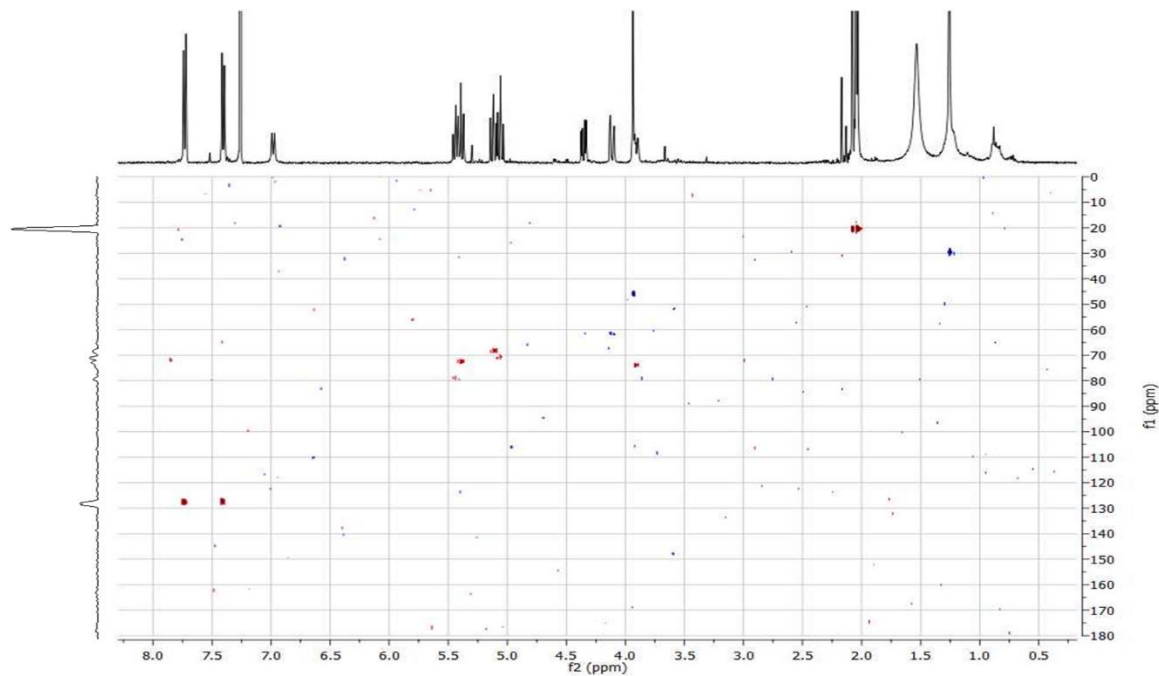


$^1\text{H NMR}$, 400 MHz, CDCl_3

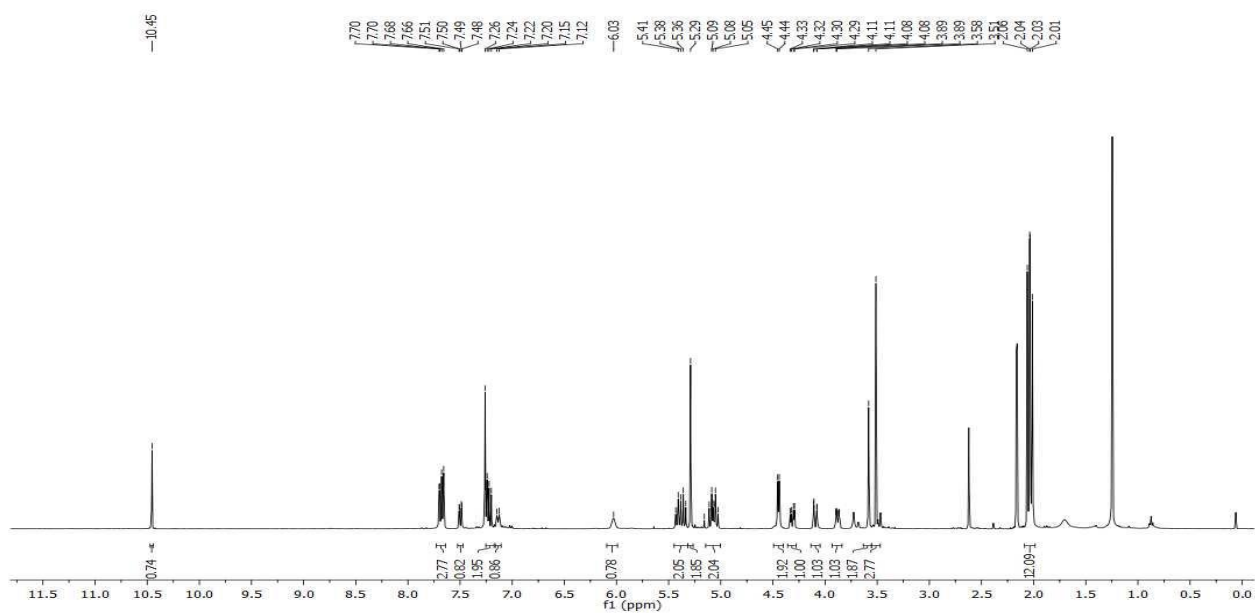


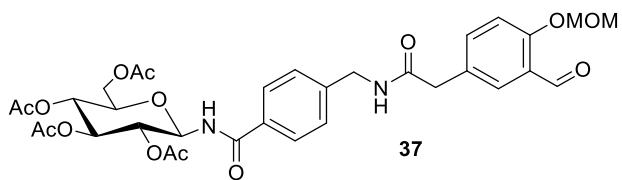


^1H - ^{13}C HSQC, CDCl_3

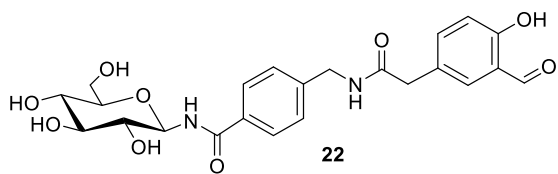
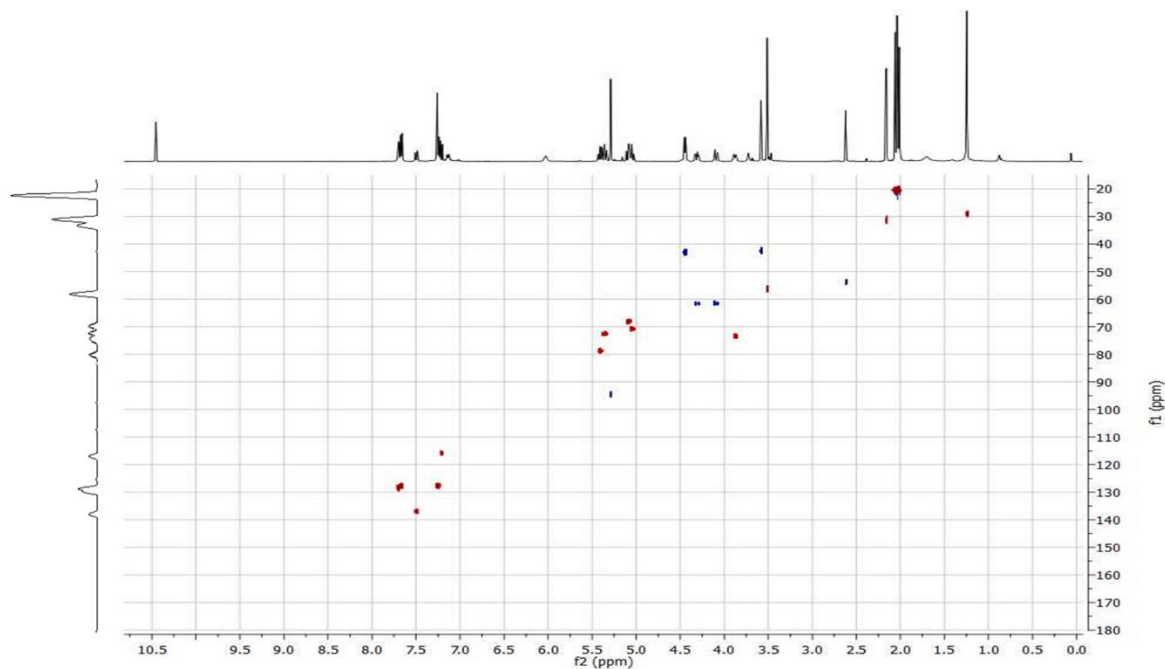


^1H NMR, 400 MHz, CDCl_3

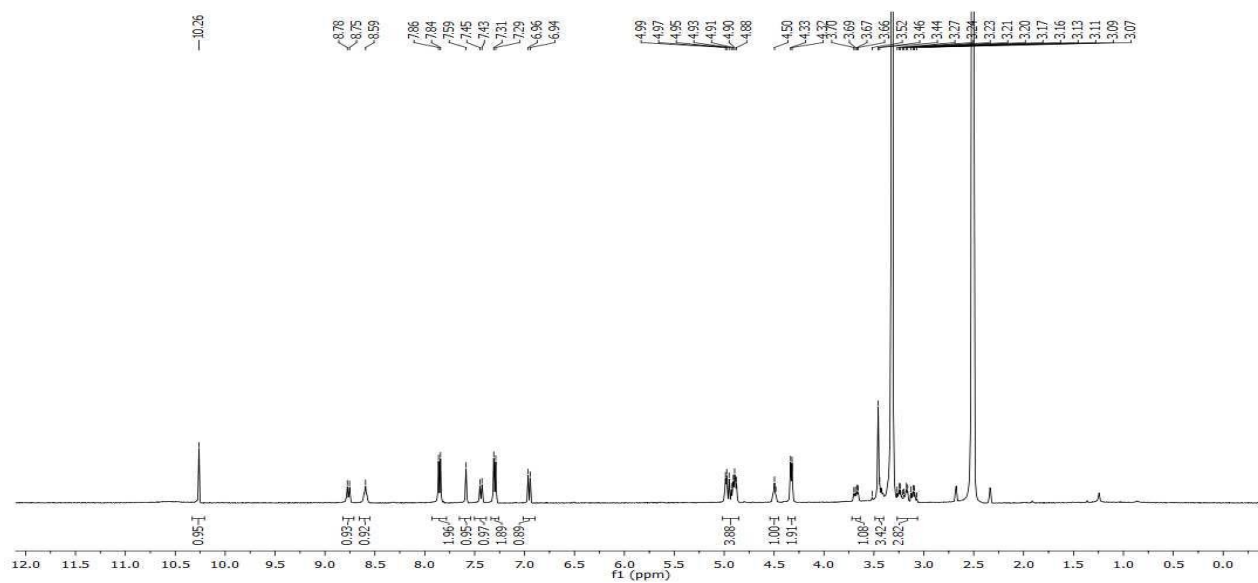


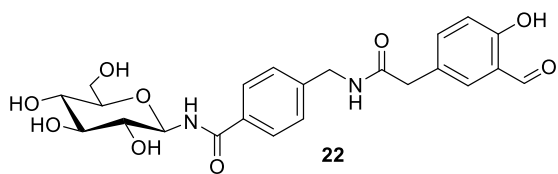


^1H - ^{13}C HSQC, CDCl_3

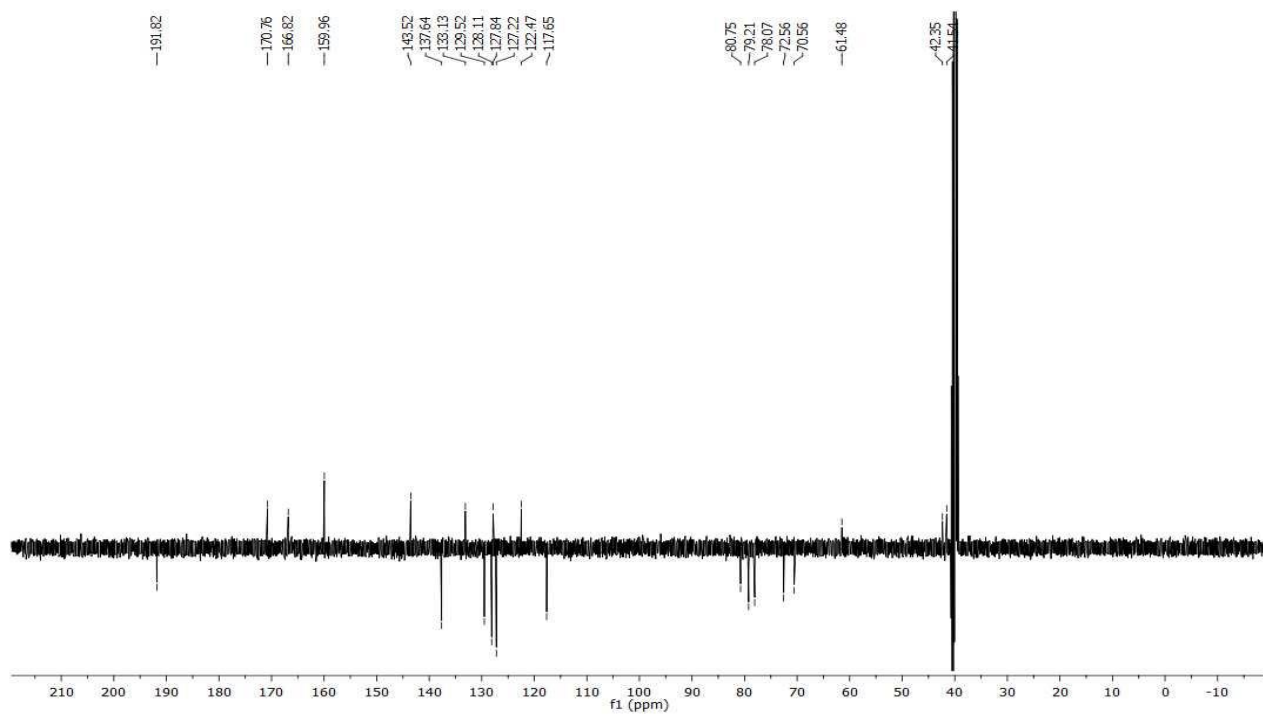


^1H NMR, 400 MHz, DMSO-d_6

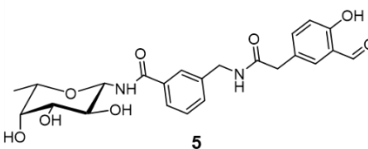
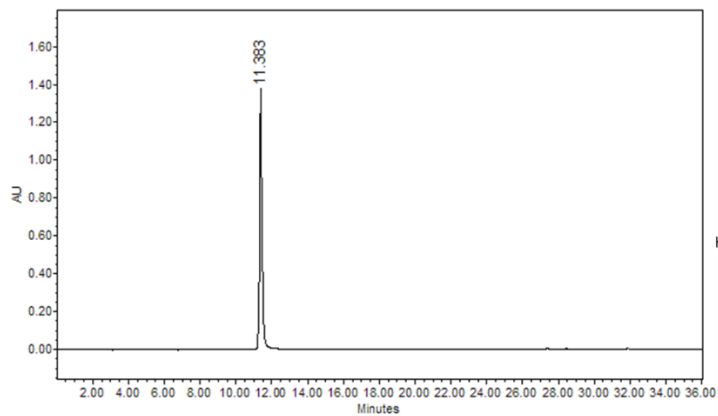
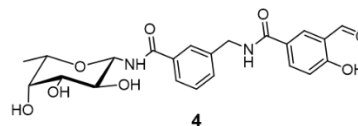
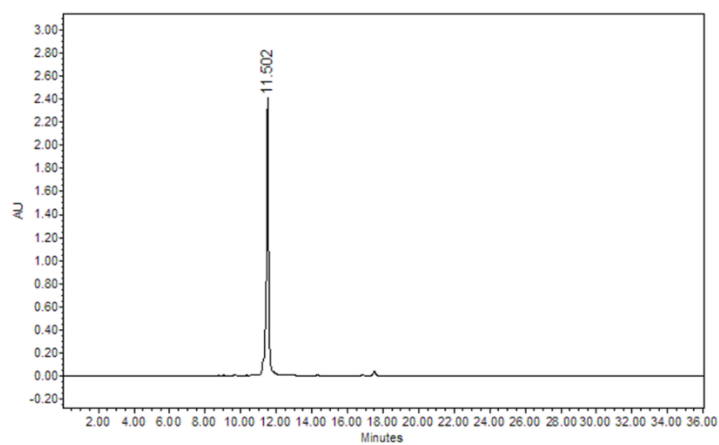
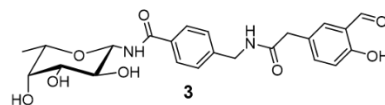
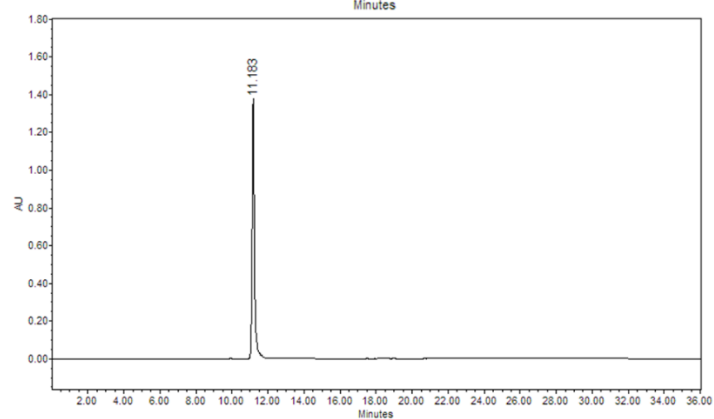
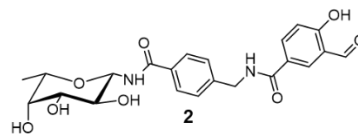
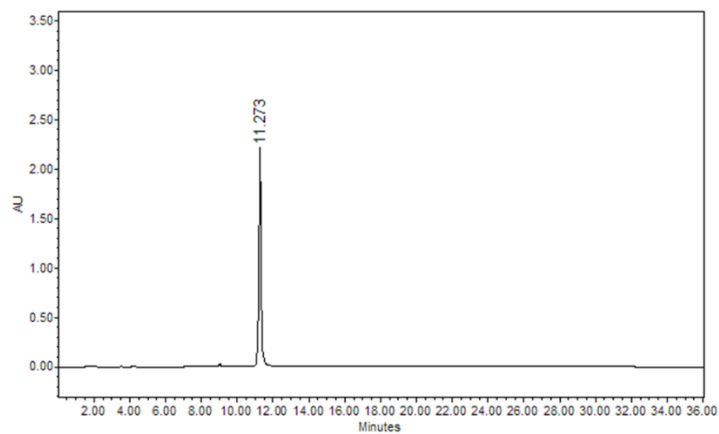


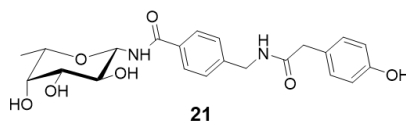
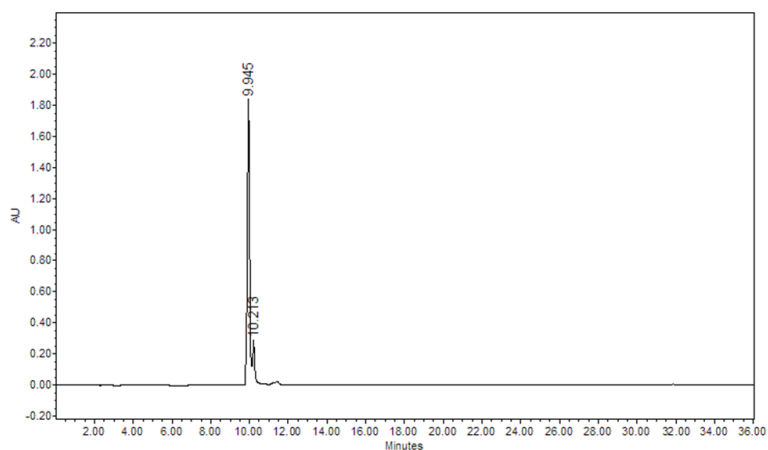


^{13}C NMR, 100 MHz, DMSO d_6

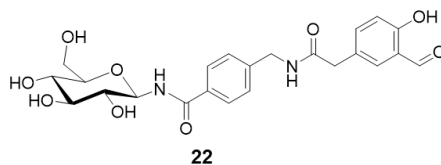
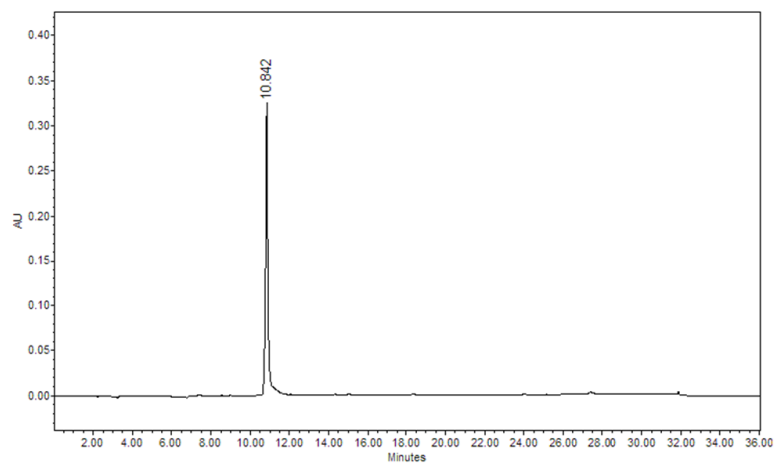


9. HPLC traces for ligands 2-5, 21 and 22





Retention time (min)	Area (μV ² sec)	% Area
9.9445	12981025	95.96
10.213	546144	4.04



Gradient (H₂O + 0.1% TFA/CH₃CN + 0.1% TFA): 0-26 min, 0-100%; 26-36 min, 100%.

10. References

- (1) Pantsar, T.; Poso, A. Binding Affinity via Docking: Fact and Fiction. *Molecules* **2018**, *23*, 1899. <https://doi.org/10.3390/molecules23081899>.
- (2) Pérez, S. ; Tvaroška, I. *Carbohydrate-Protein Interactions Molecular Modeling Insights* 2014, *71*, 9-136. <https://doi.org/10.1016/B978-0-12-800128-8.00001-7>.
- (3) Bermeo, R.; Lal, K.; Ruggeri, D.; Lanaro, D.; Mazzotta, S.; Vasile, F.; Imberty, A.; Belvisi, L.; Varrot, A.; Bernardi, A. Targeting a Multidrug-Resistant Pathogen: First Generation Antagonists of *Burkholderia Cenocepacia*'s BC2L-C Lectin. *ACS Chem Biol* **2022**, *17*, 2899–2910. <https://doi.org/10.1021/acscchembio.2c00532>.
- (4) Mazzotta, S.; Antonini, G.; Vasile, F.; Gillon, E.; Lundstrøm, J.; Varrot, A.; Belvisi, L.; Bernardi, A. Identification of New L-Fucosyl and L-Galactosyl Amides as Glycomimetic Ligands of TNF Lectin Domain of BC2L-C from *Burkholderia Cenocepacia*. *Molecules* **2023**, *28*, 1494. <https://doi.org/10.3390/MOLECULES28031494/S1>.
- (5) Antonini, G.; Civera, M.; Lal, K.; Mazzotta, S.; Varrot, A.; Bernardi, A.; Belvisi, L. Glycomimetic Antagonists of BC2L-C Lectin: Insights from Molecular Dynamics Simulations. *Front Mol Biosci* **2023**, *10*, 201630. <https://doi.org/10.3389/fmolb.2023.1201630>.
- (6) Duléry, V.; Renaudet, O.; Philouze, C.; Dumy, P. α and β L-Fucopyranosyl Oxyamines: Key Intermediates for the Preparation of Fucose-Containing Glycoconjugates by Oxime Ligation. *Carbohydr. Res.* **2007**, *342*, 894–900. <https://doi.org/10.1016/j.carres.2007.02.003>.
- (7) Palomo, C.; Aizpurua, J. M.; Balentová, E.; Azcune, I.; Santos, J. I.; Jiménez-Barbero, J.; Cañada, J.; Miranda, J. I. “Click” Saccharide/ β -Lactam Hybrids for Lectin Inhibition. *Org. Lett.* **2008**, *10*, 2227–2230. <https://doi.org/10.1021/ol8006259>.
- (8) Jiang, Y.; Pan, S.; Zhang, Y.; Yu, J.; Liu, H. Copper-Catalyzed Decarboxylative Methylation of Aromatic Carboxylic Acids with $\text{PhI}(\text{OAc})_2$. *Eur. J. Org. Chem.* **2014**, *2014*, 2027–2031. <https://doi.org/10.1002/ejoc.201301815>.
- (9) Fontán, N.; García-Domínguez, P.; Álvarez, R.; De Lera, Á. R. Novel Symmetrical Ureas as Modulators of Protein Arginine Methyl Transferases. *Bioorg. Med. Chem.* **2013**, *21*, 2056–2067. <https://doi.org/10.1016/j.bmc.2013.01.017>.
- (10) Huh, S.; Saunders, G. J.; Yudin, A. K. Single Atom Ring Contraction of Peptide Macrocycles Using Cornforth Rearrangement. *Angew. Chem. Int. Ed.* **2023**, *62*, e202214729. <https://doi.org/10.1002/anie.202214729>.
- (11) Jackson, S.; Degrado, W.; Dwivedi, A.; Parthasarathy, A.; Higley, A.; Krywko, J.; Rockwell, A.; Markwalder, J.; Wells, G.; Wexler, R.; Mousa, S.; Harlow, R. Template-Constrained Cyclic Peptides: Design of High-Affinity Ligands for GPIIb/IIIa. *J. Am. Chem. Soc.* **1994**, *116*, 3220–3230.
- (12) Bermeo Malo, R. Design, Synthesis and Evaluation of Antagonists towards BC2L-C, Université Grenoble Alpes/ Università degli Studi di Milano, 2021. <https://air.unimi.it/handle/2434/850474>.